DISCLAIMER NOTICE

THIS DOCUMENT IS THE BEST QUALITY AVAILABLE.

COPY FURNISHED CONTAINED A SIGNIFICANT NUMBER OF PAGES WHICH DO NOT REPRODUCE LEGIBLY.

ARC DISCHARGE SOURCES

Final Report
16 October 1964 to 15 November 1965

15 November 1965

Contract Nonr-4647(00)
ARPA Order No. 306-62, Code 4730

Westinghouse Research Laboratories
PITTSBURGH 35, PENNSYLVANIA

This research is part of Project DEFENDER
under the joint sponsorship of the Advanced
Research Projects Agency, the Office of
Naval Research and the Department of Defense.

ARC DISCHARGE SOURCES

FINAL REPORT

Covering Period from 16 October 1964 through 15 November 1965

15 November 1965

Contract Nonr-4647(00)

ARPA Order No. 306-62

Code No. 4730

Req. No. NR-012-55/6-26-64

A 12-Month Contract

Expiration Date 11/16/65

Cost $99,552

Charles H. Church, Principal Investigator (412) 242-1500, Etx. 678 with Richard G. Schlecht and I. Liberman with Appendixes by B. W. Swanson, E. G. F. Arnott and E. Geil

R. D. Haun, Jr., Manager, Quantum Electronics Department

Westinghouse Research Laboratories
Pittsburgh, Pennsylvania 15235

This research is part of Project DEFENDER
under the joint sponsorship of the Advanced
Research Projects Agency, the Office of
Naval Research and the Department of Defense.

TABLE OF CONTENTS

TABLE OF CONTENTS (Con't.)

PREFACE

High energy arc discharges have been used to pump lasers since the first ruby laser of Maiman, and are still the most efficient means for exciting the high energy lasers. In order to obtain larger inputs to lasers and more efficient high energy lasers, the need arose for a better understanding of the processes within the arc discharge. The literature existing on these discharges is contradictory, and the experimental evidences of such phenomena as the saturation of the discharge and dependence of efficiency upon many parameters were not readily explained.

Under these circumstances, it was felt that a more basic study of the highly radiant, high energy arc discharge was needed, in which the physical properties of these arc plasma were to be used in models for the discharges to calculate the radiant characteristics. These models for the discharge would be validated through experiment. Once the suitable models were available, the application to the specific high energy laser pumping applications would be straightforward, though not necessarily easy. The theoretical models for the pulsed arc discharge discussed in the final report possess many of the features of the actual arcs, but exhibit only semi-quantitative agreement. In part, this lack of agreement is due to deficiencies in the model, such as in not including thermal conduction power transport and such features as the Stark broadened [illegible] which are so important in the infrared between .65 and 1.0 μ. But a large portion of the disagreement is due to insufficient quantitative knowledge of the properties of dense plasmas, in particular, the spectral absorptivities and transport properties (i.e., electrical and thermal conductivity) of xenon. This lack of knowledge is not unique to xenon or the

other rare gases; there is a lack of quantitative data on dense plasmas of even nitrogen and oxygen. In the past five years, there has been a large amount effort devoted towards the investigation of those gases, using the cascade arc, and the shock tube. The availability of the digital computer has helped considerably -- if not made possible -- these studies.

The experimental measurements such as those discussed in this report indicate that the wall-stabilized pulsed arc or flash tube can provide valuable quantitative information in dense plasmas such as those that may be encountered in gases other than xenon.

ABSTRACT

This report summarizes the work to date on Contract Nonr 4647(00) towards creating models for the high energy pulsed arc discharge used for high energy laser pumping. Homogeneous temperature models are discussed in which the radiant emission is balanced by the electrical power input. These models have been evaluated at various energy levels for the temperature which has been measured within the arc (assuming local thermal equilibrium). The models included the continuum spectral absorptivity calculated according to Biberman and Norman (using the Zeta factor of Schlüter). There was found to be a semi-quantitative agreement between the Zeta factor observed experimentally, and those of Biberman and Norman, and of Schlüter. The spectral transmissivity as a function of current density calculated from the models showed reasonable agreement with the experimental values of Emmett, Schawlow, and Weinberg in the visible and ultraviolet, but differ widely in the infrared (due to the strong infrared lines of xenon).

Measurements of the time-resolved profiles of lines in the infrared, of the radial distribution of the spectral radiance in the ultraviolet, and of the electrical conductivity are also discussed. These measurements provide a means for determining the temperature dependence of these quantities within these arcs. The ultraviolet radial profiles indicate that the arc is relatively homogeneous for the range of current densities and pressures studied.

Papers and Talks Resulting From This Contract

1. "A Wide Range Ultra Rapid Scan Spectrometer" by Charles H. Church and Leonard Gampel. Accepted for publication by Applied Optics.
2. "Models for Pulsed Arc Discharges" by Charles H. Church and Richard G. Schlecht. Presented at October 1965 Meeting of the Optical Society of America.
3. "Arc Discharge Sources in the Infrared--Some Simple Models" by Charles H. Church and Richard G. Schlecht. Submitted to the Proceedings IRIS.
4. "Studies of Highly Radiative Plasmas Using the Wall Stabilized Pulsed Arc Discharge" by Charles H. Church, Richard G. Schlecht, Irving Liberman, and Bruce W. Swanson. Accepted for presentation at the A.P.S [illegible] Plasmadynamics Meeting, March 1966.
5. "Laborabory Simulation of Highly Radiative Plasmas" by Charles H. Church, Richard G. Schlecht, and Irving Liberman. Submitted for presentation at the Symposium on Interdisciplinary Aspects of Radiative Energy Transfer, February 1966.
6. "Radiation Flux in a Non-Isothermal Non-Grey Cylindrical Arc" by Bruce W. Swanson. Submitted for presentation at the Symposium on Interdisciplinary Aspects of Radiative Energy Transfer, February 1966.

CHAPTER 1

Introduction

Arc discharges are commonly used for exciting high energy lasers. The highly radiative arc discharges used for the high energy laser excitation has been examined experimentally by numerous groups in order to understand them more fully, but the results were in many respects contradictory. Furthermore, many of the characteristics observed were not readily explainable on any simple basis. Phenomena such as saturation of the arc, emission with increasing power input and the variation of the efficiency with size, shape, and the energy density, all required further explanation in order to apply these arc discharges to high energy laser pumping.

The radiative arc discharge consists of a core of high density plasma, in which the opacity varies widely for different spectral regions, surrounded by a cooler gas near the wall. Various disciplines, such as astrophysics, heat transfer, and reentry physics have considered various related aspects of such plasmas. The broader considerations must include, in addition to the widely varying opacity and the high density, the transport properties of the arc plasma and the energy transport due to radiation within those plasmas, which can possess a strongly varying temperature distribution from the wall to the center of the discharge.

Since the radiative arc discharge plays a major role in high energy laser pumping, it was felt by many that these arcs should be understood more thoroughly. Such an understanding would be of use not only in present laser design, but also for studies on the optimization and the maximum energy capabilities of future laser systems.

In the course of Contract Nonr 4647(00), some models for the highly radiative arc discharge were developed in which the resistive power input per unit volume is balanced by radiation and by thermal conduction from that volume. The arcs were optically thick (i.e., high absorptivity or opacity) over certain wavelength regions, particularly in the infrared and far ultraviolet, but also for many of the lines; elsewhere they were optically thin. Consequently the analyses of the energy transport within the arc included a wide range of spectral absorptivities (i.e., a non-gray radiative transport calculation). The temperature in the arc varied from being near the boiling point of quartz or less ($\sim 2000^{\circ}K$) at the outer wall to a temperature in the center necessary to give electrical conductivities corresponding to those of a fully ionized gas ($\sim 10{,}000^{\circ}K$). This inhomogeneity in temperature and the resulting gradient needed to be considered in any complete evaluation of the model for the radiative arc discharge. The First Semiannual Report[1] discussed many of these aspects of the considerations involved in the model studies.

In the course of the contract, models described in the First Semiannual Report were evaluated which utilized simple expressions (extended by Penner[2,3] from work of Raizer[4,5]) for the bound-free and free-free continuum absorptivities for a homogeneous temperature since the homegeneous temperature was found by experimental measurements to be a reasonable approximation for the measured temperature distribution in the arc. The calculated spectral transmission of this model was found to differ by a factor of four from experimental measurements[6].

Comparison of spectral transmissivities calculated using the spectral absorptivities computed according to the methods of Biberman, Norman, and Yankov[7-12] and of Schlüter[13] with experimentally measured spectral transmissivities of Emmett, Schawlow, and Weinberg[6], and subsequent work of Harding[14], discussed in this report, show a good correspondence at wavelengths less 0.65 μ, but wide variations for the longer wavelengths to at least 0.95 μ. Experimental measurements of the profiles of the strong of xenon lines in the infrared indicated that the broadening and the saturation of these lines in the infrared could account for a major portion of the difference in the 8000A° spectral region between the absorptivities calculated considering only free-free and free-bound transitions and the absorptivities measured.

To aid in these model studies, it was felt necessary to measure the spectral absorptivities of xenon as a function of temperature and pressure, and compare the values with theoretical calculations. The saturation of the spectral radiance at wavelengths at which the arc becomes optically thick (at the peaks of the strong lines or of the continuum, in the infrared) has allowed determination of the temperature of the core of the arc channel, (assuming the arc to be homogeneous in temperature). The temperature thus measured has been used to measure wavelength dependence of the Zeta factor (the Biberman and Norman Zeta factor[7]), which related the spectral absorptivity of the continuum to the particle density and temperature in the plasma. Comparison of the measured values with recently published theoretically calculated values of Schlüter[13] indicates a reasonable correspondence both in magnitude and variation with wavelength. The spectral radiances that we have measured at various input energy levels has been compared with theoretical calculations using the simple models for the arc plasma together with spectral absorptivities calculated using Schlüter's theoretically calculated values of the Zeta factor.

The dependence of the electrical conductivity upon temperature (and pressure) was also measured. The experimentally determined electrical conductivity was appreciably lower than the calculations made according to methods of Spitzer and his collaborators[15,16].

To improve the model investigations, techniques for handling radiative transport have been developed for calculating the radiant emittance from an inhomogeneous temperature distribution, which would include the absorption in the vacuum ultraviolet by the cool gas near the walls of the tube. This work is contained in Appendix A. The iterative solutions to the differential equations, describing the energy or power balance within the arc to find the temperature distribution, were found not to have a satisfactory rate of convergence. The techniques being developed under the contract for handling radiative transport within a non-gray inhomogeneous temperature gas are generally applicable to other plasma problems. Currently the radiative transport techniques are being applied using the continuum absorptivities calculated using the theory of Biberman, Norman, and Yankov[7-12], and an approximation to the transport properties which includes electron-electron, electron-ion, and neutral-neutral scattering (due to Fay[17]). This transport properties calculation neglects electron-neutral interactions. The theoretical calculations of the transport properties incorporating the electron-neutral scattering, which for xenon, krypton, and argon involves the Ramsauer minimum[18], which were discussed in the First Semiannual Report[1] complex than we had originally envisioned and will be dealt with in subsequent work.

The inclusion of the lines into the models has proved to be uncertain due to the lack of data on the absolute transition probabilities and the line

broadening parameters for xenon. Since some of the lines of xenon are thought to be L-S coupled (according to Moore[19]), a Bates-Damgaard[20] calculation of the absolute transition probabilities of a number of the L-S coupled lines has been made. These calculated absolute transition probabilities were used to obtain a temperature to estimate the absolute transition probabilities for the other lines of interest in the infrared from the intensities listed in the American Institute of Physics Handbook[21]. This work is described in Appendix B.

The ALGOL computer programs for the Burroughs B-5500 DISK Computer that were developed in this contract are in Appendix C.

The work in Contract Nonr 4647(00) has been directed towards formulating the model for the radiative arc, and then evaluating the model by incorporating gradually more details and features of the arc plasma. Many aspects of this problem, particularly those of radiative transport in a non-gray gas and the transport properties of a partially ionized plasma, involve basic questions in plasma physics. The techniques developed on this contract, both theoretical and experimental, will be useful in solving many other problems involving radiation transport in partially ionized plasmas.

CHAPTER 2

Theoretical Calculations of the Physical Properties of the Arc Plasma

In order to construct models for the plasma, and as the work has progressed, to provide a basis for comparison of our experimental values with theoretical calculations, we needed to calculate the spectral absorptivities and the transport properties, electrical and thermal conductivity, as a function of temperature and pressure. The basis for our choice of the calculations for these properties is discussed fully in the Semiannual Report[1] Briefly, we felt that the Biberman & Norman[7] method for calculating the spectral absorptivity of the continuum was the most satisfactory approach. Particle densities necessary to calculate the spectral absorptivities and the transport properties were calculated as a function of temperature and pressure using standard methods, similar to that of Drellishak[22,23] et al.

In the calculations to be discussed, we have used a simple method to calculate the electrical conductivity, due to Spitzer and his collaborators[15,16]. Work that we have in progress with the aid of Dr. R. S. De Voto of Stanford University seeks to determine experimentally and theoretically the values of conductivity that actually exist in the plasma. These measurements are briefly discussed in Section 4.5.

The portions of the sections that follow will expand on these brief descriptions.

2.1 Theoretical Calculation of the Spectral Absorptivity for Free-Free and Free-Bound Processes

In order to calculate the radiative emission flux from an arc plasma, the spectral absorptivity of the plasma must be determined. If the temperature

and pressure of a gas is known, and LTE can be assumed, one can in principle determine the spectral absorptivity and emission coefficient due to free-free and free-bound transitions. The emission coefficient and spectral absorptivity of the rare gases were determined using the quantum defect calculations of Biberman and Norman[7-12] as originally adapted to this problem by Seaton and Burgess[24].

For a plasma in LTE, Kirchhoff's law holds. The emission coefficient may be written as

$$\epsilon_\upsilon = \kappa'_\upsilon B_\upsilon \tag{2.1}$$

where ϵ_υ - emission coefficient

κ'_υ - spectral absorptivity

B_υ - Planck function.

The effective spectral absorptivity which includes stimulated emission is given by

$$\kappa'_\upsilon = \kappa_\upsilon \left(1-e^{-h\upsilon/kT}\right) \tag{2.2}$$

where κ_υ is the spectral absorptivity. κ_υ is given by

$$\kappa_\upsilon = \sum_i \kappa_\upsilon^i \tag{2.3}$$

where κ_υ is the spectral absorptivity of the atomic or ionic species i. In the Biberman and Norman technique for determining the spectral absorptivity of an atom or ion the energy levels of the system are divided into two classes (Fig. 3 - Reference 12). In the determination of the expression for the spectral absorptivity, the upper levels in the frequency region denoted by υ_g are integrated over. The the low lying widely separated levels, an absorption cross section is calculated for each level. This has been done by Yankov[8] for the xenon atom, for the level series up to 8s. The spectral absorptivity κ_{nl}^i for each series of levels of the species is then obtained by

$$\kappa^{i}_{nl} = \sigma_{nl} N_{nl} \tag{2.4}$$

where σ_{nl} is the absorption cross section for the nl series of levels and N_{nl} is the number density of those levels. Assuming Boltzman statistics and relating this to the ground state we have

$$\kappa^{i}_{nl} = \sigma_{nl} Ng \frac{g_{ne}}{g_g} e^{-h\upsilon_{nl}/kT} \tag{2.5}$$

where N_g is the density of the ground state and g_{nl} and g_g are the statistical weights of the nl series and the ground state respectively. The spectral absorptivity for each of the nl series is then added to the spectral absorptivity due to the integrated lines and the free-free absorption. The spectral absorptivity due to the integrated lines and the free-free spectral absorptivity for species i is given by the following[7]:

$$\kappa^{i}_{A} = A \frac{2Q_{i+1}}{Q_i} T e^{-u_1+u} \frac{Z_i^2}{\upsilon^3} \xi_i(\upsilon) N_i \text{ for } \upsilon \leq \upsilon_g \tag{2.6}$$

$$= A \frac{2Q_{1+1}}{Q_i} T e^{-u_1+u_g} \frac{Z_i^2}{\upsilon^3} \xi_i(\upsilon) N_i \text{ for } \upsilon \geq \upsilon_g \tag{2.7}$$

where

$$A = \frac{16\pi^2 ke^6}{3\sqrt{3}\, ch^4} = .89 \times 10^{24} \text{ cm}^2 \text{ sec}^{-3} {}^{o}K^{-1} \tag{2.8}$$

$u = \frac{h\upsilon}{kT}$

$u_1 = \frac{h\upsilon_1}{kT}$ where υ_1 = threshold frequency for photo ionization from ground state

$u_g = \frac{h\upsilon_g}{kT}$

Z_i = core charge of the residual ion

Q_i = internal partition function of the i^{th} species

$Q_i = \sum_j g_j^i e^{-E_j^i/kT}$ where the sum is over all energy levels of the species and E_j is the energy of the j^{th} level above the ground state.

N_i = number density of the i^{th} species

$\xi_i(\upsilon)$ = a correction factor for species i as calculated for the xenon atom by Biberman, Norman and Ulyanov[11]. (Zeta factor). (Recent work by Schlüter[13] shows quite different values for ξ that agree more closely with our experimentally determined values. See Section 4.4). Then one has for the total absorption coefficient of the species i the expression

$$\kappa_\upsilon^i = \kappa_A^i + \sum_{nl} \kappa_{nl}^i \qquad (2.9)$$

where the sum is over all series of levels considered independently, of course the more levels considered independently the greater the accuracy should be.

In order to calculate κ_A^i, one needs to know, other than the correction factor $\xi_i(\upsilon)$, each species partition function Q_i, each species density N_i and the temperature T. If one can experimentally determine the temperature then, under the assumptions stated earlier, one can calculate reasonable values for Q_i and N_i. This will be discussed now.

2.2 Partition Functions and Electron Densities

As stated earlier we have for the partition function

$$Q_i = \sum_j g_j^i e^{-E_j^i/kT} \qquad (2.10)$$

The sum is over all levels and therefore diverges for a free atom or ion. However, in a plasma, electrons tend to cluster about the ions. Thus when an ion-electron pair is produced a certain amount of energy is released. Ionization potentials are reduced by this amount of ordering energy which is dependant upon

the charge of the particle, the plasma density and the temperature. Thus the partition function summation must be truncated at an energy value of

$$E^i = I_i - \Delta I_i \tag{2.11}$$

where I_i is the isolated ionization potential of species i and ΔI_i is the ionization potential lowering of that species, given by[25]

$$\Delta I_i = 2(Z_i + 1)e^3 (\pi/kT)^{1/2} (N_e + \sum_i Z_i^2 N_i)^{1/2} \tag{2.12}$$

for a Debye-Huckel plasma. For the tables which have been tabulated by Charlotte Moore[19], g_k is given by

$$g_k = 2 J_k + 1. \tag{2.13}$$

For those nl levels which have been approximated for xenon by McChesney and Jones[26]

$$g_k = \sum_n (2 J_n + 1)_k \tag{2.14}$$

where the sum is over all J states for a given nl term.

These partition functions are then used to calculate the electron density for an LTE plasma using the Saha equations[22,27]:

$$\frac{N_{i+1} N_e}{N_i} = \left(\frac{2 mk}{h^2}\right)^{3/2} \frac{2 Q_{i+1}}{Q_i} T^{3/2} e^{-(I_i - \Delta I_i)/kT} \tag{2.15}$$

If n is the highest degree of ionization of the monatomic gas, there will be n + 2 species of particles present. The set of Saha equations then gives n equations in n + 2 unknowns. The other two equations necessary to solve for all the particle densities is given by

$$N_e = \sum_{i=1}^{n} i N_i \text{ and} \tag{2.16}$$

$$N_t = \sum_{i=0}^{n} (i+1) N_i \tag{2.17}$$

N_t is the total particle density as is given by the equation of state. The equation of state used is the ideal gas law

$$p = N_t kT \tag{2.18}$$

The corrections to this for a Debye-Huckel interaction have been discussed by Griem[25]. Therefore if one is given the temperature and pressure one can solve for the electron density and the various atom and ion densities once the partition function series sum is known. However since the truncation of this sum depends on the particle densities an iteration procedure must be employed. This has been done by Drellishak, et al.[22,23,28] for argon*. A computer program has been written and the partition functions, electron, atom, and ion densities and the ionization potential lowering for xenon were calculated. The program employs certain improvements over Drellishak's calculation. The cutoff of the partition function series and the ionization potential lowering are obtained as we described earlier rather than by a principal quantum number cutoff method assuming Bohr type orbits as employed by Drellishak. At very high electron densities and high temperatures the principal quantum number cutoff will introduce errors in the partition functions.

*NOTE: An error exists in Equation (12) of reference 24. This equation should read

$$n_e^{N+1} + \sum_{i=1}^{N} \left\{ \left[n_e^{N+1-i}\,(i+1) - n_t n_e^{N-i}\,(i) \right] \prod_{r=1}^{i} K_r \right\} = 0 \tag{2.19}$$

Although this formula is incorrectly stated in references 22, 23, and 28 the correct one is used in the computer calculations so the results of those references are not affected.

2.3 The Absorption Coefficient of the Lines

The contribution of the bound-bound state transitions, the spectral lines, to the absorption coefficient is more difficult to calculate due to the requirements for absolute values of the transition probabilities for all of the lines that may be involved including those in the infrared or ultraviolet. The relative effect of the lines upon the radiant emittance varies with temperature and pressure tending to be greater (but not always) for the lower temperatures and high pressures--conditions similar to those in flash tubes. Our calculations of the transition probabilities are discussed in Appendix B. Work is in progress towards extending the Stark broadening theory of Griem[29] and other to the lines of xenon in the infrared.

2.4 The Electrical and Thermal Conductivities for a Fully Ionized Plasma

The electrical conductivity is taken to be that of a fully ionized plasma using the theory of Spitzer and his coworkers[15,16]. As the power input to the arc which is given by σE^2, is probably only appreciable in the fully ionized portion of the arc discharge. The Spitzer theory for a fully ionized plasma considers only electron-electron and electron-ion scattering, which are the dominant processes for material that is more than about .1% ionized[30]. (We are using "fully ionized" in the sense that only those processes need be considered).

There is one major difficulty in applying the Spitzer theory to the plasmas in high energy flash tubes. This difficulty arises from the high electron density but relatively low temperature which exists in the arc discharges, for which the theory is not considered valid as the coulomb logarithm term (denoted as $\ln\Lambda$) goes to zero and the errors are of the order of $1/\ln\Lambda$, due to the

neglect of close encounters in the Fokker-Planck equation used in the derivation. Following Spitzer[31], the electrical conductivity σ is given by this equation:

$$\sigma = \frac{T^{3/2}\ \delta T_E}{3.80 \times 10^3\ Z_i \ln \Lambda_i} \quad \text{in (ohm cm)}^{-1} \tag{2.20}$$

and the thermal conductivity K by

$$K = \frac{1.95 \times 10^{-11}\ T^{5/2}\ \delta T_K}{Z_i \ln \Lambda_i} \tag{2.21}$$

δT_E and δT_K are correction factors dependent upon Z_i, which is the ionic charge (note: Z = 1 for a singly ionized gas). From Cohen et al.[16], Λ_i is the ratio of the Debye shielding parameter h to the impact parameter b_o (b_o is the distance for a 90° deflection of an electron by a positive ion).

$$\Lambda_i = \frac{h}{b_o} = \frac{3}{e^3 Z_i} \left(\frac{k^3 T^3}{4 \pi N_e (1 + Z_i)} \right)^{1/2} \tag{2.22}$$

When $\Lambda_i < 12\ \pi$, Cohen et al.[16] and others[17,32,33] suggest using for z = 1

$$\Lambda = \frac{3kT}{e^2 N_e^{1/2}} \text{ rather than the above value.} \tag{2.23}$$

This is equivalent to substituting the interionic distance ($N_e^{-1/3}$) for the Debye shielding parameter h.

In common units, for Z = 1, ln Λ from equation 3.10 is given as

$$\ln \Lambda = 9.43 + 1/2 \ln \frac{T^3}{N_e} \tag{2.24}$$

for T in °K and N_e in particles/cm^3. The correction factors δT_E and δT_K are given by Spitzer and Härm in terms of Z (the integral values of $\bar{Z}$, a value may be obtained by interpolation between the values in the following table[15]:

	Z = 1	Z = 2	Z = 4	Z = 16	Z = ∞
δT_E	.582	.683	.785	.923	1
δT_K	.225	.356	.513	.791	1

2.5 The Thermal Conductivity in the Boundary Layer (Used in Appendix A)

The thermal conductivity in (either the simple or complete case) is a source of great concern in this investigation. The major influence of the thermal conductivity heat transfer in the pulsed arc discharges lies in the boundary region between the arc discharge channel (where the σE^2 terms are dominant) and the relatively cool wall containing the arc. We say relatively cool as the temperature of the wall is assumed to be on the order of the boiling point of quartz ($2800^{\circ}K$) or probably much less. In this boundary region, there can be extremely high thermal, electron density, and neutral particle density gradients (the latter being of opposite sign from the first two). Simple approaches to thermal conduction, such as that shown graphically in Fay[17] and in Reilly[34] for argon and xenon use Spitzer conductivity down to temperatures at which the neutral particle thermal conductivity becomes dominant[35]. This may be correct, or it may be off by an order of magnitude at one temperature or another. The neglect of the electron-neutral conductivity in gases with a Ramsauer minimum, such as argon, krypton and xenon have, may lead to large errors. There have not, as yet, been any definitive experiments, that we could find in the literature, on the measurement of the thermal conductivities of partially ionized plasmas--much less those in a high temperature and electron density gradients at the particle densities we are concerned within the flash tubes.

The thermal conductivity given in the previous section is that derived from Spitzer's theory and is probably a reasonable representation of the thermal conductivity in the arc channel proper. For the boundary layer region, for the simple representation, Fay's approach[17] was used calculating the values corresponding to the pressure in the flash tube.

CHAPTER 3

The Model Studies

3.1 Introduction to the Model Studies

An arc discharge may have many different temperature distributions. If a major portion of the power put into the arc is carried away by thermal conduction, then thermal conduction power transport within the arc and external to the arc causes the variation of temperature with arc radius. This occurs when the radiative flux from the arc is small compared to the thermally conducted power; it usually occurs in low pressure arcs. If the plasma in the arc is optically very thick over a major portion of the spectral region of emission, the radiative power transport within the arc will lead to a temperature gradient similar to that of the thermal conduction. As we had mentioned in the previous report, the optically thick radiative flux is directly analogous in its effects to thermal conduction.

If the radiation emitted balances a major fraction of the input power (i.e.: thermal conduction losses are small), and the arc is optically thin over a major portion of the spectral region of interest (this case appears to be that for the pulsed flash lamp at normal energy loadings) the temperature within the arc will not change appreciably with radius except at the very edge. The temperature distribution can be taken to be constant in the arc channel.

Appendix A shows our progress towards solving the radiative transport problem for models having a non-homogeneous distribution which is necessary for solving the radiant energy balance equation discussed in the Semiannual Report[1] to obtain the temperature distribution.

The two new models that will be discussed in the following sections assume constant temperature in the arc channel; that is, the arc channel is homogeneous in temperature. Experimental measurements of the radial distribution of the spectral transmissivity[6] and of the spectral radiance is the ultraviolet (to be discussed later) support this assumption.

The arcs to be considered will be steady state arcs in which the electrical power input is balanced by the power radiated from the arc and that carried away by thermal conduction. A more complete calculation for pulsed or AC arcs would require the inclusion of the power required to ionize the gas. The calculations to be presented will also neglect thermal conduction to the arc boundaries such as the walls and the electrodes.

3.2 Analysis

The power is generated in the arc by resistive heating; this power is balanced by the sum of the radiated power and the power carried away by thermal processes, such as conduction and convection. In equation form, this balance is[36]

$$\text{div}\ (\bar{F} + \bar{F}_{HC}) = \sigma E^2 \qquad (3.1)$$

where E is the electric field in volts/cm, σ is the electrical conductivity in ohm^{-1}, $\bar{F}$ is the radiant emittance vector in watts/cm^2, and $\bar{F}_{HC}$ is the vector representing the power carried away by the thermal processes. $\bar{F}_{HC}$ and the convection heat transfer vector denoted by $\bar{F}_C$:

$$\bar{F}_{HC} = \bar{F}_H + \bar{F}_C \qquad (3.2)$$

The convection term is usually small and will be considered negligible in this calculation. The thermal conduction term $\bar{F}_H$ is usually expressed in terms of the thermal conductivity, K, by

$$\bar{F}_H = -K \text{ grad } T \tag{3.3}$$

where T is the temperature and grad T, the temperature gradient at the point at which F is being measured. The units of K, the thermal conductivity, are watts $cm^{-2}\ {}^{o}K^{-1}$ cm.

Equation 3.1 can be integrated over the volume surrounding the arc.

$$\iiint_V \text{div } (\bar{F} + \bar{F}_{HC})dV = \iiint_V \sigma E^2 \, dV \tag{3.4}$$

The integral over the arc volume can be transformed by the Gauss Theorem to an integral of the normal component over the surface are A

$$\iint_A (\bar{F} + \bar{F}_H)_{\substack{\text{normal} \\ \text{component}}} dA = \iint_A \bar{F} \ \bar{n}dA + \iint_A \bar{F}_H \ \bar{n}dA = \iiint_V \sigma E^2 \, dV \tag{3.5}$$

Let us now confine our discussion to arcs of infinite length. For a volume of unit length, the power flow through the end surfaces balance so we need to consider only the power flow through the boundary surfaces. The coordinate system for the models being considered is so chosen that the x-direction is normal to the surface, and the x-component of $\bar{F}$ and $\bar{F}_H$ is then the normal component which is to be integrated over the surface area.

The power radiated by the arc is given by $\bar{F}$, the radiant emittance. $\bar{F}$ is the integral over all frequencies (i.e., energy units) or all wavelengths of the spectral radiant emittance, $\bar{F}_\nu$ or $\bar{F}_\lambda$, in frequency or wavelength units, respectively.

$$\bar{F} = \int_c^\infty \bar{F}_\nu \, d\nu = \int_o^\infty \bar{F}_\lambda \, d_\lambda \tag{3.6}$$

$\bar{F}$ may be expressed per cm or micron of wavelength; $\bar{F}_\nu$ can be in cm^{-1}, sec^{-1} or energy units.

In converting between the units, remember that

$$\lambda = \frac{1}{n} = \frac{c}{\nu} \text{ and } \Delta\lambda = -\frac{1}{n^2} \; ; \Delta n = -\frac{c}{\nu^2} \, \Delta\nu \tag{3.7}$$

We will use cm^{-1} units in the calculation, but refer to them as frequency units.

Let us now consider the x component of the spectral radiant emittance $E_{\nu_x}(P)$. $E_{\nu_x}(P)$ is the total power per unit frequency interval flowing across a unit area perpendicular to the x-direction. It is given by the integral over all angles of the component of the spectral radiance $I(P,\bar{S})$ in the x-direction.

$$E_{\nu_x}(P) = \int_\omega I_\nu (P,\bar{S}) \cos(\bar{S},x) \, d\omega \tag{3.8}$$

Figure 1 shows this relationship. The spectral radiance, I_ν, is the basic unit in radiative power transport. For a given direction $\bar{S}$, $I_\nu(P,\bar{S})$ is the power per unit frequency (or wavelengths), per solid angle per unit area perpendicular to the direction $\bar{S}$ at a point P. I_ν has the units watts cm^{-2} cm steradian^{-1} for frequency in cm^{-1} units. (I_λ has the units watts cm^{-2} cm^{-1} steradian^{-1} for wavelengths in cm). I_ν or I_λ is also called the specific intensity of radiation. It is the radiametric unit corresponding to luminance (or brightness) in photometric units.

The spectral radiance is related to the properties of the medium through the equation of transfer which, for a medium in local thermal equilibrium [39] [40] (LTE) can be written as

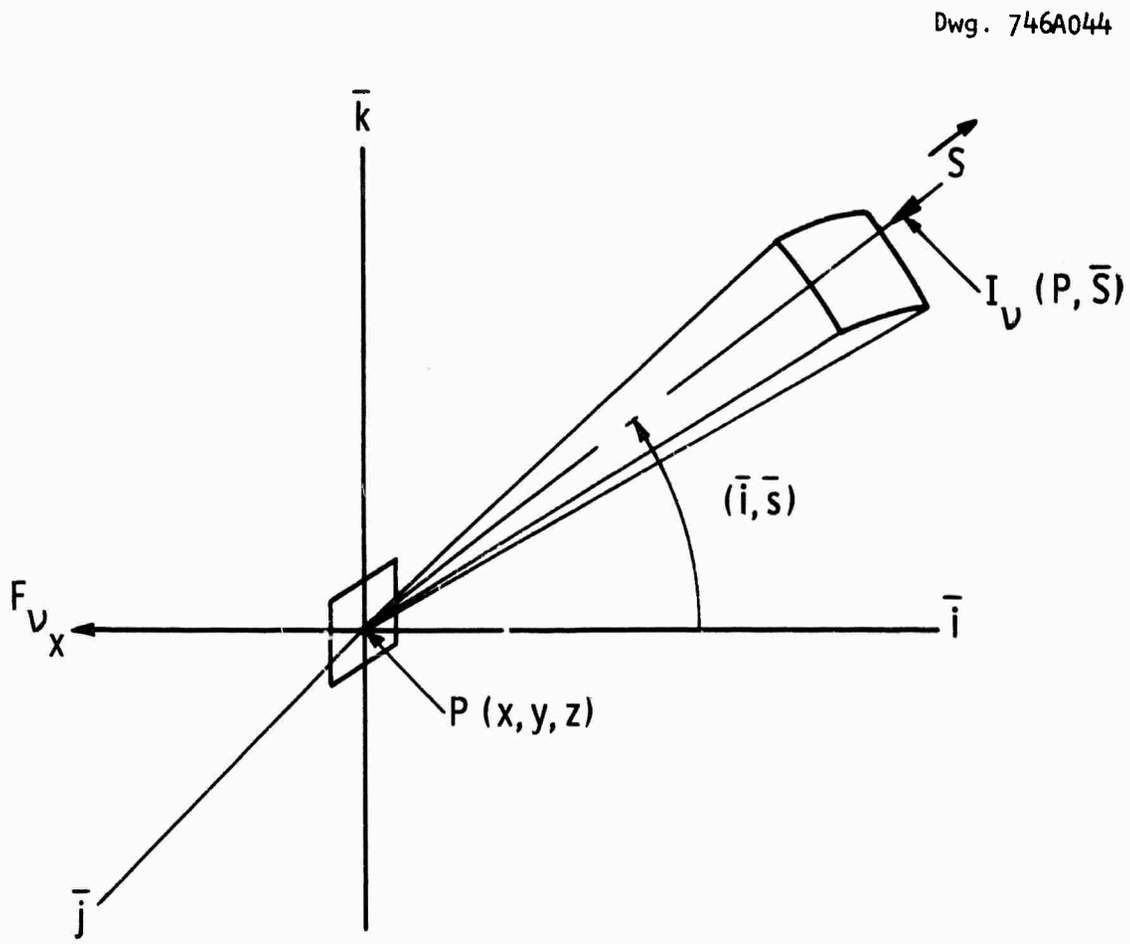

Fig. 1—The geometry of radiative transfer

$$\frac{dI_\nu(P,\bar{S})}{dS} = \kappa'_\nu [B_\nu(T) - I_\nu(P,\bar{S})] \qquad (3.9)$$

in which κ'_ν, is the spectral absorption coefficient including stimulated emission and $B_\nu(T)$ the Planck function for a temperature, T. κ'_ν is related to the more usual spectral absorption coefficient by the equation

$$\kappa'_\nu = \kappa_\nu (1 - e^{-h\nu/RT}). \qquad (3.10)$$

κ_ν, the spectral absorption, is a function of the arc medium at that temperature and pressure. It may arise from discrete transitions (lines), or from transition between bound-free or free-free states (continuum).

Following Lutz,[41] using standard techniques for solving a first order differential equation,[42] the solution can be found for equation 3.9. We assume that no radiance is incident upon the system and the temperature is homogeneous; thus, there is no variation of κ_ν with $\bar{S}$.

$$I_\nu = B_\nu(T) \quad [1 - e^{-\kappa'_\nu \quad S}] \qquad (3.11)$$

We will apply this to a plane parallel slab and a cylinder of homogeneous temperature.

3.3 Plane Parallel Slab of Homogeneous Temperature

The geometry of the plane parallel slab is shown in Figure 2. As $S = x \sec\theta$, equation 3.11 becomes

$$I_\nu = B_\nu(T) \quad [1 - e^{-\kappa'_\nu \; x \sec\theta}] \qquad (3.12)$$

We want the radiant emittance at P = P (0,0,0) in the x-direction (actually negative x). So using 3.12 in equation 3.8 yields

$$F_x = \int_{\phi=0}^{2\pi} \int_{\theta=0}^{\pi/2} B_\nu(T) \; [1 - e^{-\tau_\nu \sec\theta}] \quad \cos\theta \sin\theta d\theta d\phi \qquad (3.13)$$

where $\tau_\nu = \kappa'_\nu x$

Dwg. 746A045

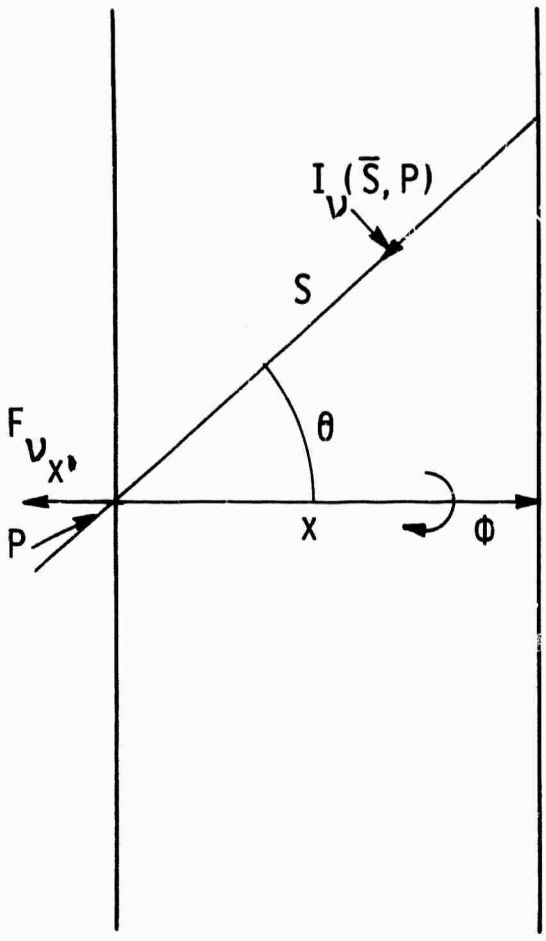

Fig. 2—A plane-parallel slab of homogeneous temperature

Integrating over ϕ yields

$$F_{\nu_x} = 2\pi B_\nu(T) \left\{ 1/2 - \int_0^{\pi/2} e^{-\tau_\nu \sec\theta} \cos\theta \sin\theta d\theta \right\} \qquad (3.14)$$

Let $u = \sec\theta$,

The integral reduces to the exponential integral of the third order[41, 43]

$$\int_0^{\pi/2} e^{-\tau \sec\theta} \cos\theta \sin\theta d\theta = \int_1^\infty \frac{e^{-\tau u}}{u^3} du = E_3(\tau) \qquad (3.15)$$

The exponential integral of third order[43] may be integrated twice by parts to the first exponential integral denoted by $E_1(\tau)$

$$E_3(\tau) = \frac{e^{-\tau}(-\tau) + \tau^2 E_1(\tau)}{2} \qquad (3.16)$$

where $E_1(\tau) = \int_1^\infty \frac{e^{-\tau u}}{u} du$, the first exponential integral. (3.17)

The properties of the first exponential integral are discussed and the values tabulated in a number of places (for example references (43) and (44)). For calculations on a computer, there are two useful expansions:[44]

For $0 \leq \tau \leq 1$

$$E_1(\tau) = \ln\tau + a_o + a_1\tau + a_2\tau^2 + a_3\tau^3 + a_4\tau^4 + a_5\tau^5 + \varepsilon(\tau) \qquad (3.18)$$

a_o	-.57721566	a_3	.05519968
a_1	.99999193	a_4	.00976004
a_2	.24991055	a_5	.00107857

where $|\varepsilon(\tau)| < 5 \times 10^{-5}$

For $1 \leq \tau \leq \infty$

$$E_1(\tau) = \frac{e^{-\tau}}{\tau} \left(\frac{\tau^2 + a_1\tau + a_2}{\tau^2 + b_1\tau + b_2} \right) + \varepsilon(\tau) \qquad (3.19)$$

a_1	= 2.33473	b_1	= 3.330657
a_2	= 0.250621	b_2	= 1.681534

where $|\epsilon(\tau)| < 5 \times 10^{-5}$

The spectral radiant emittance in the x-direction is given by

$$F_{\nu_x} = \pi B_\nu(T) \left\{ 1 + (\tau_\nu - 1)e^{-\tau_\nu} - \tau_\nu^2 E_1(\tau_\nu) \right\} \tag{3.20}$$

The radiant emittance F_x may be considered as the sum of the integrals over the optically thick and optically thin spectral regions

$$F_x = \int_0^\infty F_{\nu x} d\nu \tag{3.21}$$

$$= \sum_{TK} \int_{\nu_{TK}} F_{\nu x}(TK)\, d\nu \qquad F_{\nu x}(TN)\, d\nu + \sum_{TK} \int_{\Delta\nu_{TN}} F_{\nu x}(TN) d\nu \tag{3.22}$$

Each of the separate integrals over the various thick and thin spectral regions may be calculated to allow an estimate of the energy transfer within the plasma, which of course, is neglected in this model of homogeneous temperature.

The electrical field E was calculated to be that necessary to create twice the radiant emittance in the x direction to account for both sides radiating. The radiant emittance in the y and z directions were balanced by that from adjacent sections in the infinite extent plane parallel slab.

This balance of radiant emittance and electrical power is expressed as

$$\sigma E^2 d = 2 F_x \tag{3.23}$$

where d is the plasma thickness

$$E = \sqrt{\frac{2F_x}{\sigma d}} \tag{3.24}$$

The current density J in the plane parallel slab was calculated from

$$J = \sigma E \tag{3.25}$$

The pressure in the model was

$$p = (N_o + N_e)kT \tag{3.26}$$

where N_e is the electron density and N_o is the heavy particle density.

3.4 Cylinder of Homogeneous Temperature

The cylinder of homogeneous temperature represents another simple model for describing an arc discharge. The cylinder problem is more difficult to handle than the plane parallel slab due to the boundaries existing in two coordinates rather than only one, thereby making the integral over F more complex.

Figure 3 shows the geometry we are considering in a fashion similar to the parallel slab model; we can write the spectral radiance $I_\nu(\theta, \phi)$ at the point P (0,0,0) on the edge of the cylinder as:

$$I_\nu(\theta, \phi) = B_\nu \left[1 - e^{-\kappa_\nu S(\theta, \phi)}\right] \tag{3.27}$$

where $S(\theta, \phi)$ is the distance through which the radiation travels in the cylinder of homogeneous temperature, and diameter d. Referring to Figure 4, S is expressed as

$$S(\theta, \phi) = \frac{d}{\cos\theta + \tan\theta \sin\theta \sin^2\phi} \tag{3.28}$$

and the spectral radiance $I_\nu(\theta, \phi)$ is

$$I_\nu = B_\nu \left(1 - \exp \frac{-\kappa_\nu d}{\cos\theta \tan\theta \sin\theta \sin^2\phi}\right) \tag{3.29}$$

The spectral radiant emittance in the radial direction, F_{ν_r}, is given by

$$F_{\nu_r} = \int_0^{2\pi} \int_0^{\pi/2} I_\nu \cos\theta \sin\theta \, d\theta \, d\phi \tag{3.30}$$

Substituting the value of I_ν in this equation, the spectral radiant emittance is as follows:

Dwg. 746A049

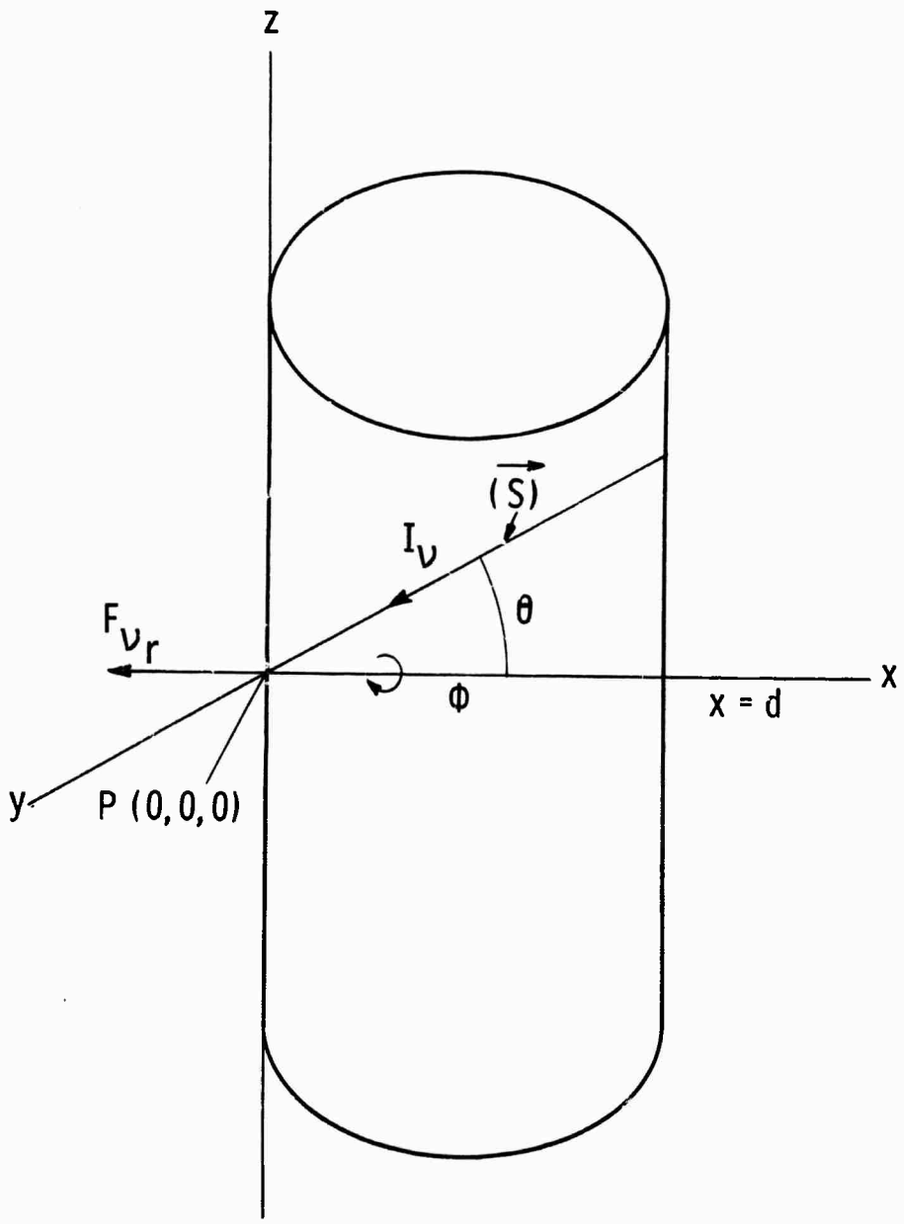

Fig. 3 —An infinite cylinder showing coordinate system

Dwg. 746A033

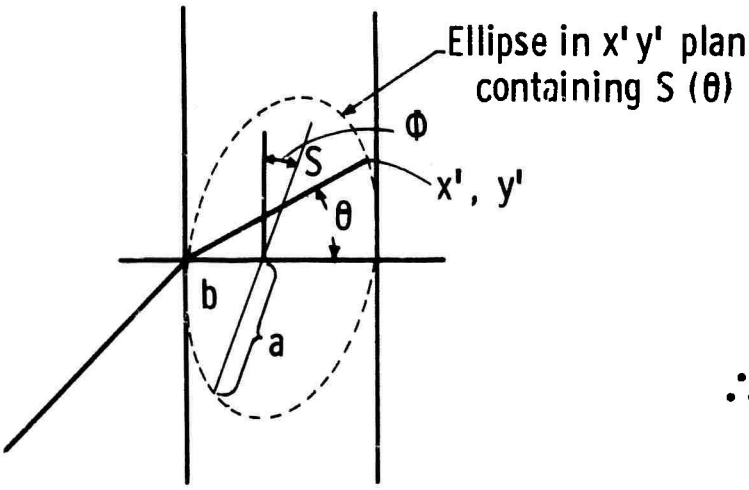

Equation of ellipse is:

$$x'^2 - x'd + y'^2 \sin^2\Phi = 0$$

where $0 \leq \Phi \leq 2\pi$, $0 \leq \theta \leq \pi/2$

and $x' = S \cos\theta$; $y' = S \sin\theta$

$$\therefore S = d/\cos\theta + \tan\theta \sin\theta \sin^2\Phi$$

Fig. 4—Radiation traveling through a cylinder of homogeneous absorption

$$F_{\nu_r} = B_\nu(T) \int_0^{2\pi} \int_0^{\pi/2} \left(1-\exp \frac{\kappa' d}{\cos\theta + \tan\theta \sin\theta \sin^2\phi}\right) \cos\theta \sin\theta d\theta d\phi \quad (3.31)$$

The first term within the integral may be integrated to yield

$$F_{\nu_r} = B_\nu(T) \quad \pi - 4 \int_0^{\pi/2} \int_0^{\pi/2} \left(\exp - \frac{\kappa' d}{\cos\theta + \tan\theta \sin\theta \sin^2\phi}\right) \cos\theta \sin\theta d\theta d\phi \quad (3.32)$$

Letting $\mu = \cos\theta$ allows this equation to be rewritten as:

$$F_{\nu_r} = B_r(\tau) \quad \pi - 4 \int_0^{\pi/2} \int_0^{1} \exp \frac{-\kappa' \nu d\mu}{\mu^2 + (1-\mu^2) \sin^2\phi} \mu d\mu d\phi \quad (3.33)$$

This integral is well-behaved so it can be readily integrated numerically. F_{ν_a} when integrated over all ν yields the radiant emittance in the radial direction.

$$F_r = \int_0^{\infty} F_{\nu_r} d\nu \quad (3.34)$$

Neglecting thermal conduction heat transfer, the radiant emittance per unit length integrated over the radiating surface can be equated to the power input to the arc plasma per unit length.

$$\int_S F_r dA = \int_V \sigma E^2 dV \quad (3.35)$$

As F_r is independent of direction and σE^2 is invariant over the volume

$$F_r = \sigma E^2 \frac{d}{4} \quad (3.36)$$

Solving for E, the electric field intensity for the cylinder of homogeneous temperature is

$$E = \sqrt{\frac{4F_r}{\sigma d}} \quad (3.37)$$

3.5 Comparison of Models with Experiment - Spectral Radiance

To evaluate these models, we needed theoretical expression for the spectral absorptivity and the electrical and thermal conductives as a function of temperature and pressure. The spectral absorptivity calculation was discussed in Chapter 2 together with the particle density calculation. Calculation of the electrical conductivity using Spitzer was in Section 2.4.

The results calculated using this cylindrical model together with the experimentally measured valves are shown in Tables I, II and III for three temperatures and pressures.

The three temperatures and pressures 10,000 K, 7.6 ATM; 11,500 K, 11ATM correspond to the three temperatures (and the pressures resulting from the homogeneous temperature assumption) measured at the peak of the arc discharge cycle. These measurements are discussed in Section 4.3 Figure 5, 6, and 7 (and Figures 19, 20, and 21 on a linear scale) show the wavelength dependence of the spectral radiances on Tables I, II, and III and the measured radiances. These results are discussed further in Section 4.4.

3.6 Comparison of Models with Experiment: Transmissivity as a Function of Current Density

In order to obtain an estimate of the validity of these homogeneous temperature models, a number of comparisons were made with experimental measurements, both by other workers and in our own laboratory. These measurements included those of spectral transmissivity, and of the radial distribution of the spectral radiance. These measurements

LN LAMBDA = 5.493E+00
ELECTRICAL CONDUCTIVITY SIGMA= 5.576E+01 INVERSE OHMS INVERSE CM
THERMAL CONDUCTIVITY K= 1.512E-02 WATTS/CM DEGREES

FROM NU=24.794 TO NU= 12.337 THE VALUE OF THE INTEGRAL OF ENU IS 1.869E+01 WATTS/CM2 THICK
FROM NU=11.807 TO NU= 0.248 THE VALUE OF THE INTEGRAL OF ENU IS 3.253E+03 WATTS/CM2 THIN
FROM NU= 0.124 TO NU= 0.012 THE VALUE OF THE INTEGRAL OF ENU IS 1.394E+01 WATTS/CM2 THICK

RADIANT EMITTANCE E= 3.285E+03 WATTS/CM2
ELECTRIC FIELD E= 1.362E+01 VOLTS/CM
CURRENT DENSITY J= 7.596E+02 AMP/CM2

THETA=0.86 EV NTOTAL=5.615E+18 NDENSITY=5.299E+18 PARTICLES/CM3
T= 10000.0 DEGREES K. P= 7.65 ATM

HNU EV	WAVELENGTH MICRONS	KAPPA-PRIME 1/CM	TAU	(=TAU) 1-E	BNU WATTS/CM	STER	ENU WATTS/CM
24.794	5.000E-02	5.213E+01	6.621E+01	1.000E+00	3.044E-09	3.044E-09	7.712E-05
22.540	5.500E-02	1.224E+02	1.554E+02	1.000E+00	3.128E-08	3.128E-08	7.926E-04
20.662	6.000E-02	1.809E+02	2.297E+02	1.000E+00	2.131E-07	2.131E-07	5.400E-03
19.072	6.500E-02	2.304E+02	2.926E+02	1.000E+00	1.060E-06	1.060E-06	2.686E-02
17.710	7.000E-02	2.729E+02	3.465E+02	1.000E+00	4.125E-06	4.125E-06	1.045E-01
16.529	7.500E-02	3.096E+02	3.933E+02	1.000E+00	1.320E-05	1.320E-05	3.345E-01
15.496	8.000E-02	3.418E+02	4.341E+02	1.000E+00	3.607E-05	3.607E-05	9.140E-01
13.774	9.000E-02	3.955E+02	5.023E+02	1.000E+00	1.868E-04	1.868E-04	4.734E+00
12.397	1.000E-01	4.384E+02	5.568E+02	1.000E+00	6.736E-04	6.736E-04	1.707E+01
11.807	1.050E-01	3.393E-03	4.309E-03	4.299E-03	1.154E-03	4.963E-06	1.251E-01
8.265	1.500E-01	6.954E-03	8.832E-03	8.793E-03	2.415E-02	2.123E-04	5.348E+00
6.199	2.000E-01	1.249E-02	1.586E-02	1.572E-02	1.121E-01	1.762E-03	4.437E+01
4.959	2.500E-01	1.974E-02	2.508E-02	2.476E-02	2.424E-01	6.007E-03	1.511E+02
4.132	3.000E-01	2.881E-02	3.659E-02	3.593E-02	3.682E-01	1.323E-02	3.325E+02
3.542	3.500E-01	3.958E-02	5.027E-02	4.902E-02	4.638E-01	2.274E-02	5.710E+02
3.099	4.000E-01	5.324E-02	6.764E-02	6.540E-02	5.252E-01	3.435E-02	8.618E+02
2.755	4.500E-01	6.739E-02	8.558E-02	8.202E-02	5.574E-01	4.576E-02	1.146E+03
2.479	5.000E-01	8.458E-02	1.074E-01	1.019E-01	5.490E-01	5.796E-02	1.450E+03
2.254	5.500E-01	6.371E-02	8.092E-02	7.773E-02	5.454E-01	4.395E-02	1.102E+03
2.066	6.000E-01	7.586E-02	9.634E-02	9.185E-02	5.529E-01	5.072E-02	1.270E+03
1.907	6.500E-01	3.168E-02	4.023E-02	3.943E-02	5.331E-01	2.102E-02	5.283E+02
1.771	7.000E-01	2.483E-02	3.153E-02	3.104E-02	5.104E-01	1.585E-02	3.986E+02
1.653	7.500E-01	2.902E-02	3.684E-02	3.619E-02	4.844E-01	1.761E-02	4.427E+02
1.550	8.000E-01	3.357E-02	4.263E-02	4.173E-02	4.622E-01	1.929E-02	4.847E+02
1.458	8.500E-01	3.845E-02	4.883E-02	4.766E-02	4.380E-01	2.088E-02	5.244E+02
1.377	9.000E-01	4.616E-02	5.842E-02	5.693E-02	4.146E-01	2.360E-02	5.925E+02
1.305	9.500E-01	5.210E-02	6.617E-02	6.403E-02	3.922E-01	2.511E-02	6.300E+02
1.240	1.000E+00	5.842E-02	7.420E-02	7.151E-02	3.709E-01	2.653E-02	6.652E+02
1.181	1.050E+00	6.512E-02	8.270E-02	7.937E-02	3.509E-01	2.785E-02	6.980E+02
1.127	1.100E+00	6.436E-02	8.174E-02	7.848E-02	3.321E-01	2.606E-02	6.532E+02
1.078	1.150E+00	5.410E-02	7.124E-02	6.876E-02	3.144E-01	2.162E-02	5.423E+02
1.033	1.200E+00	6.237E-02	7.921E-02	7.615E-02	2.979E-01	2.269E-02	5.687E+02
0.992	1.250E+00	8.726E-02	1.104E-01	1.049E-01	2.825E-01	2.964E-02	7.414E+02
0.954	1.300E+00	9.611E-02	1.221E-01	1.149E-01	2.682E-01	3.081E-02	7.702E+02
0.918	1.350E+00	1.054E-01	1.339E-01	1.253E-01	2.547E-01	3.192E-02	7.977E+02
0.886	1.400E+00	1.152E-01	1.463E-01	1.361E-01	2.422E-01	3.295E-02	8.225E+02
0.855	1.450E+00	1.254E-01	1.592E-01	1.472E-01	2.305E-01	3.393E-02	8.482E+02
0.826	1.500E+00	1.360E-01	1.728E-01	1.587E-01	2.194E-01	3.484E-02	8.682E+02
0.800	1.550E+00	1.415E-01	1.796E-01	1.644E-01	2.093E-01	3.442E-02	8.575E+02
0.775	1.600E+00	1.537E-01	1.951E-01	1.773E-01	1.998E-01	3.541E-02	8.813E+02
0.751	1.650E+00	1.663E-01	2.113E-01	1.904E-01	1.908E-01	3.633E-02	9.034E+02
0.729	1.700E+00	1.795E-01	2.280E-01	2.039E-01	1.824E-01	3.718E-02	9.234E+02
0.708	1.750E+00	1.931E-01	2.452E-01	2.175E-01	1.745E-01	3.795E-02	9.418E+02
0.689	1.800E+00	2.071E-01	2.631E-01	2.313E-01	1.671E-01	3.865E-02	9.582E+02
0.670	1.850E+00	2.216E-01	2.814E-01	2.453E-01	1.601E-01	3.927E-02	9.727E+02
0.652	1.900E+00	2.364E-01	3.002E-01	2.593E-01	1.534E-01	3.982E-02	9.854E+02
0.636	1.950E+00	2.516E-01	3.195E-01	2.735E-01	1.474E-01	4.030E-02	9.965E+02
0.620	2.000E+00	2.671E-01	3.392E-01	2.877E-01	1.416E-01	4.072E-02	1.006E+03
0.248	5.000E+00	1.754E+00	2.228E+00	8.922E-01	2.862E-02	2.553E-02	6.125E+02
0.124	1.000E+01	6.491E+00	8.243E+00	9.997E-01	7.707E-03	7.705E-03	1.931E+02
0.062	2.000E+01	2.436E+01	3.093E+01	1.000E+00	1.999E-03	1.999E-03	5.061E+01
0.025	5.000E+01	1.451E+02	1.843E+02	1.000E+00	3.268E-04	3.268E-04	8.282E+00
0.012	1.000E+02	5.701E+02	7.240E+02	1.000E+00	8.230E-05	8.230E-05	2.085E+00

Table I

LN LAMBDA = 4.910E+00
ELECTRICAL CONDUCTIVITY SIGMA= 7.695E+01 INVERSE OHMS INVERSE CM
THERMAL CONDUCTIVITY K= 2.542E-02 WATTS/CM DEGREES

FROM NU=24.794 TO NU= 12.397 THE VALUE OF THE INTEGRAL OF ENU IS 1.414E+02 WATTS/CM2 THICK
FROM NU=11.807 TO NU= 0.620 THE VALUE OF THE INTEGRAL OF ENU IS 1.779E+00 WATTS/CM2 THIN
FROM NU= 0.248 TO NU= 0.012 THE VALUE OF THE INTEGRAL OF ENU IS 1.213E+02 WATTS/CM2 THICK

RADIANT EMITTANCE F= 1.805E+04 WATTS/CM2
ELECTRIC FIELD E= 2.71E+01 VOLTS/CM
CURRENT DENSITY J= 2.092E+03 AMP/CM2

THETA=0.99 EV NTOTAL=4.127E+18 NDENSITY=5.264E+19 PARTICLES/CM3
T= 11500.0 DEGREES K. P= 9.61 ATM

HNU EV	WAVELENGTH MICRONS	KAPPA-PRIME 1/CM	TAU	(-TAU) 1-E	BNU WATTS/CM	ING STER	ENU WATTS/CM
24.794	5.000E-02	4.574E+01	5.509E+01	1.000E+00	1.299E-07	1.299E-07	3.289E-03
22.540	5.500E-02	1.073E+02	1.363E+02	1.000E+00	9.485E-07	9.485E-07	2.403E-02
20.662	6.000E-02	1.587E+02	2.015E+02	1.000E+00	4.862E-06	4.862E-06	1.232E-01
19.077	6.500E-02	2.021E+02	2.567E+02	1.000E+00	1.902E-05	1.902E-05	4.819E-01
17.710	7.000E-02	2.394E+02	3.040E+02	1.000E+00	6.020E-05	6.020E-05	1.526E+00
16.529	7.500E-02	2.716E+02	3.450E+02	1.000E+00	1.611E-04	1.611E-04	4.083E+00
15.496	8.000E-02	2.999E+02	3.809E+02	1.000E+00	3.766E-04	3.766E-04	9.542E+00
13.774	9.000E-02	3.469E+02	4.404E+02	1.000E+00	1.503E-03	1.503E-03	3.809E+01
12.397	1.000E-01	3.843E+02	4.881E+02	1.000E+00	4.399E-03	4.399E-03	1.115E+02
11.807	1.050E-01	1.363E-02	1.731E-02	1.716E-02	4.895E-03	1.183E-04	2.978E+00
8.265	1.500E-01	2.798E-02	3.553E-02	3.491E-02	8.438E-02	2.945E-03	7.406E+01
6.199	2.000E-01	5.034E-02	6.393E-02	6.193E-02	2.869E-01	1.777E-02	4.458E+02
4.959	2.500E-01	7.997E-02	1.016E-01	9.657E-02	5.154E-01	4.980E-02	1.246E+03
4.132	3.000E-01	1.171E-01	1.487E-01	1.382E-01	8.932E-01	9.578E-02	2.390E+03
3.542	3.500E-01	1.612E-01	2.047E-01	1.851E-01	1.302E-01	1.485E-01	3.694E+03
3.099	4.000E-01	2.191E-01	2.782E-01	2.429E-01	1.541E-01	2.074E-01	5.139E+03
2.755	4.500E-01	2.771E-01	3.519E-01	2.966E-01	1.756E-01	2.567E-01	6.338E+03
2.479	5.000E-01	3.449E-01	4.443E-01	3.587E-01	1.513E-01	3.054E-01	7.508E+03
2.254	5.500E-01	2.752E-01	3.495E-01	2.950E-01	1.217E-01	2.424E-01	5.984E+03
2.066	6.000E-01	3.279E-01	4.166E-01	3.406E-01	1.837E-01	2.469E-01	6.570E+03
1.907	6.500E-01	1.633E-01	2.073E-01	1.872E-01	1.420E-01	1.389E-01	3.455E+03
1.771	7.000E-01	1.242E-01	1.577E-01	1.459E-01	1.992E-01	1.020E-01	2.545E+03
1.653	7.500E-01	1.451E-01	1.843E-01	1.683E-01	1.571E-01	1.106E-01	2.754E+03

1.550	8.000E-01	1.677E-01	2.129E-01	1.918E-01	1.167E-01	1.183E-01	2.941E+03
1.458	8.500E-01	1.919E-01	2.438E-01	2.163E-01	5.785E-01	1.251E-01	3.106E+03
1.377	9.000E-01	2.311E-01	2.935E-01	2.544E-01	5.426E-01	1.380E-01	3.417E+03
1.305	9.500E-01	2.607E-01	3.311E-01	2.819E-01	5.092E-01	1.435E-01	3.547E+03
1.240	1.000E+00	2.922E-01	3.711E-01	3.100E-01	4.782E-01	1.482E-01	3.656E+03
1.181	1.050E+00	3.255E-01	4.133E-01	3.386E-01	4.495E-01	1.522E-01	3.746E+03
1.127	1.100E+00	3.269E-01	4.152E-01	3.398E-01	4.230E-01	1.437E-01	3.538E+03
1.079	1.150E+00	2.958E-01	3.756E-01	3.131E-01	3.985E-01	1.248E-01	3.077E+03
1.033	1.200E+00	3.281E-01	4.167E-01	3.408E-01	3.758E-01	1.281E-01	3.153E+03
0.992	1.250E+00	4.582E-01	5.819E-01	4.412E-01	3.549E-01	1.566E-01	3.829E+03
0.954	1.300E+00	5.037E-01	6.396E-01	4.725E-01	3.355E-01	1.585E-01	3.871E+03
0.918	1.350E+00	5.514E-01	7.003E-01	5.035E-01	3.176E-01	1.599E-01	3.898E+03
0.886	1.400E+00	6.014E-01	7.638E-01	5.341E-01	3.010E-01	1.608E-01	3.911E+03
0.855	1.450E+00	6.537E-01	8.302E-01	5.640E-01	2.856E-01	1.611E-01	3.913E+03
0.826	1.500E+00	7.083E-01	8.995E-01	5.932E-01	2.713E-01	1.609E-01	3.904E+03
0.800	1.550E+00	7.429E-01	9.435E-01	6.107E-01	2.580E-01	1.575E-01	3.819E+03
0.775	1.600E+00	8.089E-01	1.027E+00	6.420E-01	2.456E-01	1.577E-01	3.817E+03
0.751	1.650E+00	8.777E-01	1.115E+00	6.720E-01	2.340E-01	1.573E-01	3.803E+03
0.729	1.700E+00	9.491E-01	1.205E+00	7.004E-01	2.232E-01	1.564E-01	3.778E+03
0.708	1.750E+00	1.023E+00	1.299E+00	7.273E-01	2.132E-01	1.550E-01	3.743E+03
0.689	1.800E+00	1.099E+00	1.396E+00	7.525E-01	2.037E-01	1.533E-01	3.700E+03
0.670	1.850E+00	1.178E+00	1.496E+00	7.760E-01	1.949E-01	1.512E-01	3.650E+03
0.652	1.900E+00	1.259E+00	1.599E+00	7.979E-01	1.866E-01	1.489E-01	3.593E+03
0.636	1.950E+00	1.342E+00	1.703E+00	8.181E-01	1.788E-01	1.463E-01	3.531E+03
0.620	2.000E+00	1.427E+00	1.812E+00	8.367E-01	1.715E-01	1.435E-01	3.465E+03
0.248	5.000E+00	9.780E+00	1.229E+01	1.000E+00	3.356E-02	3.356E-02	8.462E+02
0.124	1.000E+01	3.618E+01	4.595E+01	1.000E+00	8.949E-03	8.949E-03	2.267E+02
0.062	2.000E+01	1.364E+02	1.733E+02	1.000E+00	2.309E-03	2.309E-03	5.852E+01
0.025	5.000E+01	8.151E+02	1.035E+03	1.000E+00	3.766E-04	3.766E-04	9.542E+00
0.012	1.000E+02	3.206E+03	4.071E+03	1.000E+00	9.473E-05	9.473E-05	2.401E+00

Table I

LN LAMBDA = 4.701E+00
ELECTRICAL CONDUCTIVITY SIGMA= 8.490E+01 INVERSE OHMS INVERSE CM
THERMAL CONDUCTIVITY K= 3.142E-02 WATTS/CM DEGREES

FROM NU=24.794 TO NU= 12.397 THE VALUE OF THE INTEGRAL OF FNU IS 3.450E+02 WATTS/CM2 THICK
FROM NU=11.807 TO NU= 0.670 THE VALUE OF THE INTEGRAL OF FNU IS 3.189E+04 WATTS/CM2 THIN
FROM NU= 0.652 TO NU= 0.012 THE VALUE OF THE INTEGRAL OF FNU IS 1.931E+03 WATTS/CM2 THICK

RADIANT EMITTANCE F= 3.416E+04 WATTS/CM2
ELECTRIC FIELD E= 3.479E+01 VOLTS/CM
CURRENT DENSITY J= 3.093E+01 AMP/CM2

THETA=1.06 EV NTOTAL=4.564E+18 NDENSITY=5.265E+18 PARTICLES/CM3
T= 12300.0 DEGREES K. P= 11.01 ATM

HNU EV	WAVELENGTH MICRONS	KAPPA-PRIME 1/CM	TAU	(-TAU) 1-E	HNU WATTS/CM	INU STER	FNU WATTS/CM
24.794	5.000E-02	4.982E+01	5.185E+01	1.000E+00	6.609E-07	6.609E-07	1.674E-02
22.540	5.500E-02	9.581E+01	1.217E+02	1.000E+00	4.144E-06	4.164E-06	1.055E-01
20.662	6.000E-02	1.416E+02	1.759E+02	1.000E+00	1.887E-05	1.887E-05	4.782E-01
19.072	6.500E-02	1.804E+02	2.291E+02	1.000E+00	6.649E-05	6.649E-05	1.685E+00
17.710	7.000E-02	2.136E+02	2.713E+02	1.000E+00	1.925E-04	1.925E-04	4.878E+00
16.529	7.500E-02	2.424E+02	3.079E+02	1.000E+00	4.768E-04	4.768E-04	1.208E+01
15.496	8.000E-02	2.677E+02	3.399E+02	1.000E+00	1.041E-03	1.041E-03	2.638E+01
13.774	9.000E-02	3.097E+02	3.933E+02	1.000E+00	3.712E-03	3.712E-03	9.404E+01
12.397	1.000E-01	3.433E+02	4.359E+02	1.000E+00	9.926E-03	9.926E-03	2.515E+02
11.807	1.050E-01	2.356E-02	2.999E-02	2.954E-02	1.497E-02	4.411E-04	1.118E+01
8.265	1.500E-01	4.841E-02	6.149E-02	5.963E-02	1.452E-01	8.658E-03	2.173E+02
6.199	2.000E-01	8.725E-02	1.108E-01	1.049E-01	4.313E-01	4.524E-02	1.132E+03
4.959	2.500E-01	1.389E-01	1.763E-01	1.617E-01	7.159E-01	1.157E-01	2.883E+03
4.132	3.000E-01	2.037E-01	2.586E-01	2.279E-01	9.136E-01	2.082E-01	5.164E+03
3.542	3.500E-01	2.807E-01	3.564E-01	2.998E-01	1.020E+00	3.058E-01	7.547E+03
3.099	4.000E-01	3.835E-01	4.871E-01	3.856E-01	1.058E+00	4.078E-01	1.001E+04
2.755	4.500E-01	4.849E-01	6.159E-01	4.598E-01	1.051E+00	4.832E-01	1.181E+04
2.479	5.000E-01	6.144E-01	7.803E-01	5.417E-01	1.018E+00	5.513E-01	1.341E+04
2.254	5.500E-01	4.928E-01	6.259E-01	4.652E-01	9.704E-01	4.514E-01	1.103E+04
2.066	6.000E-01	5.873E-01	7.459E-01	5.257E-01	9.164E-01	4.817E-01	1.173E+04
1.907	6.500E-01	3.151E-01	4.002E-01	3.298E-01	8.605E-01	2.838E-01	6.990E+03
1.771	7.000E-01	2.365E-01	3.003E-01	2.594E-01	8.054E-01	2.089E-01	5.171E+03
1.653	7.500E-01	2.762E-01	3.507E-01	2.958E-01	7.525E-01	2.226E-01	5.495E+03
1.550	8.000E-01	3.190E-01	4.052E-01	3.331E-01	7.027E-01	2.341E-01	5.764E+03
1.458	8.500E-01	3.651E-01	4.637E-01	3.710E-01	6.562E-01	2.435E-01	5.981E+03
1.377	9.000E-01	4.402E-01	5.591E-01	4.283E-01	6.132E-01	2.626E-01	6.428E+03
1.305	9.500E-01	4.965E-01	6.305E-01	4.677E-01	5.735E-01	2.682E-01	6.550E+03
1.240	1.000E+00	5.561E-01	7.063E-01	5.065E-01	5.370E-01	2.720E-01	6.628E+03
1.181	1.050E+00	6.193E-01	7.865E-01	5.444E-01	5.034E-01	2.741E-01	6.666E+03
1.127	1.100E+00	6.264E-01	7.955E-01	5.487E-01	4.724E-01	2.593E-01	6.304E+03
1.079	1.150E+00	5.757E-01	7.311E-01	5.186E-01	4.442E-01	2.304E-01	5.610E+03
1.033	1.200E+00	6.381E-01	8.103E-01	5.553E-01	4.182E-01	2.322E-01	5.643E+03
0.992	1.250E+00	8.901E-01	1.130E+00	6.771E-01	3.942E-01	2.669E-01	6.453E+03
0.954	1.300E+00	9.776E-01	1.242E+00	7.111E-01	3.721E-01	2.646E-01	6.390E+03
0.918	1.350E+00	1.069E+00	1.358E+00	7.428E-01	3.517E-01	2.612E-01	6.306E+03
0.886	1.400E+00	1.165E+00	1.480E+00	7.724E-01	3.328E-01	2.571E-01	6.203E+03
0.855	1.450E+00	1.266E+00	1.608E+00	7.996E-01	3.154E-01	2.522E-01	6.086E+03
0.826	1.500E+00	1.371E+00	1.741E+00	8.246E-01	2.992E-01	2.467E-01	5.956E+03
0.800	1.550E+00	1.443E+00	1.833E+00	8.400E-01	2.842E-01	2.387E-01	5.764E+03
0.775	1.600E+00	1.573E+00	1.998E+00	8.643E-01	2.703E-01	2.336E-01	5.640E+03
0.751	1.650E+00	1.708E+00	2.169E+00	8.858E-01	2.573E-01	2.279E-01	5.502E+03
0.729	1.700E+00	1.849E+00	2.348E+00	9.045E-01	2.452E-01	2.218E-01	5.354E+03
0.708	1.750E+00	1.995E+00	2.533E+00	9.206E-01	2.340E-01	2.154E-01	5.198E+03
0.689	1.800E+00	2.145E+00	2.724E+00	9.344E-01	2.234E-01	2.088E-01	5.038E+03
0.670	1.850E+00	2.300E+00	2.921E+00	9.461E-01	2.134E-01	2.021E-01	4.876E+03
0.652	1.900E+00	2.460E+00	3.124E+00	9.560E-01	2.040E-01	1.954E-01	4.715E+03
0.634	1.950E+00	2.624E+00	3.332E+00	9.643E-01	1.951E-01	1.887E-01	4.555E+03
0.620	2.000E+00	2.792E+00	3.546E+00	9.712E-01	1.876E-01	1.822E-01	4.431E+03
0.248 -	5.000E+00	1.921E+01	2.439E+01	1.000E+00	3.620E-02	3.620E-02	9.142E+02
0.124	1.000E+01	7.210E+01	9.156E+01	1.000E+00	9.611E-03	9.611E-03	2.436E+02
0.062	2.000E+01	2.725E+02	3.460E+02	1.000E+00	2.475E-03	2.475E-03	6.272E+01
0.025	5.000E+01	1.430E+03	2.070E+03	1.000E+00	4.031E-04	4.031E-04	1.021E+01
0.012	1.000E+02	6.411E+03	8.142E+03	1.000E+00	1.014E-04	1.014E-04	2.549E+00

Table III

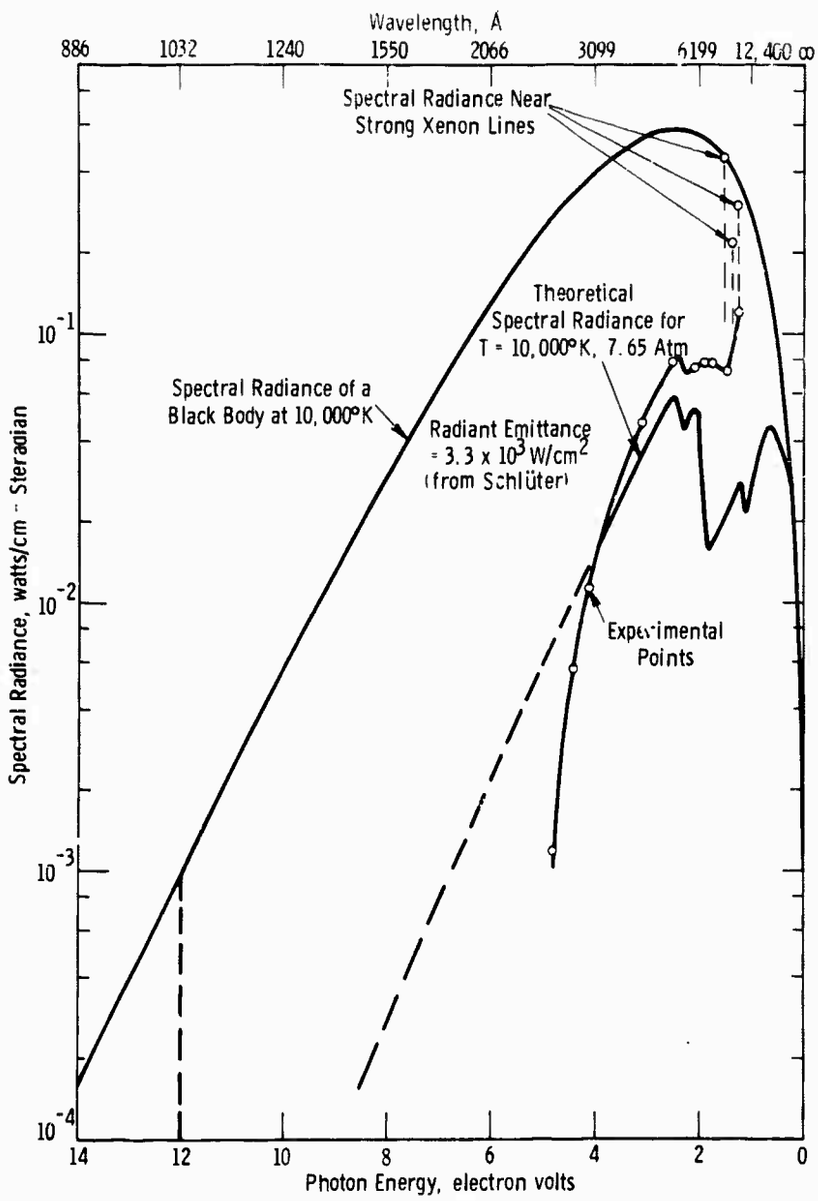

Fig. 5— Experimental & theoretically determined peak spectral radiance of a 1.27 cm thick xenon plasma; theoretical calculation used Schlüter's value. or ξ (dotted portion was extrapolated). Experimental conditions: Energy: 780J, V_B = 1.4 KV, C = 800 μF, L = 100 μH Flash Tube: 1.27 cm inside diameter, 30 cm arc length, 150 torr initial pressure Peak Current Density: 1000 A/cm^2; Peak Electric Field: 32 V/cm

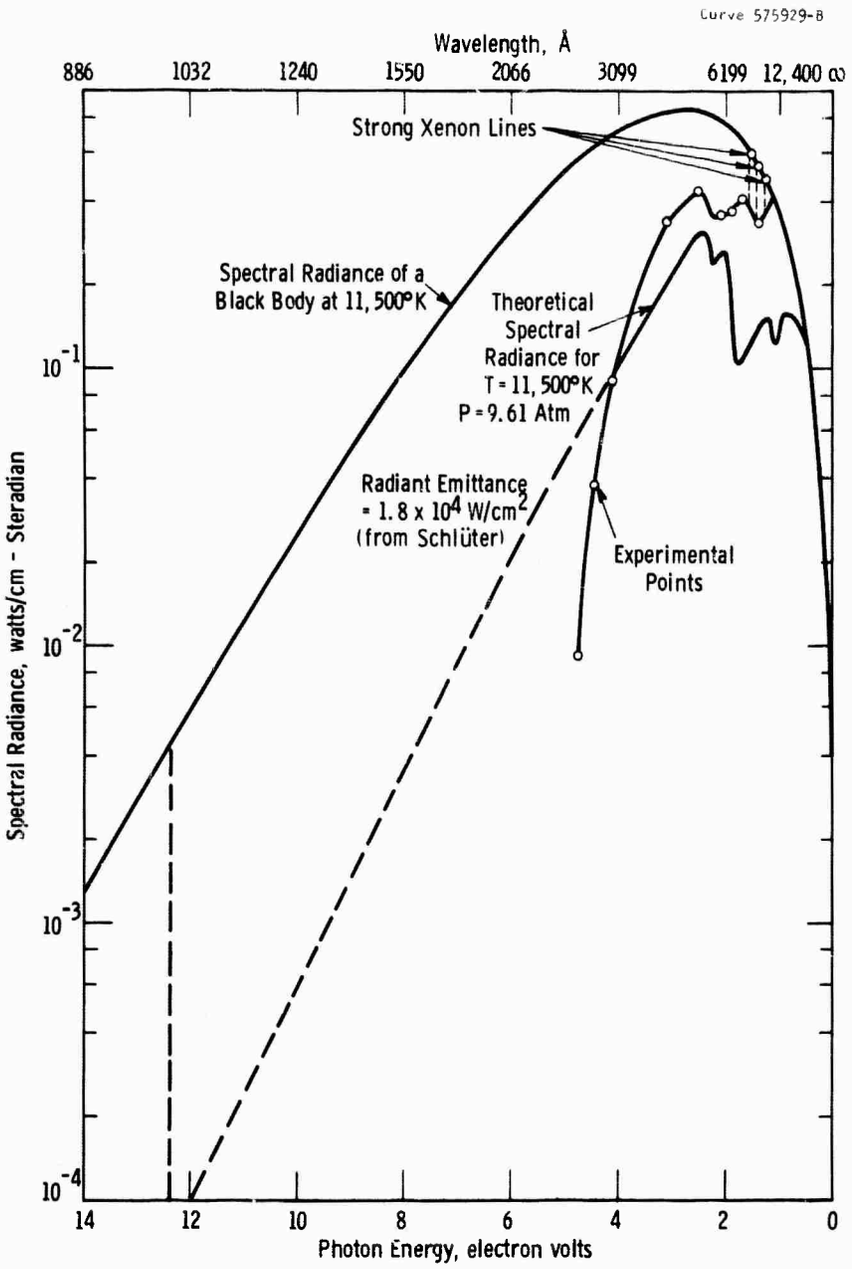

Fig. 6— Experimental & theoretically determined peak spectral radiance of a 1.27 cm thick xenon plasma; theoretical calculation used Schlüter's values for ξ (dotted portion was extrapolated). Experimental conditions: Energy: 3140J, V_B = 2.8 KV, C = 800 μF, L = 100 μH Flash Tube: 1.27 cm inside diameter, 30 cm arc length, 150 torr initial pressure Peak Current Density: 2580 A/cm^2; Peak Electric Field: 54.3 V/cm

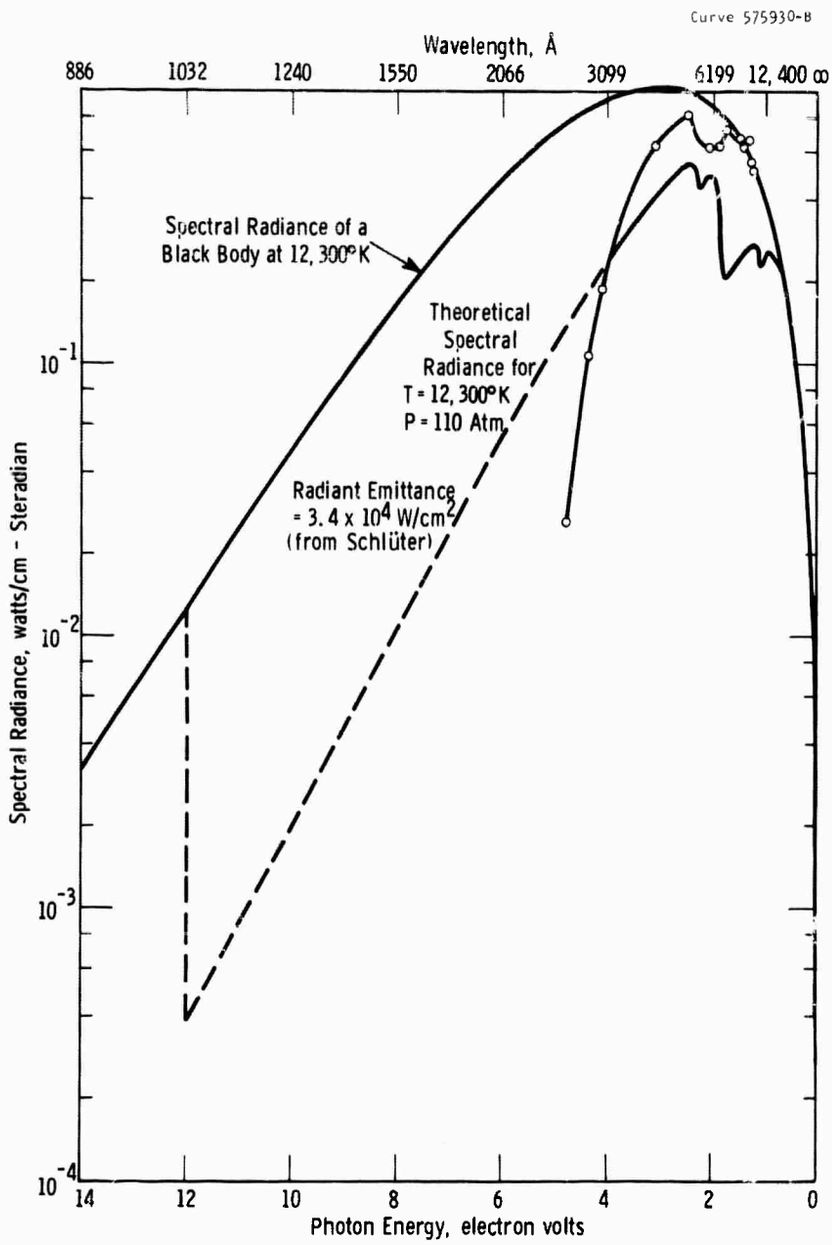

Fig. 7 - Experimental and theoretically determined peak spectral radiance of a 1.27 cm thick xenon plasma; theoretical calculation used Schlüter's values for E, (dotted portion was extrapolated). Experimental conditions: Energy: 6400J, V_B = 4.0 KV, C = 800μF, L = 100μH Flash tube: 1.27 cm inside diameter, 30 cm arc length, 150 torr initial pressure Peak Current Density: 4480 A/cm^2; Peak Electric Field: 69.1 V/cm

led to a means to measure the temperature within the discharge, and thus in turn means to measure various properties of the arc plasma as a function of temperature.

Emmett, Schawlow, and Weinberg[6] had measured the transmissivity at various wavelengths in the ultraviolet, in the visible and in the near infrared as a function of current density. By plotting $e^{-\tau}$ from the model versus the current density predicted by the balance with the radiated power, we could calculate similar plots for the slab and cylindrical geometries. Figures 8, 9, and 10 show the comparison of the calculated and observed values for 3000A°, 5000A°, and 8000A°. The former two plots are within the error of the measurements. The latter results, in Figure 10, at 8000A°, differed strongly between theory and experiment. This high, measured value for the opacity was caused (as we shall show later in Section 4.3) by the broadened and saturated strong infrared lines of xenon.

The results in this section utilized purely theoretical calculations for the special absorptivity and electrical conductivities which are not truly representative of the values in the arc plasma. As better theoretical calculations are developed for the continuum, lines, and conductivities, through these studies and others, the agreement at all wavelength measured by Emmett, Schawlow, and Weinberg[6] should improve.

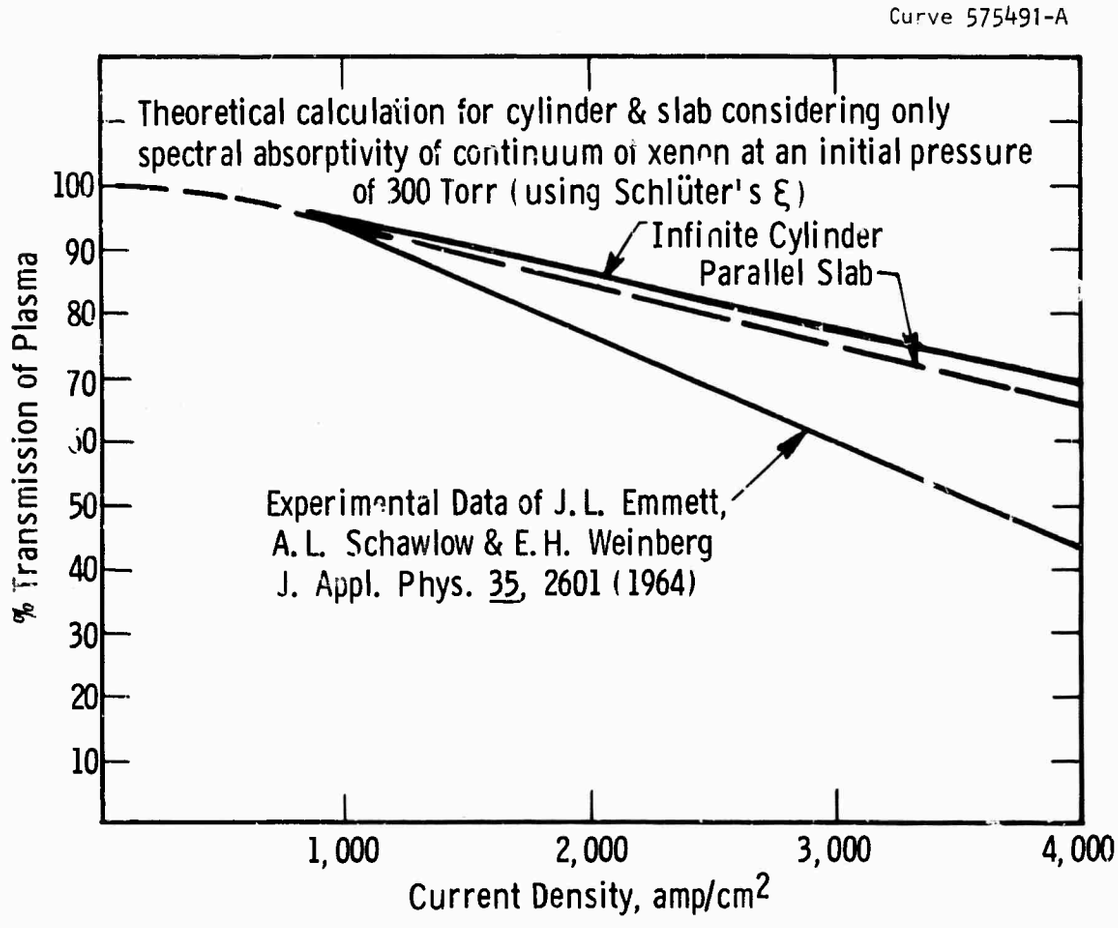

Fig. 8—Transmission of a 1 cm thick layer of xenon of homogeneous temperature at 3000 Å

Curve 575493-A

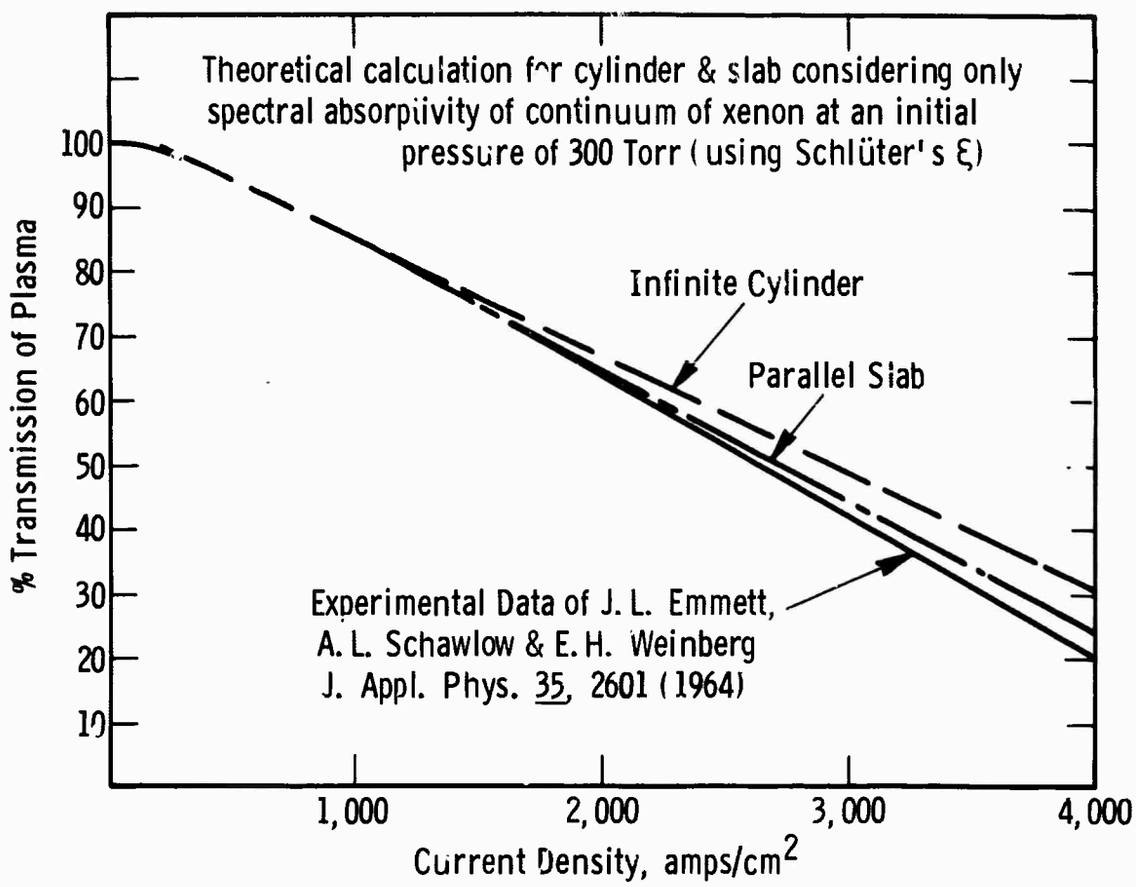

Fig. 9—Transmission of a 1 cm thick layer of xenon of homogeneous temperature at 5000 Å

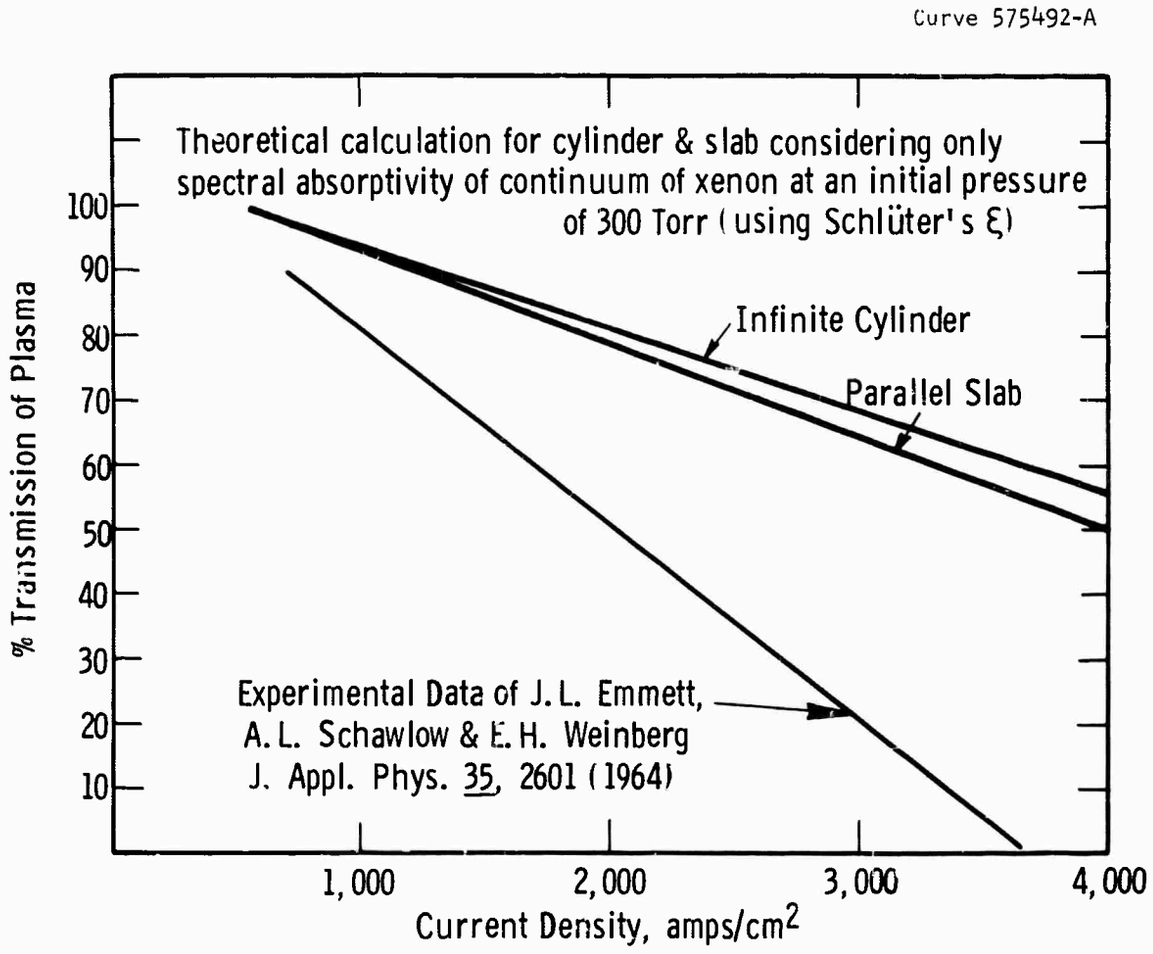

Fig. 10—Transmission of a 1 cm thick layer of xenon of homogeneous temperature at 8000 Å

CHAPTER 4

Experimental Measurements

4.1 Experimental Measurements Measured on the Pulsed Arc

The spectral radiance in a high current pulsed arc was measured at a number of wavelengths and positions within the arc. The voltage and the currents through the arc were also measured simultaneously with the time varying spectral radiance. These measurements were first used to determine the temperature and then the temperature dependence of the spectral absorptivity and electrical conductivity of the xenon arc.

The experimental arrangement for these measurements is shown in Figure 11. A 12.7 mm bore tube filled to a pressure of 150 torr of xenon was used. Two off-axis paraboloidal mirrors of 1 meter focal length imaged the arc discharge upon the entrance slit. The various radial portions of the discharge were studied by traversing the monochromator across the image between firings of the bank, with the monochromator set for the wavelength at which the spectral radiance was to be measured. The power input and electrical conductivity of the discharge was monitored through recording the voltage and current for each shot (with the capacitance .800 μF and the inductance .100 μH held constant for the whole series). The energy input was varied by charging the capacitor bank voltage. The current was measured with a T&M coaxial current shunt (.001 r), the voltage with a Tektronix voltage divider. The entire optical system, including the mirrors, monochromator and photomultiplier detector was calibrated for spectral radiance by the substitution method, using a synchronous detector recorder with a tungsten strip filament lamp (GE 30A/T24/17) being used as the standard. This lamp in turn had been calibrated by Eppley Laboratories.

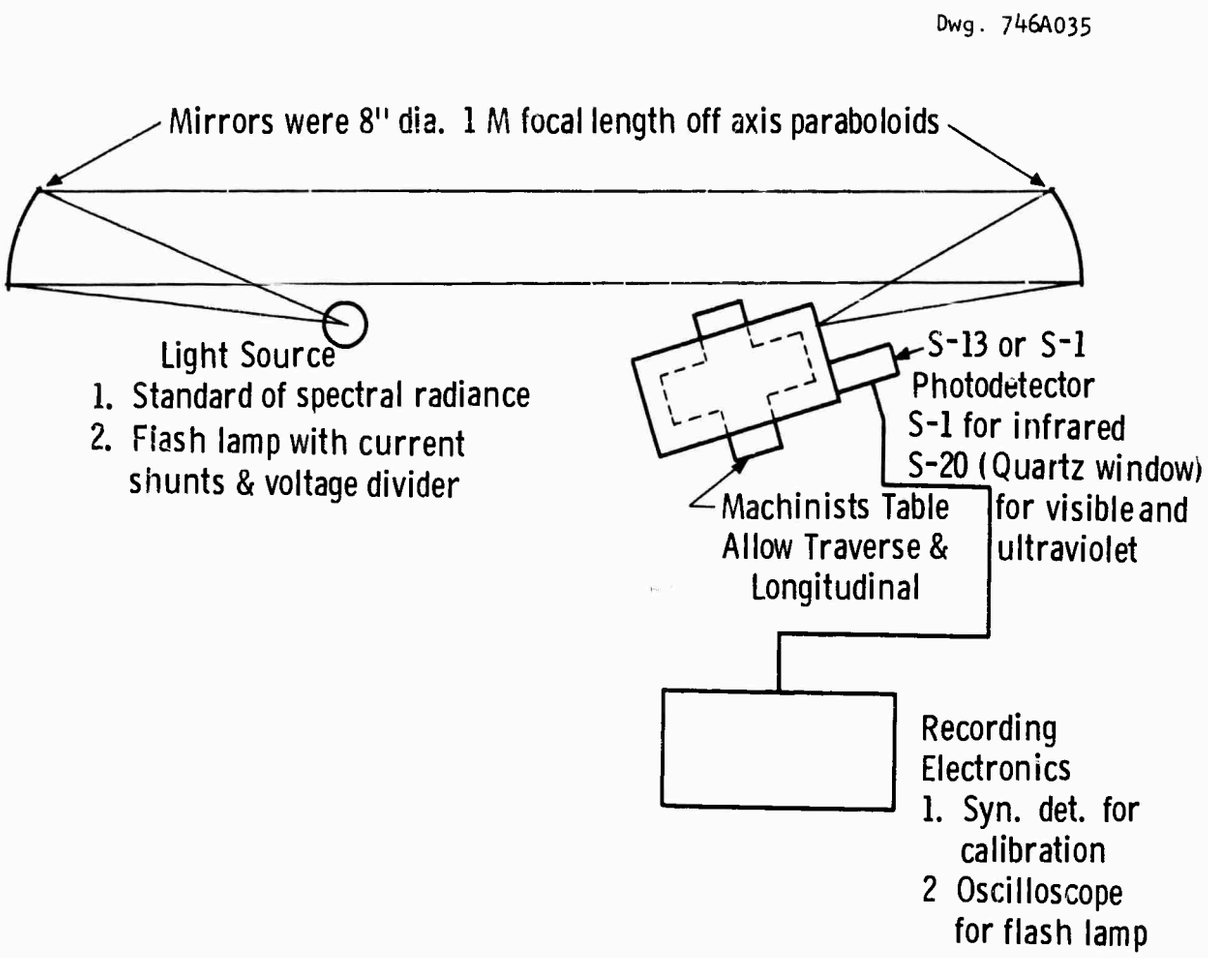

Fig. 11—Monochromator arrangement for studies on flash lamps

4.2 Radial Distribution of Spectral Radiance

The spectral radiance was measured on the central axis for a number of wavelengths in the ultraviolet where the plasma should be optically thin[6]. There were no emission lines noted in this spectral region in the xenon short arc spectra discussed in section 5.5 of the First Semiannual Report.

The radial distribution of the spectral radiance was measured at 2600, 2800 and 3000Å at a number of different radial positions on each side of the center line. The results of these measurements are shown in Figures 12 and 13 for two different energy levels and thus current densities.

The spectral radiance at 3000Å near the tube wall was measured to ascertain, if possible, the boundary layer thickness. The values shown are the raw values of spectra radiance at various diameters, not as yet corrected to the radial dependence by means of the Abel inversion using techniques described in Freeman and Katz[45] and many other papers. These values indicate roughly that the homogeneous temperature model is reasonable as a rough approximation. The homogeneous temperature distribution is shown in dashed lines. The walls of the tube were at ± .25 inches (i.e.: ± .635 cm). The high radiance in the wall region is not readily explicable, but is probably due to reflections from the quartz wall interfaces. Frost[46] and Maecker[47] have shown that no lens effect exists in the region inside the walls (i.e.: a distance from the centerline outside the tube corresponds to the spectral radiance that distance from the centerline. Figure 14 shows a simple proof of this.

4.3 Time-Resolved Spectral Radiance in the Infrared - Temperature Measurements

The spectral radiance in the center of the arc was measured as a function of time in the immediate vicincity of some strong lines of xenon in the

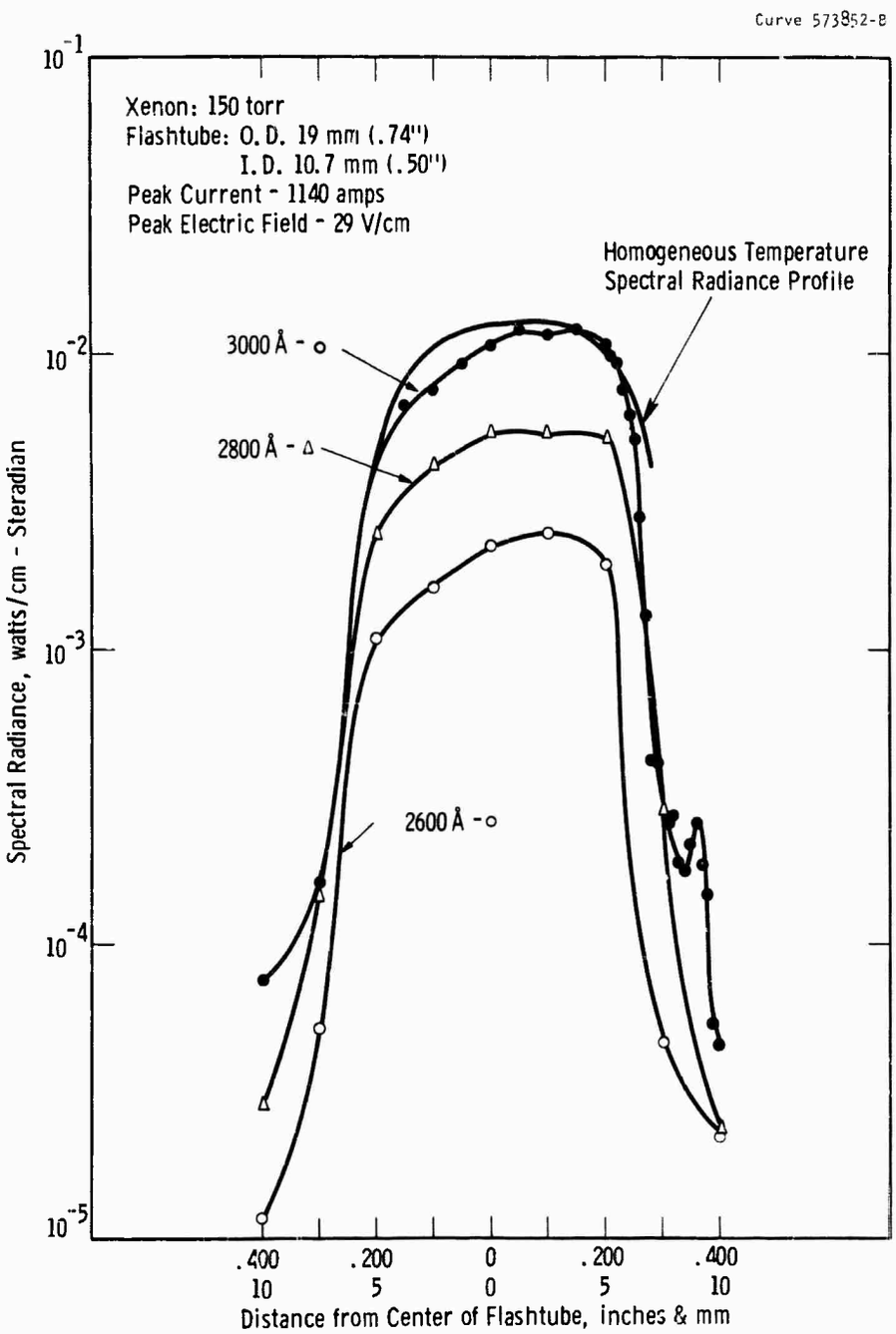

Fig. 12 -Peak spectral radiance at different distances from flashtube center at three wavelengtns for 780 J input. (not corrected Abel inversion). Homogeneous temperature profile indicated

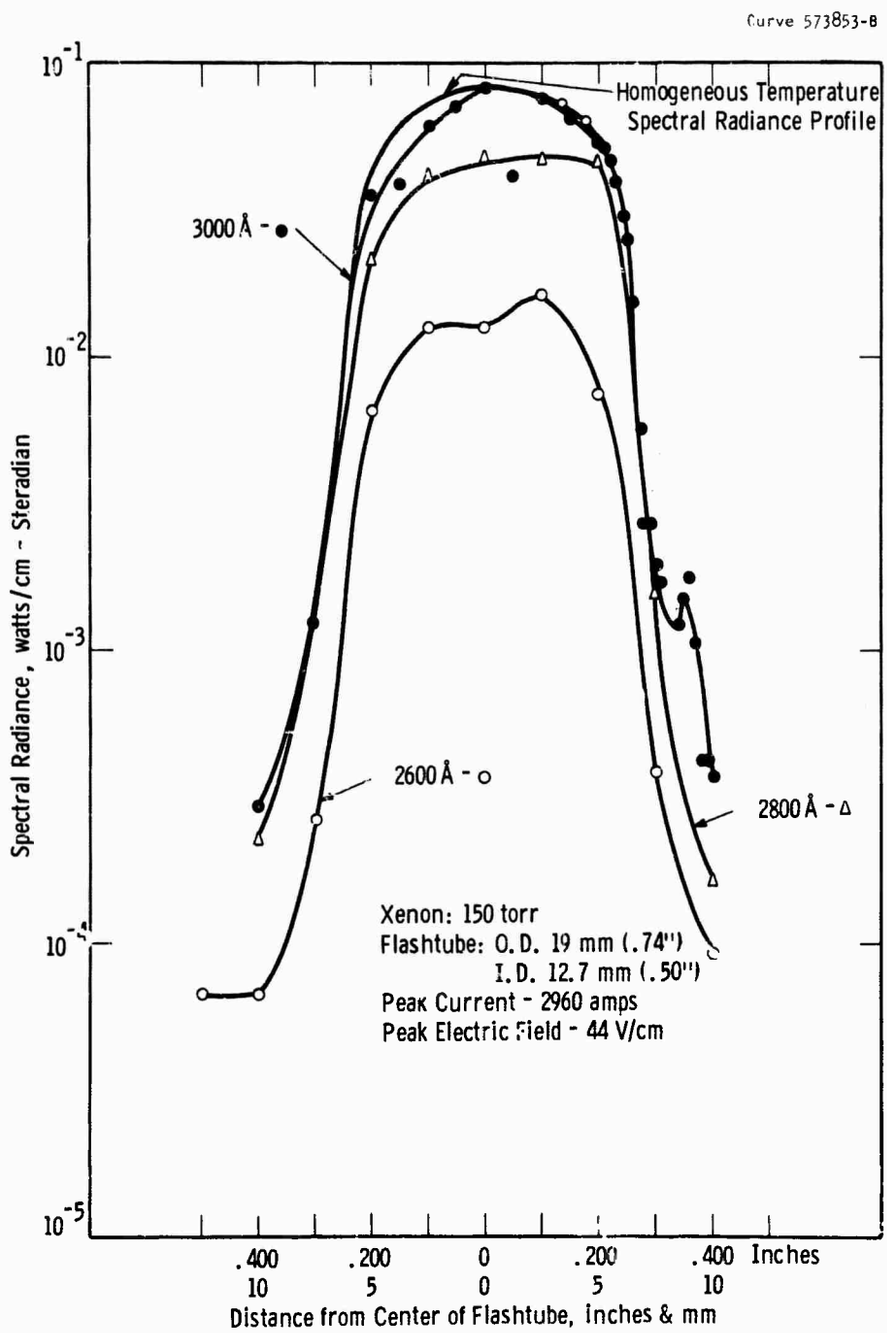

Fig. 13—Peak spectral radiance at different distances from flashtube center at three wavelengths for 3140 J input. (not corrected Abel inversion). Homogeneous temperature profile indicated

Curve 575937-A

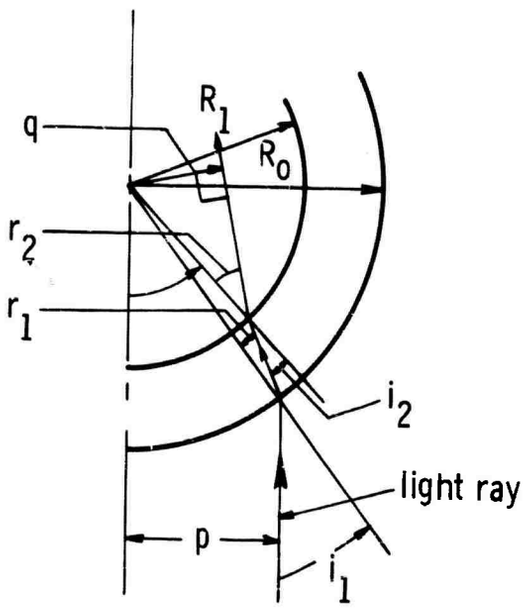

Let i_1 = angle of incidence with respect to axis

$\sin i_1 = \frac{p}{R_0}$ where R_0 is the outer radius of the tube

$\sin r_1 = \frac{\sin i_1}{n}$; n = index of refraction of cylinder

i_2 = angle of incidence from cylinder to plasma

$\sin i_2 = \frac{R_0}{R_1} \sin r_1$

$\sin r_2 = n \sin i_2$

Tracing whole route of the ray through cylinder yields:

$\sin r_2 = n \sin i_2 = nR_0/R, \sin r_1 = R_0/R_1 \sin i_1$

$\sin r_2 = p/R_0 \times R_0/R_1 = p/R_1$

$q/R_1 = \sin r_2 = p/R_1 : q = p$ where q is the perpendicular distance of the ray in the cylinder to the center of the cylinder

Fig. 14—Derivation of Frost's and Maecher's center line distance relation

infrared. The slit width of the monochromator was set for a spectral resolution of just under 1A° to avoid over lapping of the spectral radiance determinations. Figure 15 shows two oscilloscope traces, the upper with twice the gain of the lower. The lower trace was taken at the unshifted center of the 8231.6A° line of xenon; the upper trace was taken at 8198A°, approximately 34A° away towards the shorter wavelength. The current trace is the upper curve on both pictures. The energy input to the 12.7 mm diameter, 30 cm arc length tube was 780J. To be noted on these traces is the saturation and long persistance of the line at 8231.6A° particularly in comparison with the current or the 8198A° trace. Figure 16 is a cross section in wavelength of the spectral radiance about the line for different time intervals. Each wavelength setting was a separate shot (note the reproducibility at the peak). To be noted is the shift and broadening of the line with increasing current. The wings of the line contribute strongly to the spectral absorptivity of the continuum away from the line center.

The saturation of the spectral radiance of the line provides a means to determine the temperature within the arc. If the arc is homogeneous, this temperature so determined is that of the arc core. If the arc is not homogeneous, further measurements would be required of the radial distribution of the saturated radiance. The units were converted to temperatures using Walker's tables[48] which list spectral radiances for black bodies.

Temperature measurements by means of spectral radiance measurements in the infrared require high precision in the measurement of the spectral radiance and the other quantities for which the temperature dependence being measured. Source of error in the methods for measured temperature, particularly

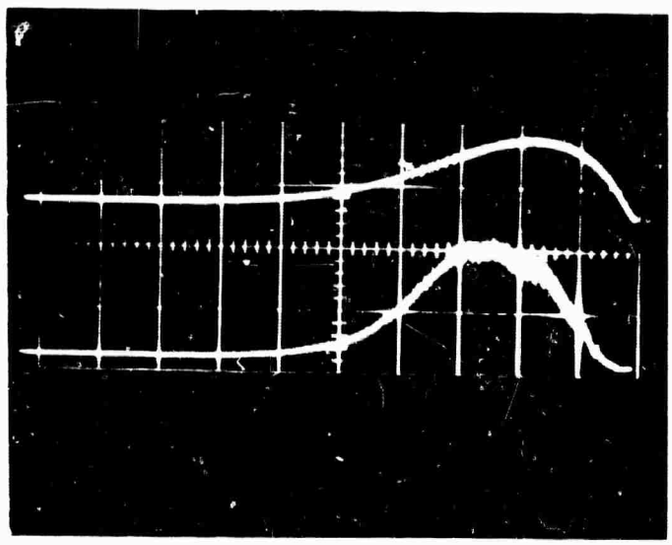

a) 8198 Å (Continuum) Gain 100 mv/ cm
(2 x (b))

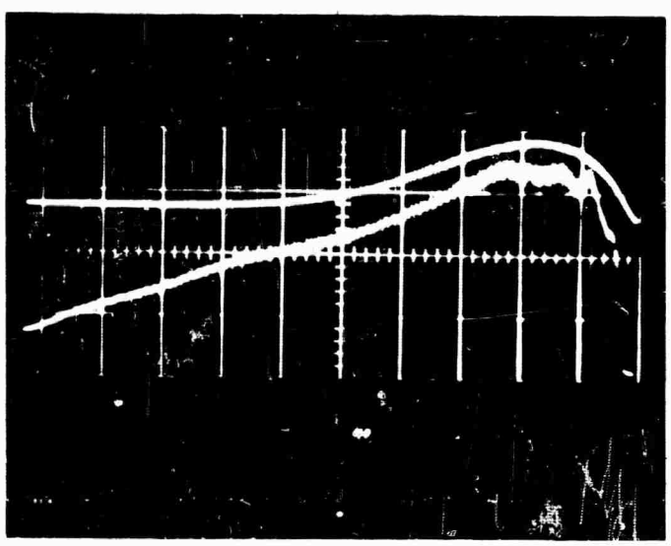

b) 8231.6 Å (Line) (Gain 200 mv/cm)

Fig. 15—Oscilloscope traces of the voltage representing the spectral radiance at the center of the 8231.6 Å line and at 8198 Å (in the continuum). The 8198 Å trace has twice the gain of the other trace. The upper curve in both cases is the current. The time scale is 100 μ sec/scale division

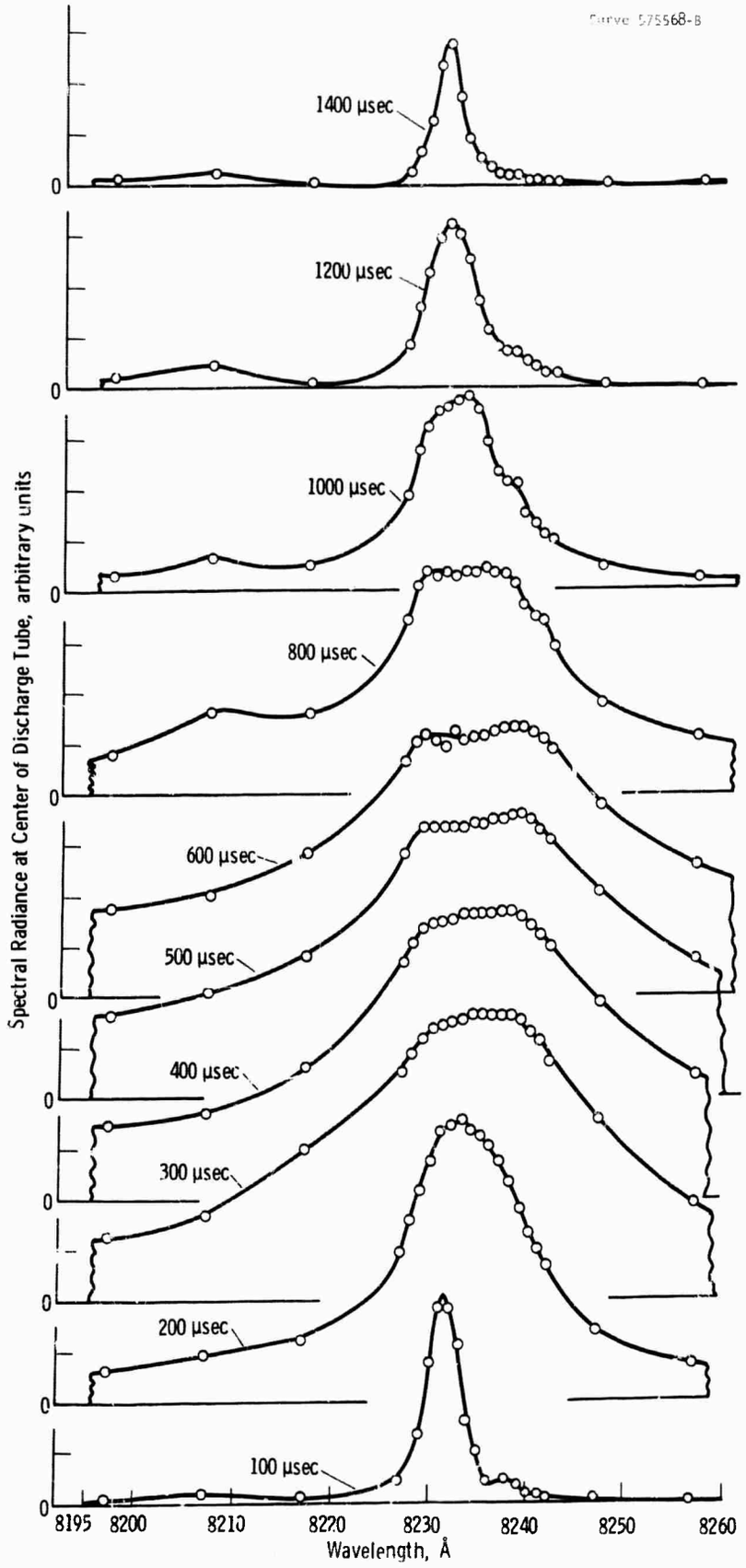

Fig. 16— Time history of 8231.6 Å line of xenon
780J input, 12.7mm dia. tube, 150 torr initial pressure
Peak current 1140 amps
Peak electric field, 29 v/cm

with the pulsed discharge, are the shot to shot variations (simultaneous measurements are to be preferred) and the difficulties in reading oscilloscope deflections accurately, in addition to the more usual problems of accurate measurements of spectral radiance (i.e.: those of the standard lamp and of the same viewing geometry, etc.). The technique has the supreme virtue of yielding a temperature without assumptions on the detailed properties of the plasma.

The temperatures obtained by this method were used to measure the temperature dependence of the spectral radiance and of the electrical conductivity of the arc to be discussed in subsequent sections.

4.4 Measurements of the Spectral Absorptivity and the ξ Factor of Biberman & Norman

Earlier measurements of the radial distribution of the spectral radiance in the ultraviolet in the First Semiannual Report[1], and analyzed more thoroughly in this report, and spectral transmissivity measurements[6] indicated that the arc plasma at current densities to at least 3000 amp (cm^2) was nearly homogeneous in spectral absorptivity, and therefore in temperature. During the development of the models, the need for some confirmation of the values of the spectral absorptivity used in the models was required.

Measurements of the spectral radiance at wavelengths for the arc was thick (at the peak of a strong line or the continuum in the infrared) had led to the determination of the temperature of this homogeneous plasma. Using the values of temperature thus determined, the pressure was calculated assuming that the entire volume of the tube was of homogeneous temperature. Figure 17 is a chart derived from the particle density versus pressure calculations to aid this computation. By comparing the spectral radiance observed on the flash

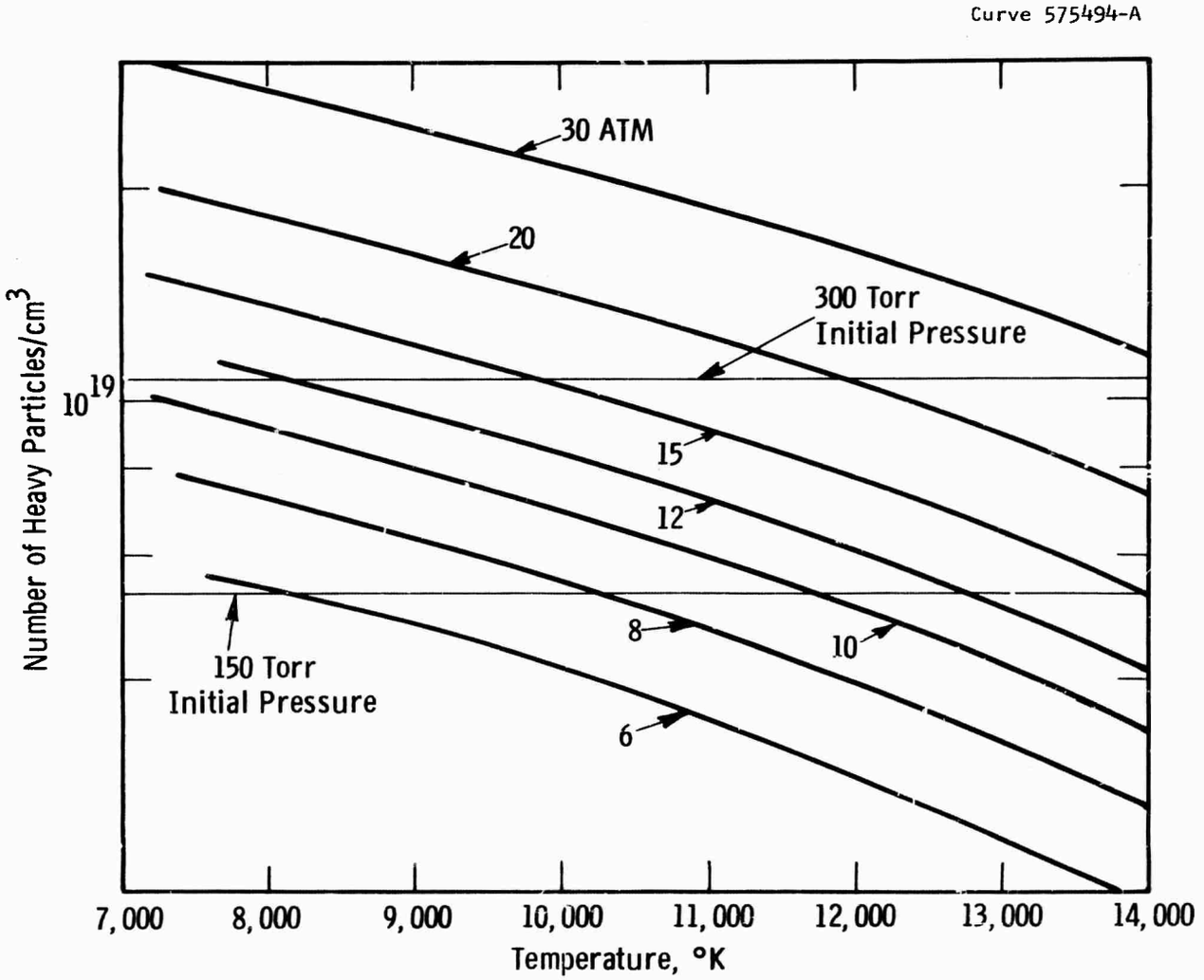

Fig. 17—Heavy particle (atoms + ions) density as function of temperature for various pressures. For homogeneous temperature model, dynamic pressure is given by horizontal line representing initial pressure and thus particle density

tube with that calculated using the Biberman & Norman continuum theory[7] using Schlüter's values for the ξ factor for the same pressure and temperature, an experimental value of the variation of ξ with wavelength was obtained. The experimentally determined values are shown in Figure 18 together with the theoretically calculated values of Biberman & Norman[7], and of Schlüter[13]. The measured values have a semi-quantitative agreement with the wavelength variation and the magnitude of Schlüter's values but still differ widely in the infrared between .7 and 1.0 μ. The large values of ξ measured between 7500A° and 10000° is probably due to the effects of the wings of the strong lines of xenon in the infrared (as shown in Section 4.3). Furthermore, accurate measurements of ξ particularly in the ultraviolet below 2600A°, and in the infrared beyond 10000A°, would provide further insight into the actual values of ξ for further theoretical calculations as would be the extension of his theory to the shorter wavelengths where the slope of Schlüter's values of ξ differ widely from our experimental values shown in Figure 18. Figure 19 is a plot of the spectral radiance at 3000A° with temperature for various pressures. The arc discharge in the flash tube which may be considered to be a constant heavy particle processes follows the heavy lines indicated.

Figures 20, 21, and 22 present on a linear scale for clarity the experimentally measured values of the spectral radiance together with the black body radiance and the spectral radiance calculated using Schlüter's values for ξ corresponding to the temperatures measured in the arc in Section 4.3. These figures are linear plots of Figures 5, 6, 7 which are semi-log. The linear plot shows the detailed correspondence and theoretical distribution more

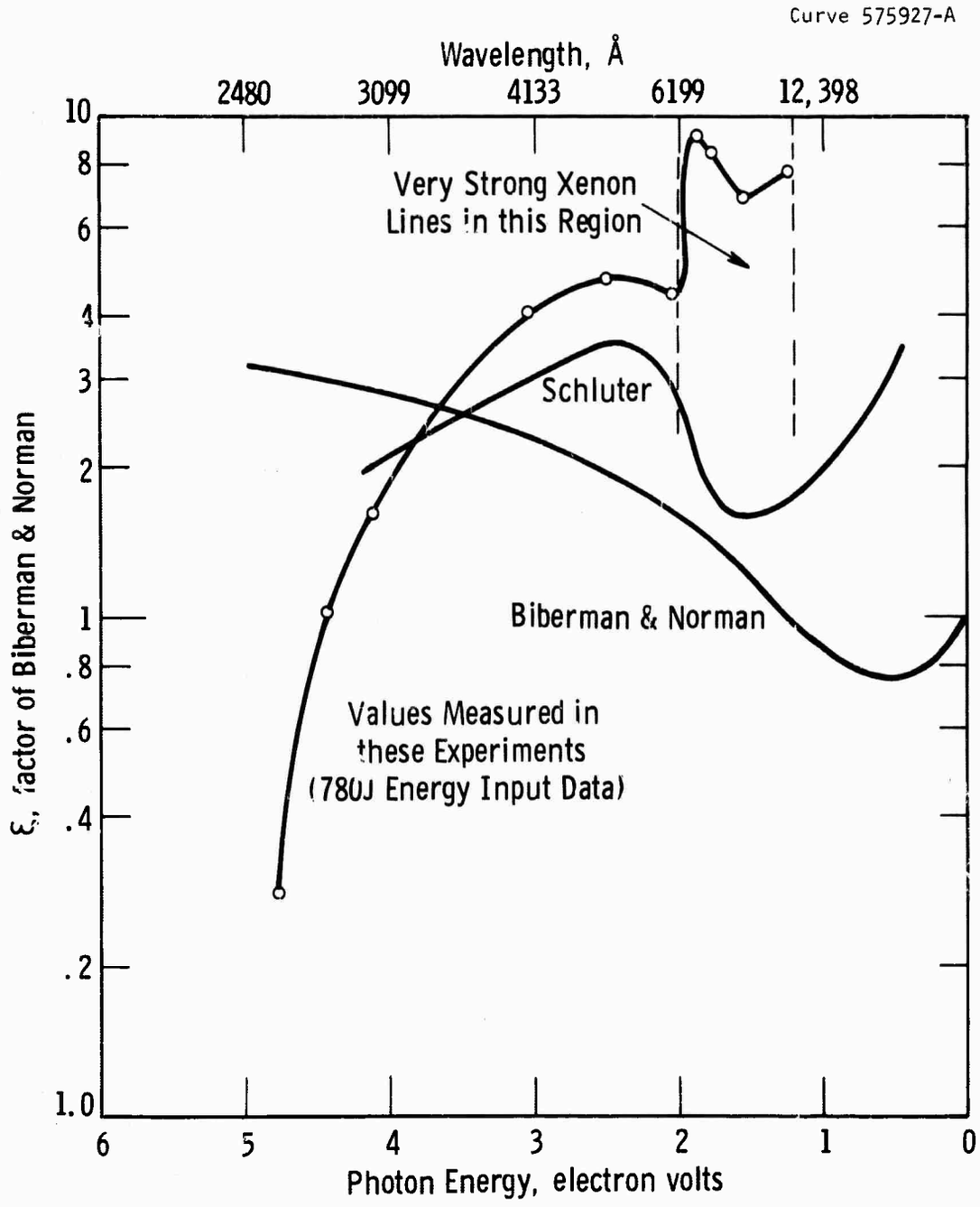

Fig. 10-Comparison of experimentally measured values of Biberman & Norman ξ Factor with theoretical calculated values of Schluter (Z. Astrophys. 61,67 (1965) and of Biberman & Norman (J. Quant. Spectr. Rad. Transfer 3, 221 (1963)

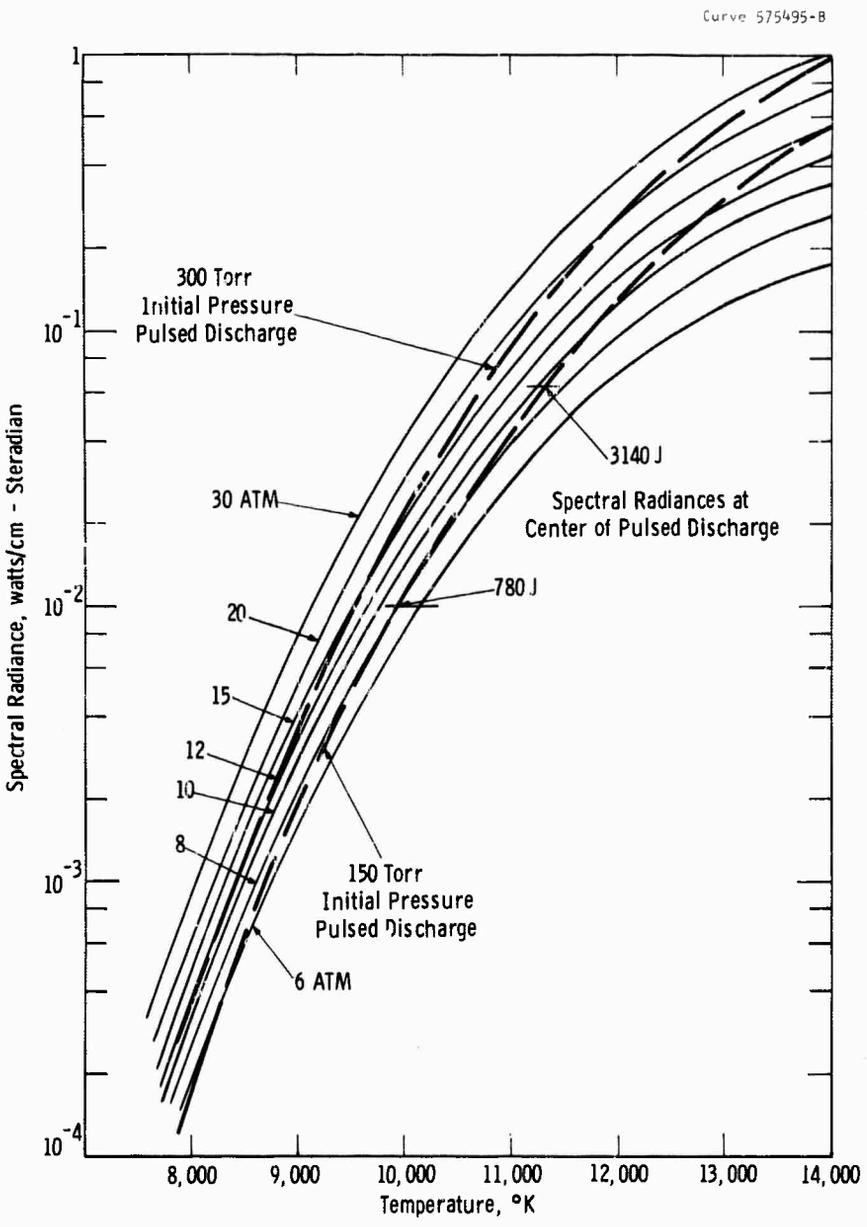

Fig. 19- Spectral radiance at 3000 Å at a constant pressure of a 1 cm thick layer of xenon. The pulsed discharge curves are for a homogeneous temperature plasma with a constant heavy particle concentration derived from the initial pressure

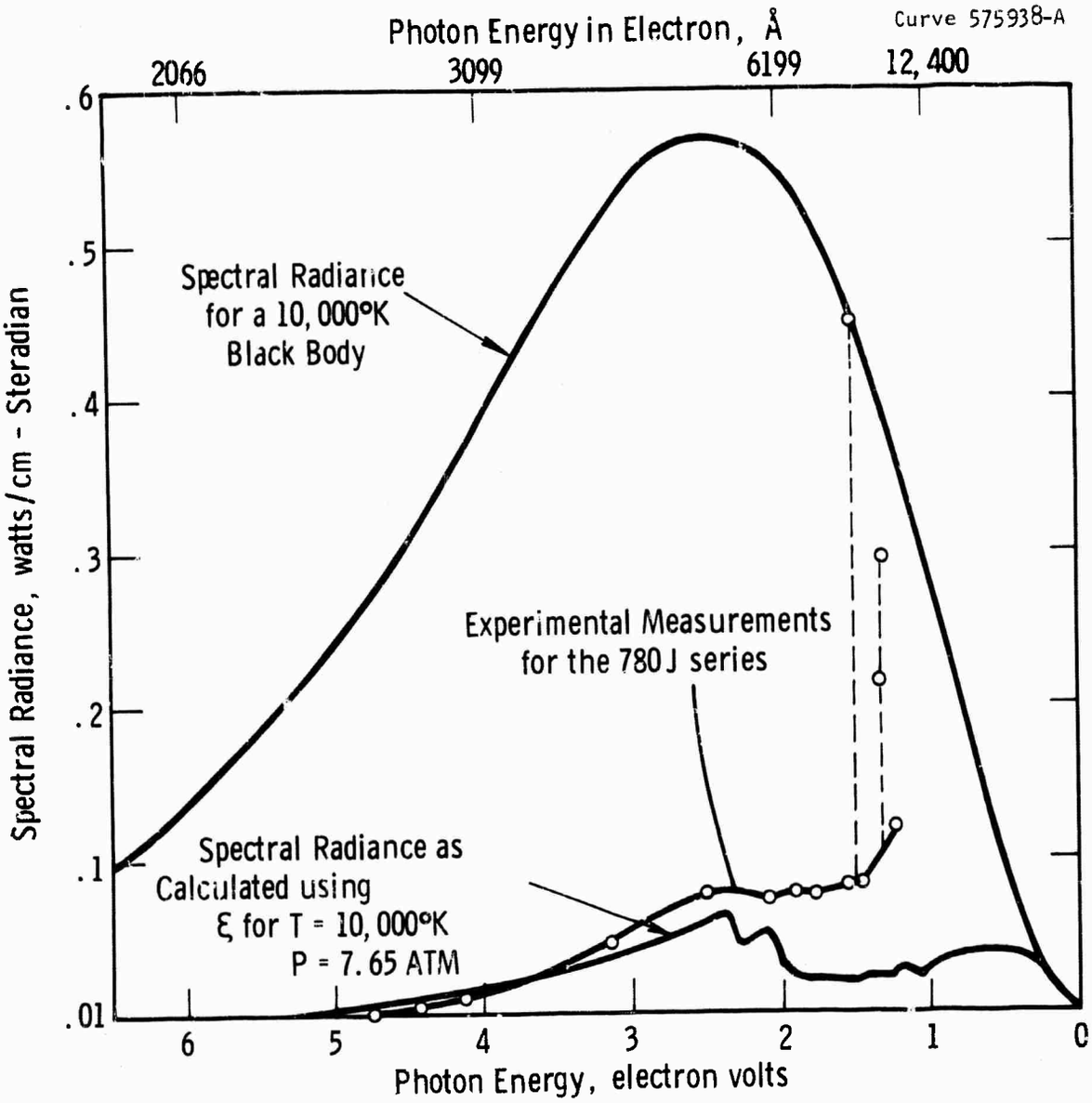

Fig. 20 –Linear plot of the experimental and theoretical values for the spectral radiance of a 1.27 cm thick xenon plasma of homogeneous temperature corresponding to the 780 J - 1000 A/cm^2 peak current density series Flashtube: 1.27 cm inside dia. 30 cm long filled to 150 torr xenon

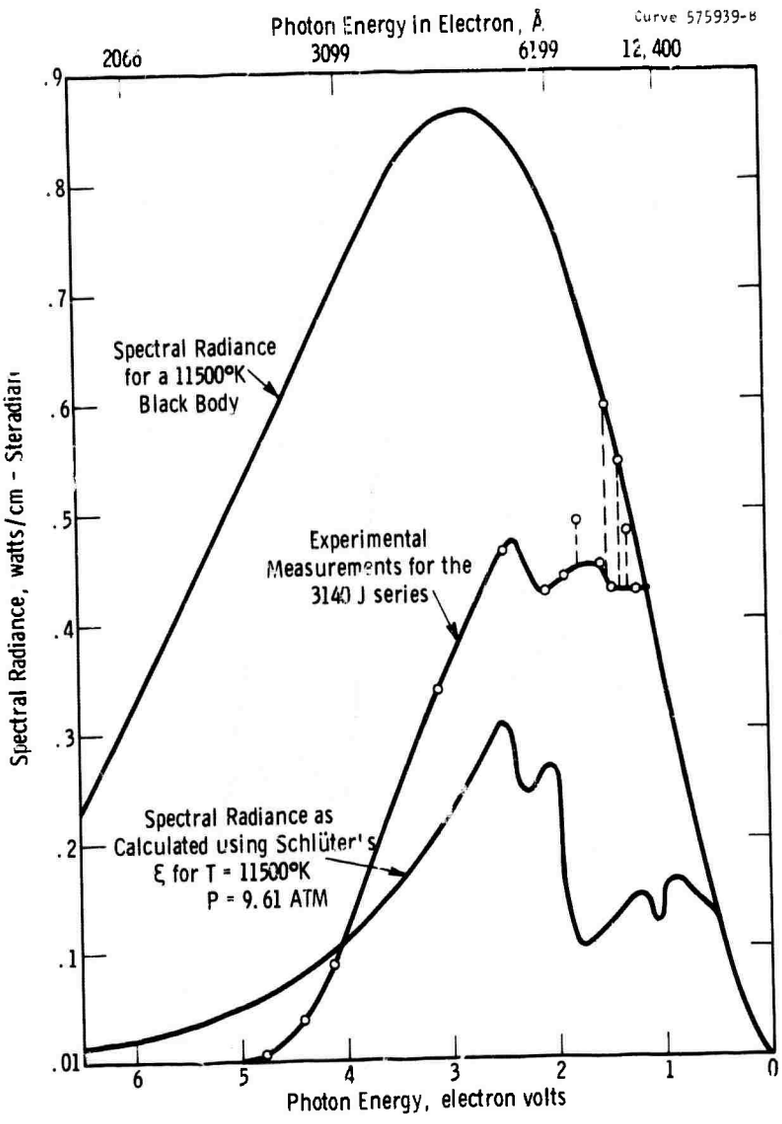

Fig. 21 –Linear plot of the experimental and theoretical values for the spectral radiance of a 1.27 cm thick xenon plasma of homogeneous temperature corresponding to the 3140 J - 2580 A/cm^2 peak current density series
Flashtube: 1.27 cm inside dia. 30 cm long filled to 150 torr xenon

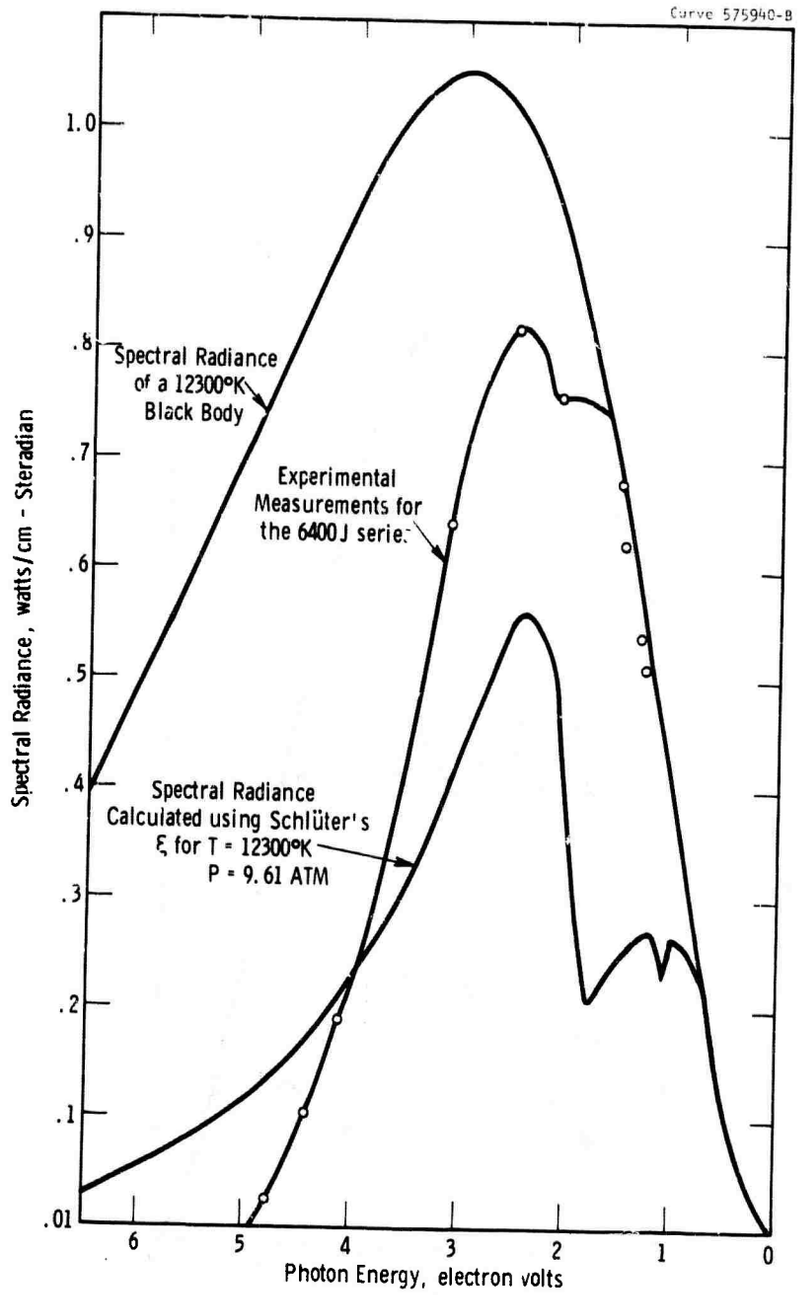

Fig. 22 -Linear plot of the experimental and theoretical values for the spectral radiance of a 1.27 cm thick xenon plasma of homogeneous temperature corresponding to the 6400 J - 4480 A/cm^2 peak current density series
Flashtube: 1.27 cm inside dia 30 cm long filled to 150 torr xenon

clearly while the semi-log plot shows well the wide variation with wavelength of the spectral radiance and in optical thickness.

4.5 Temperature Dependence of the Electrical Conductivity

The electrical conductivity in the xenon plasma was measured as a function of temperature using the temperature as determined in Section 4.3. The temperature dependence (for the same number of heavy particles) is shown in Figure 23. The voltage drop at the electrodes was considered to be negligible (Gonz[49] estimated the voltage drop to be 10 to 20 volts in similar flash tubes). The electrical conductivity measured is the average value over the cross section of the tube. The average value will equal the actual value if the flash tube is completely filled with a homogeneous plasma. The correction factor necessary to allow for the boundary layer has not yet been determined; though the radial spectral radiance profiles (Section 4.2) indicated the boundary layer should be small.

The measured electrical conductivity is considerably smaller than that calculated using Spitzer's theory[15,16] for the same temperature and pressure also shown in Figure 22. This is not wholly unexpected as the electron-neutral scattering could be important at 10000°K, (and 7.6 atm.) even though the gas is about 10% ionized. As the electron density was calculated to be about 1×10^{18} for these conditions, Spitzer's theory and in particular the Coulomb term may be beyond its limits of validity. Both areas (i.e.: electron neutral effects and high density corrections) need further investigation.

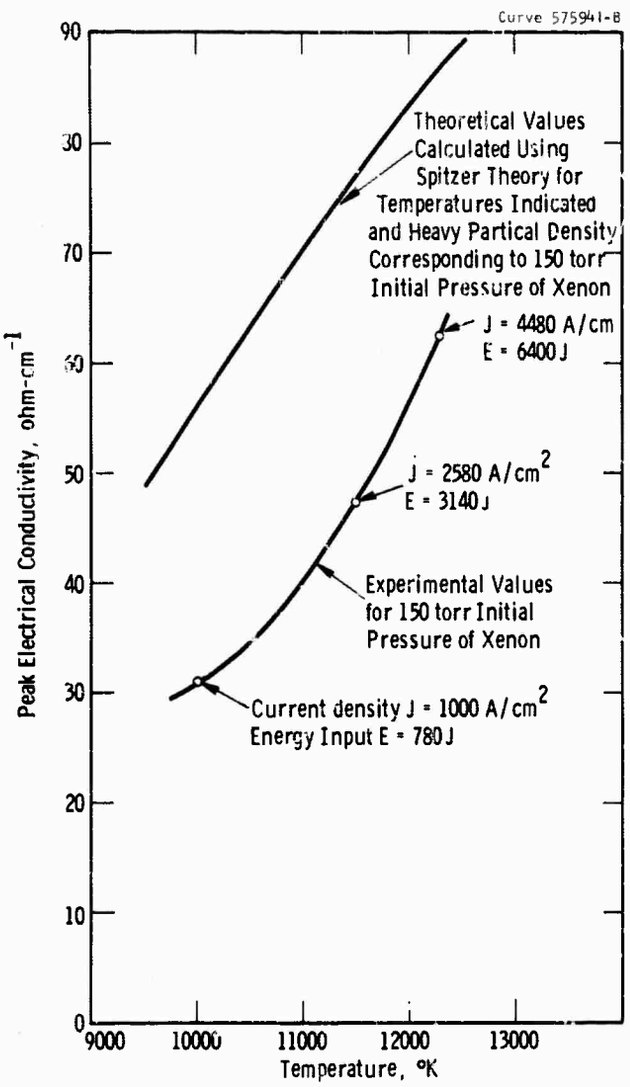

Fig. 23 –Experimental and theoretical dependence of electrical conductivity of xenon upon temperature at a constant heavy particle density

STATUS OF THE PROBLEM AND FUTURE WORK

In this report, we have presented some simple models for the arc discharge. The models have many features that agree in a semi-quantitative fashion with the actual arc. These areas of agreement include 1) the arc is thick in the infrared and visible, and thin in the ultraviolet, 2) large changes in input power can lead to relatively small changes in spectral radiance in the infrared where the arc is thick, but very large changes of the spectral radiance in the ultraviolet where the arc is thin. To utilize these models and to develop more complete models that include energy transport within the arc and to the walls the physical properties of the arc need to be better known. Future work on these arcs should include experimental and theoretical studies to improve the quantitative agreement between the theory of the spectral absorptivity of the continuum (Section 4.4) and the actual experimental values. Inclusion of the pressure broadened lines in the infrared would probably improve the agreement, particularly for arcs of moderate current densities ($\sim$1000 A/cm^2) which are becoming of more interest due to the advances in laser efficiency.

We have neglected thermal conductivity and have used a simple representation for electrical conductivity in these model calculations. Quantitative models particularly in the current density range ($\sim$1000 A/cm^2) should include thermal conduction and better values of electrical conductivities to allow calculation of the power balance as the energy transfer by thermal conduction and the heating away from the central core becomes more important in the lower power-lower pressure arcs.

The extension of these models to more complex arc systems in which the power balance between radiation and thermal conduction is a factor that requires an extension of radiative transport theory beyond that of Appendix A. As the techniques improve, we must see what simplifications are warranted and how and when to include the walls, be they transparent or reflective. It should also be possible to apply these theories and the model calculations to actual laser pumping situations such as is found in a coaxial laser pump closely coupled to the laser rod.

The techniques devised in this work, both experimental and theoretical, can be applied to other problems of radiative plasma such as those occurring in lightning arcs, in light sources, and in simulating plasmas of astrophysical interest.

ACKNOWLEDGMENTS

We wish to thank Dr. Elliot Weinburg of ONR-London and Dr. R. D. Haun, Jr. of Westinghouse for their aid and counsel in our pursuit of these models. We also wish to thank many of the personnel of Westinghouse Research Laboratories who have assisted in this work, particularly J. Lesnick, M. Uman, J. Lowke, C. Chen, W. A. Stewart, E. Somers, A. Sletten, A. Phelps, L. Frost, and E. Corinaldesi. Many people in the Quantum Electronics Department have contributed through advice or through loan of equipment. We also wish to thank R. Grassell, J. Humphreys, Jr., and L. Criscella for their good services gathering the experimental data.

The contributions of Ethel Marko and Martha Fischer to the typing; J. Getsko, M. Bowman, and others in Drafting to the figures; K. Moelk, H. Payne, and others in Graphic Arts for the reproduction are also appreciated.

REFERENCES

1. C. H. Church and R. G. Schlecht, "Arc Discharge Sources, Semi-Annual Technical Report in Contract Nonr 4647(00), Westinghouse Research Laboratories, Pittsburgh, Pa. (May 15, 1965).
2. S. S. Penner and M. Thomas, "Approximate Theoretical Calculation of Continuum Opacities," A.I.A.A.J., 2, 1572-1575 (1964).
3. R. A. Pappert and S. S. Penner, "Approximate Opacity Calculations for Polyelectronic Atoms at High Temperatures," J. Quant. Spect. Rad. Transfer, 1; 259-268 (1961).
4. Yu. P. Raizer, "A Simple Method of Calculating the Degree of Ionization and Thermodynamic Functions of a Multiply Ionized Ideal Gas," Sov. Phys.-J.E.T.P., 9, 1124-1125 (1959).
5. Yu. P. Raizer, "Simple Method for Computing the Mean Range of Radiation in Ionized Gases at High Temperatures," Sov. Phys.-J.E.T.P., 10, 769 (1960).
6. J. E. Emmett, A. L. Schawlow, and E. H. Weinberg, "Direct Measurement of Flashtube Opacity," J. Appl. Phys., 35, 2601-2604 (1964).
7. L. M. Biberman and G. E. Norman, "Plasma Radiation due to Recombination and Bremstrahlung Processes," J. Quant. Spect. Rad. Transfer, 3, 221-245 (1963) General Atomics-San Diego Translation GA tr 4943.
8. V. V. Yankov, "On the Distribution of Energy in the Continuous Absorption Spectrum of Xenon," Optics and Spectroscopy, 14, 14-17 (1963).
9. L. M. Biberman and G. E. Norman, "On the Calculation of Photoionization Absorption," Optics and Spectroscopy, 8, 230-232 (1960).
10. L. M. Biberman, G. E. Norman, and K. N. Ulyanov, "The Photoionization of Excited Complex Atoms and Ions," Sov. Astronomy - AJ 6, 77-83 (1962).

11. L. M. Biberman, G. E. Norman, and K. N. Ulyanov, "On the Calculation of Photoionization Absorption in Atomic Gases," Optics and Spectroscopy, 10, 297-299 (1961).

12. L. M. Biberman, Yu. N. Toropkin, and K. N. Ulyanov, "The Theory of Multistage Ionization and Recombination," Soc. Phys. - Tech. Phys. 7, 605-609 (1963).

13. D. Schlüter, "Die Berechnung der Übergangswahr scheinlichkeiten von Seriengrenzkontinua mit Anwendung auf die schweren Edelgase," Z. Astrophys. 61, 67-76 (1965).

14. G. O. Harding, "Laser Flashlamp Final Report," Contract Nonr-4122(00), PEK Labs. Inc., Sunnyvale, California.

15. L. Spitzer, Jr. and R. Härm, "Transport Phenomena in a Completely Ionized Gas," Phys. Rev., 89, 977-981 (1953).

16. R. S. Cohen, L. Spitzer, Jr. and P. Routly, "The Electrical Conductivity of an Ionized Gas," Phys. Rev., 80, 230-238 (1950).

17. J. Fay, "High Temperature Aspects of Hypersonic Flow," Ed. by W. C. Nelson, Pergamon Press Inc., New York (1964).

18. L. S. Frost and A. V. Phelps, "Momentum Transfer Cross Sections for Slow Electrons in He, Av, Kr, and Xe from Transport Coefficients," Phys. Rev. 136, A1538-A1545 (1964).

19. C. E. Moore, "Atomic Energy Levels," National Bureau of Standards Circular 467, Government Printing Office, Washington, D.C. (Vol. I, 1949; Vol. II, 1952; Vol. III, 1958).

20. D. R. Bates and A. Damgaard, "The Calculation of the Absolute Strengths of Spectral Lines," Phil. Trans. Roy. Soc. (London), 242A, 101-120 (1949).

21. "American Institute of Physics Handbook," 2nd Edition, edited by D. E. Gray, McGraw Hill Book Company, Inc., New York (1963).

22. K. Drellishak, C. Knopp, and A. B. Cambel, "Partition Functions and Thermodynamic Properties of Argon Plasma", Phys. Fluids 6, 1280-1288 (1963).

23. K. S. Drellishak, C. F. Knopp, and A. B. Cambel, "Partition Functions and Thermodynamic Properties of Argon Plasma" AEDC-TDR-63-146, Northwestern University, Evanston, Illinois (August 1963).

24. A. Burgess and M. J. Seaton, "A General Formula for the Calculation of Atomic Photo-Ionization Cross Sections," Mon. Not. Roy. Astron. Soc. 120, 121-151 (1960).

25. H. Griem, "High Density Corrections in Plasma Spectroscopy," Phys. Rev. 128, 997-1003 (1962).

26. M. McChesney and N. R. Jones, "Equilibrium Properties of Shock Ionized Xenon," Proc. Phys. Soc. 84, 983-1000 (1964).

27. H. Griem, Plasma Spectroscopy, McGraw-Hill Book Co., New York (1964).

28. K. S. Drellishak, "Partition Functions and Thermodynamic Properties of High Temperature Gases," AEDC-TDR-64-22, Northwestern University, Evanston, Illinois (January 1964).

29. H. R. Griem, "Stark Broadening of Isolated Spectral Lines in a Plasma," U.S. Naval Research Laboratory, NRL Report 6084 (June 1964), AD 443 76Z.

30. I. P. Shkarofsky, "The A.C. Conductivity of Air at Temperatures of 300-12,000^{o}K in the Presence of a Static Magnetic Field", Can. J. Phys.

31. L. Spitzer, Jr., Physics of Fully Ionized Gases, 2nd Edition, Interscience Publishers, John Wiley and Sons, Inc., New York (1962).

32. J. A. Fay and N. H. Kemp, "Theory of End Wall Heat Transfer in a Monatomic Gas, Including Ionization Effects," BSD-TDR-63-47, AVOC-Everett Research Laboratory (March 1963) AD 425461.

33. M. Camac, J. A. Fay, R. M. Feinberg, and N. H. Kemp, "Heat Transfer from High Temperature Argon," Proceedings of the 1963 Heat Transfer and Fluid Mechanics Institute, Stanford University Press (1963).

34. J. P. Reilly, "Stagnation-Point Heating in Ionized Monatomic Gases," Phys. Fluids 7, 1905-1912 (1964).

35. I. Amdur and E. A. Mason, "Properties of Gases at Very High Temperatures," Phys. Fluids 1, 370-383 (1959).

36. Private communication from Dr. E. Caproitti.

37. See for example J. C. Slater and N. H. Frank, "Electromagnetism," McGraw Hill Book Co., New York, p. 200-201, (1947).

38. S. Chandrasekar, "An Introduction to the Study of Stellar Structure," Dover, New York (1939).

39. R. M. Goody, Atmospheric Radiation, Vol. I, Theoretical Basis, Oxford Univ. Press, London (1964).

40. H. Mayer, "Opacity Calculations, Past and Future," J. Quant, Spect. Rad. Transfer 4, 585-95 (1964).

41. M. A. Lutz, "Radiant Energy Loss from a Cesium-Argon Plasma to an Infinite Plane Parallel Enclosure", BSD-TDR-64-6, AVOC Everett Research Laboratory (Sept. 1963). AD 431640.

42. W. Kaplan, "Advanced Calculus", Addison-Wesley Press Inc., Cambridge, Mass. (1952).

43. S. Chandrasekar, Radiative Transfer, Dover Publications, Inc., New York (1960).

44. M. Abramowitz and I. Stegun, Editors, "Handbook of Mathematical Functions with Formulas, Graphs, and Mathematical Tables," National Bureau of Standards Applied Methematical Series 55. U.S. Government Printing Office, Washington 20402 (June 1964).

APPENDIX A

RADIATION FLUX IN A NON-ISOTHERMAL NON-GREY CYLINDRICAL ARC

by

B. W. Swanson

Nomenclature

ΔA	element of area	cm^2
B_λ	Planck function $B_\lambda = \dfrac{2c^2h}{\lambda^5\left[\exp\left(\frac{ch}{\lambda k T}\right)-1\right]}$	(watt/cm^3)
$B[T]$	$B[T] = \int_0^\infty B_\lambda(T)\,d\lambda = \sigma' T^4/\pi$	(watt/cm^2)
$B[s]$	$B[s] = B[T(s)]$	(watt/cm^2)
b	constant in equation 44	
C_1	integration constant in equation 20	
c	velocity of light $c = 3.0 \times 10^{10}$ cm/sec	
$d\omega$	differential element of solid angle	
d_λ	differential element of wavelength	(cm)
ds	differential element of length along a ray	(cm)
E	electric field	(volts/cm)
F(r)	radiation flux; equation 16	(watts/cm^2)
$\hat{F}(r)$	approximate radiation flux; equation 42	(watts/cm^2)
f_1	$f_1 = -\sin\theta\cos\phi\cos\theta' - \sin\theta\sin\phi\sin\theta'$	
f_2	$f_2 = \sin\theta\cos\phi\sin\theta' - \sin\theta\sin\phi\cos\theta'$	
f_3	$f_3 = -\cos\theta$	
$G_n(x)$	$G_n(x) = \int_0^{\frac{\pi}{2}} e^{-\frac{x}{\sin\theta}} (\sin\theta)^n d\theta$	

Nomenclature (cont'd)

h	Plancks constant $h = 6.625 \times 10^{-34}$ watt sec^2	
$I_\lambda(r,\vec{\omega})$	intensity of radiation at r in direction $\vec{\omega}$; equation 5	(watts/cm^3)
$\vec{i}$	unit vector along x axis	
$\vec{j}$	unit vector along y axis	
$\vec{k}$	unit vector along z axis	
$\bar{K}$	constant absorption coefficient	(cm^{-1})
$\bar{K}$	Boltzmann constant $\bar{K} = 1.380 \times 10^{-23}$	(watt sec/deg)
K_P	Planck mean absorption coefficient $K_P(T) = \dfrac{\int_0^\infty k_\lambda(T) B_\lambda(T) d\lambda}{B(T)}$	(cm^{-1})
K	thermal conductivity	(watt/cm deg)
K_R	Rosseland mean absorption coefficient; equation 48	(cm^{-1})
K_a	mean absorption coefficient; equation 44	(cm^{-1})
M	projection of point Q into x-y plane; Figure 1	
$\vec{n}$	unit vector normal to $\triangle A$	
Q	intersection of ray with arc boundary; Figure 1	
R	point internal to arc; Figure 1	
r	radial coordinate	(cm)
R_A	arc radius	(cm)

Nomenclature (cont'd)

$\vec{R}_{OM}$	radial vector from origin to point M	
$\vec{R}_{OR}$	radial vector from origin to point R	
$\vec{R}_{OS}$	radial vector from origin to point s on ray R-M; Figure 1	
R_o	$R_o = \lvert \vec{R}_{or} \rvert$	(cm)
$\vec{R}_{RM}$	vector from point R to point M along ray R-M; Figure 1	
$\vec{R}_{RS}$	vector from point R to point s along ray R-M; Figure 1	
R_M	$R_M = \lvert \vec{R}_{RM} \rvert$	(cm)
R_Q	length of ray Q-R	(cm)
$\vec{r}$	cylindrical coordinate unit vector; Figure 1	
s''	variable of integration	
s'	point on ray Q-R; Figure 1	
s	distance along ray R-M; Figure 1	(cm)
Δt	differential time increment; equation 5	(sec)
T	arc temperature	(°K)
$T(s)$	temperature at point s on ray R-M	(°K)
T_o	constant temperature	(°K)
α	angle between vectors $\vec{R}_{OR}$ and $\vec{R}_{OM}$; Figure 1	
θ'	cylindrical coordinate; Figure 1	(radian)
θ	spherical coordinate; Figure 1	(radian)
$\vec{\theta}$	cylindrical coordinate unit vector; Figure 1	
χ_λ	absorption coefficient	(cm^{-1})

Nomenclature (cont'd)

$\overline{\kappa}_\lambda$	average absorption coefficient	(cm^{-1})
λ	wavelength of radiation	(cm)
λ_{min}	minimum wavelength for numerical integration	(cm)
λ_{max}	maximum wavelength for numerical integration	(cm)
s	variable of integration	
σ	electrical conductivity	$(ohm\text{-}cm)^{-1}$
σ'	Stefan Boltzmann constant $\sigma' = 5.6686 \times 10^{-12}$ watts/cm^2 deg^{-4}	
$\tilde{\tau}_P(s)$	Planck optical length along ray M-R; equation 46	
$\tilde{\tau}_\lambda$	optical thickness	
$\tilde{\tau}_R(s)$	Rosseland optical length along ray M-R; equation 45	
ϕ	spherical coordinate; Figure 1	(radian)
$\vec{\omega}$	unit direction vector along ray Q-R; Figure 1	
γ	angle between vectors $\vec{n}$ and $\vec{\omega}$	

Scientific Paper 65-8D8-GASDY-P1 November 1, 1965
PROPRIETARY CLASS 3 Mod.

RADIATION FLUX IN A NON-ISOTHERMAL NON-GREY CYLINDRICAL ARC*

B. W. Swanson

Abstract

In a study of highly radiative arc discharges, an analysis has been made for determining the radiation flux (i.e., radiant emittance) throughout the interior of a non-grey cylindrical arc. These flux calculations are necessary to determine the divergence of the flux which is needed to obtain a solution of the integro-differential arc energy equation. The flux is expressed as a triple integral where the integrand is the product of absorption coefficient, Planck function and an attenuation factor which involves a line integral of the absorptivity. A computer program performs the integration with respect to wavelength, a spherical coordinate and the distance along a radiation vector. Separate programs calculate the spectral absorptivities and transport properties for use in the flux program. The cases to be discussed include only the free-free and bound-free continuum. Radial flux distributions are presented for xenon at pressures of 15 and 20 atmospheres for the following temperature distributions: (a) isothermal arcs at 20,000°K and 15,000°K; (b) linear arcs from 15,000°K to 12,000°K and 2000°K; (c) a non-linear "parabolic" arc from 15,000°K to 5000°K.

* This research is part of Project DEFENDER under joint sponsorship of the Advanced Research Projects Agency, the Office of Naval Research, and the Department of Defense.

Introduction

Neglecting convection, the steady state energy equation for an arc is given by

$$\vec{\nabla}\cdot(K\vec{\nabla}T) - \vec{\nabla}\cdot\vec{F} + \sigma(P,T)E^2 = 0 \qquad (1)$$

where $\vec{F}$ is the radiation flux vector, K(T) the thermal conductivity, T the arc temperature, σ the electrical conductivity, P the arc pressure and E the electric field. In addition the arc temperature must satisfy certain boundary conditions which depend upon the application. In turn the divergence of F is given by*

$$\vec{\nabla}\cdot\vec{F} = 4\pi\int_0^\infty \kappa_\lambda(T)B_\lambda(T)\,d\lambda - \int_0^\infty \kappa_\lambda \int_{\omega=4\pi} I_\lambda\,d\omega\,d\lambda + \frac{F}{r} \qquad (2)$$

where κ_λ is the non-grey absorption coefficient, B_λ the Planck function, I_λ the intensity of radiation and F the radiation flux. Equation 1 is an integro-differential equation which can be solved using an iteration technique. In the iteration process, a temperature distribution is assumed, and the flux F and the second integral in equation 2 are evaluated as functions of r. Equation 1 is then solved for a new temperature distribution and this process repeated until the temperature solutions converge. If the axis temperature is held constant, a value of E is associated with each temperature solution and the values of E also converge. To obtain an arc temperature distribution, it is therefore necessary to calculate the flux as a function of radial position. This paper is concerned with making

---

* Appendix

flux calculations for a non-grey cylindrical xenon arc for several assumed temperature distributions. Future work will employ the flux program to solve the arc energy equation.

Radiation Flux Integral

The flux vector $\vec{F}$ is defined by the equation

$$\vec{F}(r, \theta', z) = \int_0^\infty \vec{F}_\lambda (r, \theta', z)\, d\lambda \tag{3}$$

where λ is the wavelength and r and θ' are cylindrical coordinates. In turn, F_λ is given by

$$\vec{F}_\lambda (r, \theta', z) = \int_{\omega = 4\pi} I_\lambda (r, \theta', z, \vec{\omega})\, \vec{\omega}\, d\omega \tag{4}$$

where $\vec{\omega}$ is a unit direction vector and $I_\lambda (r,\theta',z,\vec{\omega})$ is the monochromatic intensity of radiation. In general the intensity I_λ depends on position coordinates r,θ',z and the direction signified by the vector $\vec{\omega}$. To define I_λ, let ΔA denote a small element of area; $\vec{n}$ the outward drawn normal vector to ΔA; $\vec{\omega}$ a vector enclosed by a solid angle $\Delta\omega$ which makes an angle γ with $\vec{n}$; $\Delta\lambda$ the wavelength interval between λ and $\lambda + \Delta\lambda$; and Δq_r the amount of radiant energy in the interval $\Delta\lambda$ which is transferred across ΔA, confined to the solid angle $\Delta\omega$ during the time interval Δt. Then I_λ is given by the following limit:[1]

$$I_\lambda (r, \theta', z, \vec{\omega}) = \lim_{\Delta A, \Delta t, \Delta\omega, \Delta\lambda \to 0} \left| \frac{\Delta q_r}{(\cos\gamma)\Delta A \Delta\omega \Delta t \Delta\lambda} \right| \tag{5}$$

In Figure 1 is shown a point R in the arc with coordinates r,θ', 0. Through R is drawn a ray defined by the spherical coordinates ϕ and θ which intersects the arc boundary at point Q. The integration of all radiation contributions from points on the ray from Q to R defines the intensity $I_\lambda(r,\theta',0,\vec{\omega})$ in the direction $\vec{\omega}$ along the ray. Because of the definitions of θ and ϕ, the vector $\vec{\omega}$ is given by

$$\vec{\omega} = -\sin\theta\cos\phi\,\vec{i} - \sin\theta\sin\phi\,\vec{j} - \cos\theta\,\vec{k} \tag{6}$$

Expressing the Cartesian vectors $\vec{i}$ and $\vec{j}$ in terms of the cylindrical vectors $\vec{r}$ and $\vec{\theta}$

$$\vec{i} = \vec{r}\cos\theta' - \vec{\theta}\sin\theta' \tag{7}$$

and

$$\vec{j} = \vec{r}\sin\theta' + \vec{\theta}\cos\theta' \tag{8}$$

The vector $\vec{\omega}$ in terms of $\vec{r}$, $\vec{\theta}$ and $\vec{k}$ is given by

$$\vec{\omega} = f_1\vec{r} + f_2\vec{\theta} + f_3\vec{k} \tag{9}$$

where

$$f_1 = -\sin\theta\cos\phi\cos\theta' - \sin\theta\sin\phi\sin\theta' \tag{10}$$

$$f_2 = \sin\theta\cos\phi\sin\theta' - \sin\theta\sin\phi\cos\theta' \tag{11}$$

$$f_3 = -\cos\theta \tag{12}$$

Using equation 9, equation 4 becomes

$$\vec{F}_\lambda(r,\theta',z) = \vec{r}\int_{\omega=4\pi} I_\lambda f_1 d\omega + \vec{\theta}\int_{\omega=4\pi} I_\lambda f_2 d\omega + \vec{k}\int_{\omega=4\pi} I_\lambda f_3 d\omega \qquad (13)$$

Assuming a symmetrical temperature distribution, the $\vec{\theta}$ and $\vec{k}$ components of F_λ must vanish. Hence

$$\vec{F}_\lambda(r,\theta',z) = \vec{F}_\lambda(r) = \vec{r}\int_{\omega=4\pi} I_\lambda f_1 d\omega = \vec{r}\, F_\lambda(r) \qquad (14)$$

Then

$$\vec{F} = \vec{r}\, F(r) \qquad (15)$$

where

$$F(r) = \int_0^\infty \int_{\omega=4\pi} I_\lambda f_1 d\omega\, d\lambda \qquad (16)$$

For convenience θ' may be set equal to zero. Since $d\omega = \sin\theta d\theta d\phi$, and making use of symmetry, equation 16 becomes

$$F(r) = -4\int_0^\infty \int_0^\pi \int_0^{\pi/2} I_\lambda \sin^2\theta \cos\phi\, d\theta d\phi\, d\lambda \qquad (17)$$

An expression is now needed for $I_\lambda(r,\theta,\phi)$ In Figure 1, let s' represent a point along the ray from Q to R. The intensity satisfies the transfer equation

$$\frac{dI_\lambda}{ds'} = -K_\lambda(s')I_\lambda(s') + K_\lambda(s')B_\lambda(s') \qquad (18)$$

where the Planck function B_λ is given by

$$B_\lambda(T) = \frac{2c^2h}{\lambda^5\left[\exp\left(\frac{ch}{\lambda\bar{k}T}\right) - 1\right]} \qquad (19)$$

where c is the velocity of light, and $\bar{k}$ and h are the Boltzmann and Planck constants respectively. Implicit in equation 18 is the assumption that the gas is non-scattering. An integrating factor of equation 18 is $e^{\int_0^{s'} K_\lambda ds}$.

Carrying out the integration yields

$$I_\lambda(s) = C_1 e^{-\int_0^s K_\lambda ds''} + \int_0^s K_\lambda(s')B_\lambda(s') e^{-\int_{s'}^s K_\lambda ds''} ds' \qquad (20)$$

where C_1 is a constant of integration which equals the intensity at $s' = 0$. Referring to Figure 1, $s' = 0$ corresponds to point Q and $s' = s$ corresponds to point R. The initial intensity of radiation entering the arc at point Q is assumed to be zero which makes C_1 zero. In the numerical integration, it is more convenient to reverse the integration and to let $s' = 0$ correspond to point R. Letting R_Q denote the length of the ray from R to Q, the intensity at R in the direction $\vec{\omega}$ can be written as

$$I_\lambda(R, \vec{\omega}) = \int_0^{R_Q} K_\lambda(s')B_\lambda(s') e^{-\int_0^{s'} K_\lambda(s'') ds''} ds' \qquad (21)$$

Using equation 21, equation 17 becomes

$$F(R) = -4\int_0^{\infty}\int_0^{\pi}\int_0^{\pi/2}\int_0^{R_Q} \kappa_\lambda(s')B_\lambda(s')\, e^{-\int_0^{s'}\kappa_\lambda(s'')ds''}\, ds'\sin^2\theta\cos\phi\, d\theta d\phi d\lambda \tag{22}$$

Equation 22 can be further simplified. Referring to Figure 1, consider point s' on the ray from Q to R, and its projection s on the ray from M to R. Point M is the projection of point Q onto the x-y plane. Since ds' = ds/sinθ, then

$$\int_0^{s'}\kappa_\lambda(s'')ds'' = \int_0^{s}\frac{\kappa_\lambda(s'')ds''}{\sin\theta} \tag{23}$$

Furthermore, letting $\beta_\lambda(s) = \int_0^s \kappa_\lambda(s'')ds''$, equation 22 can be written as

$$F(R) = -4\int_0^{\infty}\int_0^{\pi}\int_0^{\pi/2}\int_0^{R_M(\phi)} \kappa_\lambda(s)B_\lambda(s)\, e^{-\frac{\beta_\lambda(s)}{\sin\theta}}\sin\theta\cos\phi\, ds\, d\theta d\phi d\lambda \tag{24}$$

where R_M is the length of the ray from M to R and is a function of ϕ. Defining the function $G_n(x)$ by the equation

$$G_n(x) = \int_0^{\pi/2} e^{-\frac{x}{\sin\theta}}(\sin\theta)^n d\theta \tag{25}$$

and interchanging the orders of integration with respect to θ and s in equation 24 yields

$$F(R) = -4\int_0^{\infty}\int_0^{\pi}\int_0^{R_M(\phi)} \kappa_\lambda(s)B_\lambda(s)\, G_1[\beta_\lambda(s)]\cos\phi\, ds\, d\phi d\lambda \tag{26}$$

Equation 26 is the desired integral expression for the flux as a function of radial position. In analyzing the radiation from an axisymmetric rocket engine plume, deSoto[2] evaluated an integral similar to the one in equation 22. For the arc, the cylindrical geometry permits equation 22 to be reduced to equation 26. To evaluate this integral, it is necessary to know how R_M varies with ϕ, and for a given ϕ, how temperature varies with s along the ray.

Arc Geometry

The coordinate system in Figure 1 is redrawn in Figure 2 with θ' set equal to zero. Let $\vec{R}_{OM}$ and $\vec{R}_{OR}$ denote vectors from the origin to points M and R respectively, and $\vec{R}_{RM}$ the vector from R to M. Furthermore let R_A denote the radius of the arc, i.e. $R_A = |\vec{R}_{OM}|$. Then

$$\vec{R}_{OM} = R_A \cos\alpha\, \vec{r} + R_A \sin\alpha\, \vec{\theta} \tag{27}$$

and

$$\vec{R}_{OR} = R_o \vec{r} \tag{28}$$

where $R_o = |\vec{R}_{OR}|$

Solving for $\vec{R}_{RM}$ from the vector equation

$$\vec{R}_{OR} + \vec{R}_{RM} = \vec{R}_{OM} \tag{29}$$

gives

$$\vec{R}_{RM} = (R_A \cos\alpha - R_o)\vec{r} + R_A \sin\alpha\, \vec{\theta} \tag{30}$$

and

$$R_M = |\vec{R}_{RM}| = \left[(R_A \cos\alpha - R_o)^2 + (R_A \sin\alpha)^2\right]^{\frac{1}{2}} \tag{31}$$

To determine R_M as a function of ϕ it is necessary to determine α as a function of ϕ. From Figure 2

$$\tan\phi = \frac{R_A \sin\alpha}{R_A \cos\alpha - R_o} \tag{32}$$

which yields the equation

$$\cos\alpha = \frac{\left(\frac{R_o}{R_A}\right)\tan^2\phi \pm \sqrt{1+(\tan^2\phi)\left(1-\left(\frac{R_o}{R_A}\right)^2\right)}}{1+\tan^2\phi} \tag{33}$$

Two values of α are calculated from equation 33, the correct one being that value which also satisfies equation 32.

To evaluate the integrand $\kappa_\lambda(s)\, B_\lambda(s)\, G_\perp(\beta_\lambda(s))$ in equation 38, it is necessary to know the temperature distribution $T(s)$ along the ray defined by ϕ. A unit vector along the ray from R to M is given by $\vec{R}_{RM}/R_M$. Let $\vec{R}_{OS}$ and $\vec{R}_{RS}$ be vectors from the origin and point R to a point s on the vector $\vec{R}_{RM}$. Then

$$\vec{R}_{RS} = s\,\frac{\vec{R}_{RM}}{R_M} \tag{34}$$

where s denotes distance along the vector $\vec{R}_{RM}$ and

$$\vec{R}_{OS} = \vec{R}_{OR} + \vec{R}_{RS} \tag{35}$$

or

$$\vec{R}_{OS} = R_O \vec{r} + \frac{S}{R_M}\left[(R_A \cos\alpha - R_O)\vec{r} + R_A \sin\alpha\, \vec{\theta}\right] \quad (36)$$

Solving for $|\vec{R}_{OS}|$,

$$|\vec{R}_{OS}| = \left[\left(R_O + \frac{S}{R_M}(R_A\cos\alpha - R_O)\right)^2 + \left(\frac{S}{R_M}R_A\sin\alpha\right)^2\right]^{\frac{1}{2}} \quad (37)$$

Assuming that the radial temperature distribution $T(r)$ is known for $0 \leqq r \leqq R_A$, the value of $T(s)$ for a given value of s is defined by

$$T(s) = T\left[|\vec{R}_{OS}|\right] \quad (38)$$

Knowing $R_M(\phi)$ and $T(s)$, the integral in equation 26 can be evaluated.

As an aid in checking the computer program, it is convenient to consider the case of a grey isothermal arc. Let

$$\begin{aligned} \chi_\lambda &= K = \text{constant} \\ T(r) &= T_O = \text{constant} \end{aligned} \quad (39)$$

Then equation 26 reduces to

$$F(R) = \frac{4\sigma' T_O^4}{\pi}\int_0^{\pi} G_2\left[K R_M(\phi)\right]\cos\phi\, d\phi \quad (40)$$

Equation 40 was programmed and used to check the flux program for the evaluation of equation 26, under the conditions of equation 39.

Flux Approximation

Before discussing flux computations for assumed temperature distributions, a word is in order on making approximate flux calculations. On a Burroughs B-5000 computer, it takes an average of 100 seconds to evaluate equation 26 for one value of r. Based on present computing rates, the corresponding cost is approximately $10 per point. If the flux is evaluated at 10 points to compute a radial distribution, the cost of a flux distribution for an assumed temperature distribution is of the order of $100. Since it is not known a'priori how many iterations of equation 1 are needed to obtain a convergent solution, it is obvious that computing costs could become prohibitive. It is therefore necessary to consider the possibility of making approximate flux calculations.

For the case of a plane-parallel geometry, Sampson[3] used the general grey gas expression for the flux, but chose the mean absorption coefficient to be functions of the Planck and Rosseland mean absorption coefficients and the optical depth. By using Planck and Rosseland means, the integration with respect to wavelength is eliminated which significantly reduces machine time. Sampson's flux approximation is exact in the limits of very optically thin and very optically thick gases. For a non-grey gas of intermediate optical thickness, he found that exact and approximate flux calculations differed by no more than a factor of two. For a cylindrical geometry, the radiative intensity I_λ must be approximated instead of the flux, and the flux then obtained from the equation

$$F(r) = \int_0^\infty \int_{\omega=4\pi} I_\lambda \vec{\omega} \, d\omega \, d\lambda \qquad (41)$$

Following Sampson, approximations[4] have been obtained for the radiative intensity and the flux. The quality of the approximation has not yet been checked, but if it is comparable to Sampson's, it will be useful in making temperature calculations with a significant reduction in cost.

Only the results of this approximation analysis are presented here. The approximate flux is given by the equation

$$\hat{F}(r) = -4\int_0^{\pi}\int_0^{R_M(\phi)} \kappa_a(s)\, B(s)\, G_1\left[\int_s^{R_M(\phi)} \kappa_a(\xi)\,d\xi\right] \cos\phi\, ds\, d\phi \qquad (42)$$

where B(s) is given by

$$B(s) = \int_0^{\infty} B_\lambda[T(s)]\,d\lambda = \frac{\sigma' T^4(s)}{\pi} \qquad (43)$$

and the mean absorption coefficient $\kappa_a(s)$ is defined by the equation

$$\kappa_a(s) = \left[\frac{b}{b+\tau_p(s)}\right]\left[\frac{b+\tau_R(s)}{b+\tau_p(s)}\right]\kappa_p(s) + \left[\frac{\tau_p(s)}{b+\tau_p(s)}\right]\kappa_R(s) \qquad (44)$$

The term b is a constant of the order of unity which can be varied to improve the approximation.

The terms $\tau_R(s)$ and $\tau_P(s)$ are the Rosseland and Planck optical lengths along the ray from point M to point R in Figure 2, and are given by

$$\tau_R(s) = \int_0^s \kappa_R(\xi)\,d\xi \qquad (45)$$

$$\tau_p(s) = \int_0^s \kappa_p(\xi)\,d\xi \qquad (46)$$

where the Planck and Rosseland absorption coefficients are given by

$$\kappa_P(T) = \frac{\int_0^\infty \kappa_\lambda(T)\, B_\lambda(T)\, d\lambda}{\frac{\sigma' T^4}{\pi}} \tag{47}$$

and

$$\kappa_R(T)^{-1} = \frac{\int_0^\infty \frac{1}{\kappa_\lambda(T)} \frac{dB_\lambda}{dT}\, d\lambda}{\frac{4\sigma' T^3}{\pi}} \tag{48}$$

In equation 42, 45 and 46, s = 0 corresponds to point M in Figure 1, and therefore the integration proceeds along a ray from the arc exterior to an internal point R. When $s = R_M$, τ_P and τ_R represent optical thicknesses of the arc in the direction of the angle ϕ. Depending on the temperature distribution, pressure and location of the point R, the arc could be optically thin when $\phi = 0$ and optically thick when $\phi = \pi$. The dependence of the optical thickness on the angle ϕ is a characteristic of the cylindrical geometry.

Under optically thin conditions, when τ_P and τ_R are much less than unity, the mean absorption coefficient κ_a approaches the Planck absorption coefficient κ_P and equation 42 is exact.

Under optically thick conditions when τ_P and τ_R are both much greater than unity, κ_a approaches the Rosseland mean κ_R and equation 42 is a good approximation. The quality of the approximation afforded by equation 42 when the rays are neither optically thin nor thick will be determined by comparison with exact flux calculations.

Results

The purpose of this investigation is to determine radiant flux distributions throughout an arc corresponding to hypothetical temperature distributions. Calculations have been made for xenon at pressures of 15 and 50 atmospheres.

In Figures 3, 4, 5, and 6 the absorption coefficient of xenon is plotted versus wavelength for pressures of 15 and 50 atmospheres and for temperatures of 5,000°, 10,000°, 15,000° and 20,000°K respectively. These continuum absorptivities were calculated by Messrs. Church and Schlect[5] following the theory of Biberman and Norman[6,7] and Yankov[8], using partition functions and particle densities derived from a modification of Drellishaks[9,10,11] procedure. A separate computer program was written for the absorptivity calculations and the computed absorptivities stored on disc for the flux program.

The optical thickness τ_λ is defined by the equation

$$\tau_\lambda = \int_0^{R_M(\phi)} K_\lambda(s)\,ds \cong \overline{K}_\lambda\, R_M(\phi) \qquad (49)$$

From Figure 3, for a pressure of 50 atmospheres, $\overline{K}_\lambda$ is of the order of 1×10^{-6} cm^{-1}. If the arc radius is one centimeter, and $R_M(\phi)$ is of the order of one centimeter, $\tau_\lambda << 1$ and a 5000°K arc is optically thin in all radial directions. From Figure 5, for a pressure of 50 atmospheres, $\overline{K}_\lambda$ is of the order of 10 and $\tau_\lambda >> 1$ so that a 15,000°K arc is optically thick in all radial directions. Between 10,000°K and 15,000°K the arc is neither optically thin nor thick. Furthermore between 5,000°K and 15,000°K, the absorptivity varies by eight orders of magnitude.

For the flux calculations, isothermal, linear and "parabolic" temperature distributions were assumed. Although the arc temperature is always conduction controlled near the flashtube wall, under certain conditions the arc may be fairly isothermal. In general, the arc temperature would be expected to be "parabolic", but a combination of isothermal and linear profiles might be used to bound the flux distribution.

In Figure 7 the flux distribution is shown for an isothermal arc of 20,000°K at a pressure of 50 atmospheres. From equation 26, when r = 0, $R_M(\phi)$ is equal to the arc radius for all values of ϕ and the flux must

vanish. From Figure 6, $\bar{\kappa}_\lambda$ is of the order of 5 cm^{-1}. Letting $\bar{\kappa}_\lambda = \bar{\kappa}$, then from equation 40, the shape of the flux curve is essentially determined by the integral $\int_0^{\pi} G_2[\bar{\kappa} R_m(\phi)] \cos\phi \, d\phi$

In Figure 8 are shown two temperature profiles T_1 and T_2 and the corresponding flux distributions F_1 and F_2. Temperature T_1 is constant at 20,000°K up to r = 0.9 cm where it drops linearly to 2000°K at r = 1.0 cm. This temperature profile to some extent simulates the effect of a thermal conduction layer near the arc boundary. The corresponding flux distribution F_1 follows the flux distribution of Figure 7 until the "conduction layer" reduces its boundary value. Temperature T_2 decreases linearly from 20,000°K at r = 0 to 2000°K at r = 1.0 cm. Both flux distributions F_1 and F_2 assume maximum values at interior points.

In Figure 9 the flux distribution is shown for an isothermal arc at 15,000°K. The fluxes in Figures 7 and 9 are almost in the ratio of $(20,000/15,000)^4$ as would be expected from equation 40 since the "average" absorptivities are approximately equal, i.e., of the order of 5 to 6 cm^{-1}.

In Figure 10, the temperature varies linearly from 15,000°K at r = 0 to 12,000°K at r = 1.0 cm, and fluxes are shown for pressures of 15 and 50 atmospheres. An inspection of Figures 3 to 6 shows that the absorptivity for 15 atmospheres is always less than that for 50 atmospheres. From equation 26, the integrand $\kappa_\lambda(s) B_\lambda(s) G_1[\beta_\lambda(s)]$ gives the amount of radiation leaving a point s which arrives at a fixed point R. The Planck function $B_\lambda(s)$ is independent of pressure. Therefore, two arcs with the same temperature distribution, but at different pressures, will have different flux distributions because of differences in the product $\kappa_\lambda G_1[\beta_\lambda(s)]$. The term $\kappa_\lambda(s) G_1[\beta_\lambda(s)]$ behaves like the function $\kappa_\lambda e^{-\bar{\kappa}_\lambda s}$ which approaches zero for small and large values of κ_λ and which has a maximum for some value κ_λ^*. For a given s, if $\kappa_\lambda < \kappa_\lambda^*$, a reduction in κ_λ due to a reduction in pressure causes a reduction in the amount of radiation leaving s and arriving at point R. Therefore, the overall effect of a reduction in pressure is a reduction in flux distribution.

In Figure 11, the temperature varies linearly from 15,000°K to 2000°K. As in Figure 10, the flux at 15 atmospheres is less than the flux at 50 atmospheres for the reasons just given.

The last temperature distribution is shown in Figure 12. This "parabolic" temperature profile was observed in a nitrogen arc by Schmitz[12] and is most likely to occur in xenon. The flux distribution for 15 atmospheres is again less than that for 50 atmospheres and both flux profiles have maxima, which is characteristic of wall cooling effects.

These hypothetical temperature profiles have been used to illustrate radial flux computations for a one centimeter xenon arc. For operating conditions that could produce an isothermal arc with a thin conduction layer, or a "parabolic" arc, the value of the flux at r = 1.0 cm gives the radiation of the arc to its surroundings.

For the arc temperature in Figure 8, the arc radiation is 50×10^4 watts/cm^2 which is equivalent to 1.59×10^9 Btu/hr ft^2. Therefore, radiation from high pressure-high temperature self-absorbing arcs can be significant.

Acknowledgements

The author wishes to acknowledge the efficient computer programming by Mrs. E. Geil and Mr. B. Wang of the Computer Sciences Department, Westinghouse Research Laboratories.

Appendix A

Evaluation of $\vec{\nabla} \cdot \vec{F}$

From equation 14,

$$\vec{F}_\lambda = \int_{\omega=4\pi} \vec{r}\, I_\lambda f_1 \, d\omega \tag{A-1}$$

Taking the divergence of both sides of equation A-1

$$\vec{\nabla} \cdot \vec{F}_\lambda = \int_{\omega=4\pi} \vec{\nabla} \cdot (\vec{r}\, I_\lambda) f_1 \, d\omega \tag{A-2}$$

or

$$\vec{\nabla} \cdot \vec{F}_\lambda = \int_{\omega=4\pi} f_1 I_\lambda \vec{\nabla} \cdot \vec{r}\, d\omega + \int_{\omega=4\pi} f_1 \vec{r} \cdot \vec{\nabla} I_\lambda \, d\omega \tag{A-3}$$

In cylindrical coordinates

$$\vec{\nabla} \cdot \vec{r} = \frac{1}{r} \tag{A-4}$$

Since the arc is symmetrical,

$$\vec{\nabla} I_\lambda = \vec{r}\, \frac{dI_\lambda}{dr} \tag{A-5}$$

and

$$\vec{r} \cdot \vec{\nabla} I_\lambda = \frac{dI_\lambda}{dr} \tag{A-6}$$

Now from equation 9,

$$\vec{\omega} = f_1 \vec{r} + f_2 \vec{\theta} + f_3 \vec{\pi} \tag{A-7}$$

and

$$\vec{\omega} \cdot \vec{\nabla} I_\lambda = \frac{dI_\lambda}{ds} = f_1 \frac{dI_\lambda}{dr} \tag{A-8}$$

Using equations A-4, A-6 and A-8, equation A-3 becomes

$$\vec{\nabla} \cdot \vec{F_\lambda} = \frac{1}{r} \int_{\omega=4\pi} f_1 I_\lambda d\omega + \int_{\omega=4\pi} \frac{dI_\lambda}{ds} d\omega \tag{A-9}$$

From equation 18,

$$\frac{dI_\lambda}{ds} = K_{1\lambda} B_\lambda - K_\lambda I_\lambda \tag{A-10}$$

and from equation 14

$$F_\lambda(r) = \int_{\omega=4\pi} I_\lambda f_1 d\omega \tag{A-11}$$

Using equations A-10 and A-11, A-9 becomes

$$\vec{\nabla} \cdot \vec{F}_\lambda = 4\pi \kappa_\lambda B_\lambda - \kappa_\lambda \int_{\omega=4\pi} I_\lambda d\omega + \frac{F_\lambda}{r} \qquad \text{(A-12)}$$

Since

$$F(r) = \int_0^\infty F_\lambda(r)\, dr \qquad \text{(A-13)}$$

integrating equation A-12 with respect to λ from 0 to ∞ yields

$$\vec{\nabla} \cdot \vec{F} = 4\pi \int_0^\infty \kappa_\lambda B_\lambda d\lambda - \int_0^\infty \kappa_\lambda \int_{\omega=4\pi} I_\lambda d\omega d\lambda + \frac{F(r)}{r} \qquad \text{(A-14)}$$

also, since

$$\vec{\nabla} \cdot \vec{F} = \frac{dF}{dr} + \frac{F}{r} \qquad \text{(A-15)}$$

it follows from equation A-14 that

$$\frac{dF}{dr} = 4\pi \int_0^\infty \kappa_\lambda B_\lambda d\lambda - \int_0^\infty \kappa_\lambda \int_{\omega=4\pi} I_\lambda d\omega d\lambda \qquad \text{(A-16)}$$

References

1) R. Viskanta, "Heat Transfer in Thermal Radiation Absorbing and Scattering Media," Dissertation, 1960, University Microfilms, Inc., Ann Arbor, Michigan.

2) S. deSoto, "The Radiation from an Axisymmetric, Real Gas System with a Non-Isothermal Temperature Distribution," A.I.Ch.E.-A.S.M.E. Heat Transfer Conference, August 1964.

3) D. H. Sampson, "Choice of an Appropriate Mean Absorption Coefficient for Use in the General Grey Gas Equations," General Electric Space Sciences Lab., Report R64SD77, November 1964.

4) B. W. Swanson, "Radiation Flux Approximation in a Non-Grey Cylindrical Arc," Westinghouse Research Report 65-8D8-GASDY-R1, 1965 (unpublished)

5) C. H. Church, R. G. Schlect, "Arc Discharge Radiation Sources for the Infrared - Some Simple Models," Westinghouse Scientific Paper 65-9C1-148-P3, 1965.

6) L. Biberman and G. Norman, "Plasma Radiation Due to Recombination and Bremstrahlung Processes," J. Quant. Spect. Rad. Transfer 3, 221-245 (1963) General Atomics - San Diego Translation GA tr 4943.

7) L. M. Biberman, Yu. N. Toropkin, and K. N. Ulyanov, "The Theory of Multistage Ionization and Recombination," Sov. Phys. - Tech Phys. 7, 605-609 (1963).

8) V. V. Yankov, "On the Distribution of Energy in the Continuous Absorption Spectrum of Xenon," Optics and Spectroscopy 14, 14-17 (1963).

9) K. Drellishak, C. Knopp, and A. B. Cambel, "Partition Functions and Thermodynamic Properties of Argon Plasma," Phys. Fluids 6, 1280-1288 (1963).

10) K. S. Drellishak, C. F. Knopp, and A. B. Cambel, "Partition Functions and Thermodynamic Properties of Argon Plasma," AEDC-TDR-146, Northwestern University, Evanston, Illinois, August 1963.

11) C. H. Church and R. G. Schlect, "Arc Discharge Sources," Semi-Annual Technical Report in Contract NONR 4647(00), Westinghouse Research Laboratories, Pittsburgh, Pennsylvania, May 15, 1965.

12) G. Schmitz, "The Profile of the Arc Column," Aeronautical Research Laboratories Report ARL 62-401, August 1962.

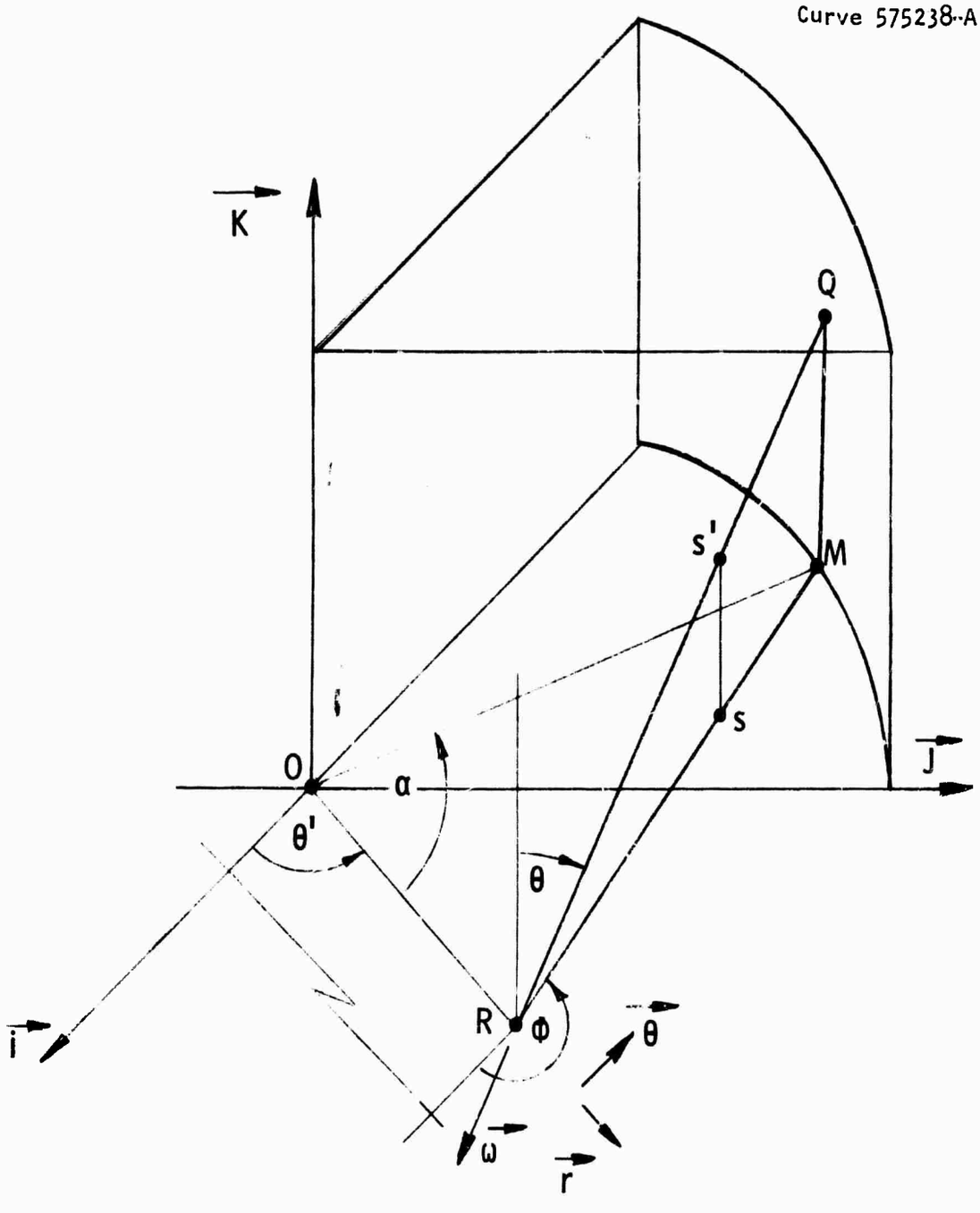

Fig. 1—Arc geometry

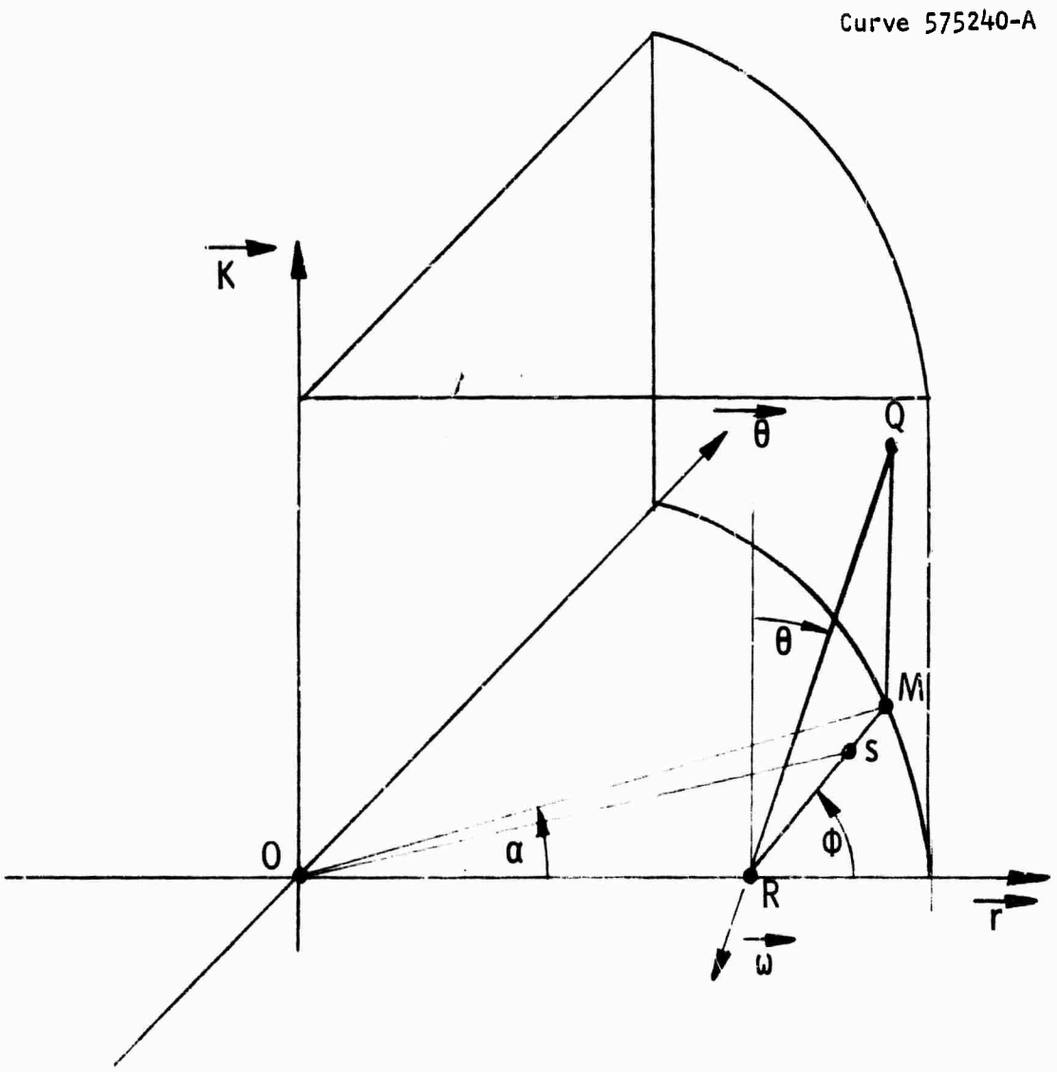

Fig. 2—Arc geometry with $\theta' = 0$

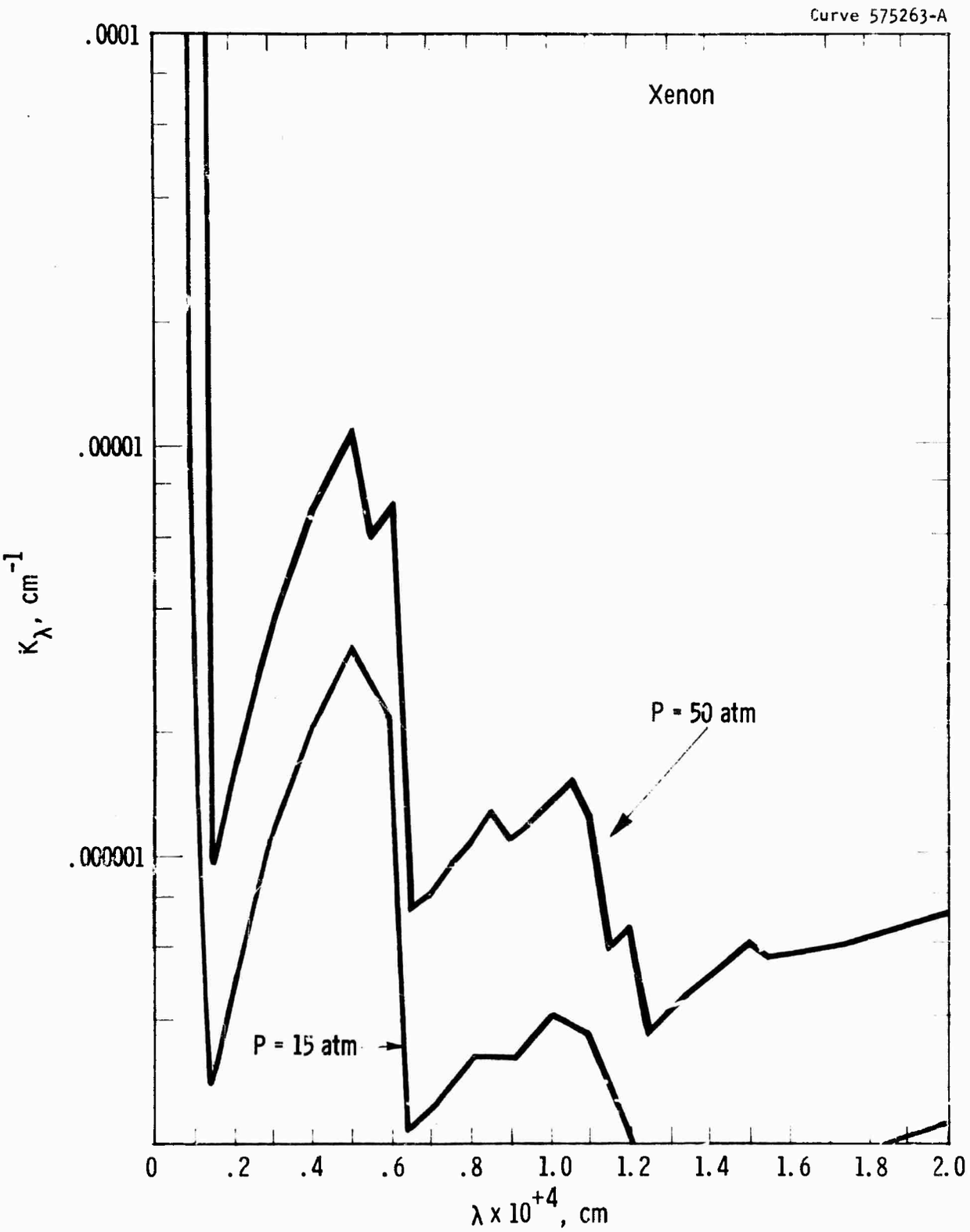

Fig. 3—Absorption coefficient vs wavelength: T = 5000°K

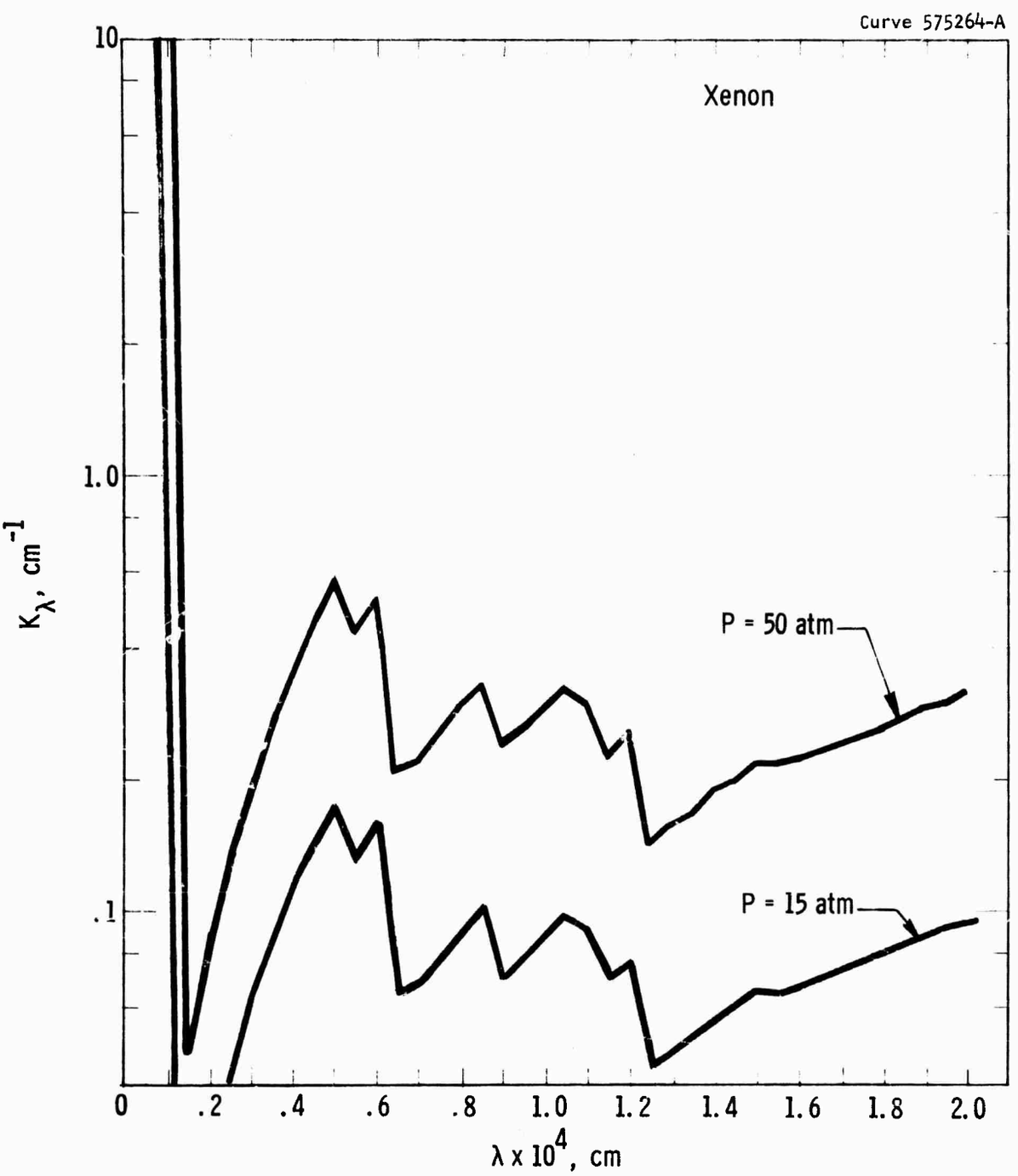

Fig. 4—Absorption coefficient vs wavelength: T = 10000°K

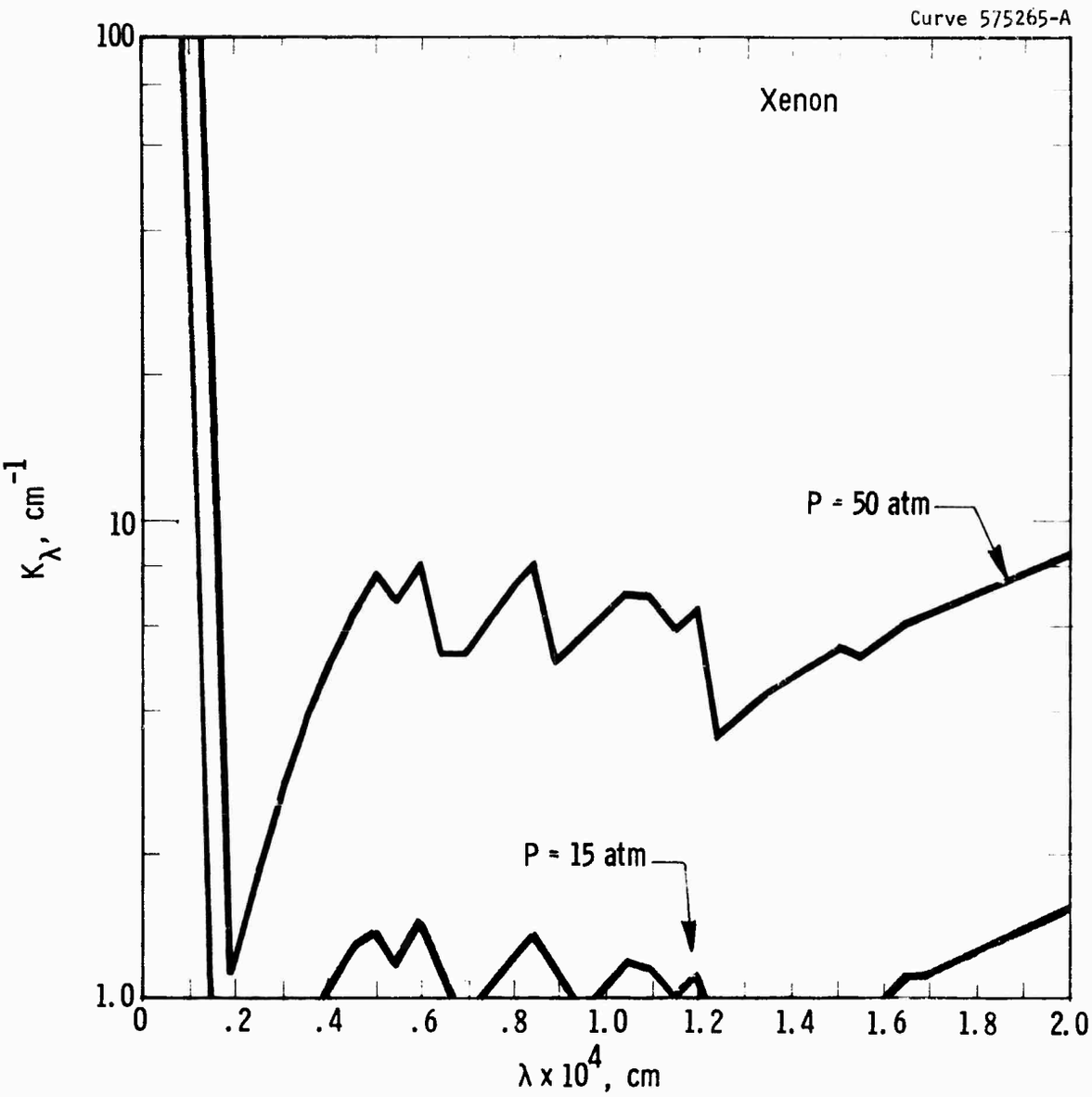

Fig. 5—Absorption coefficient vs wavelength: T = 15000°K

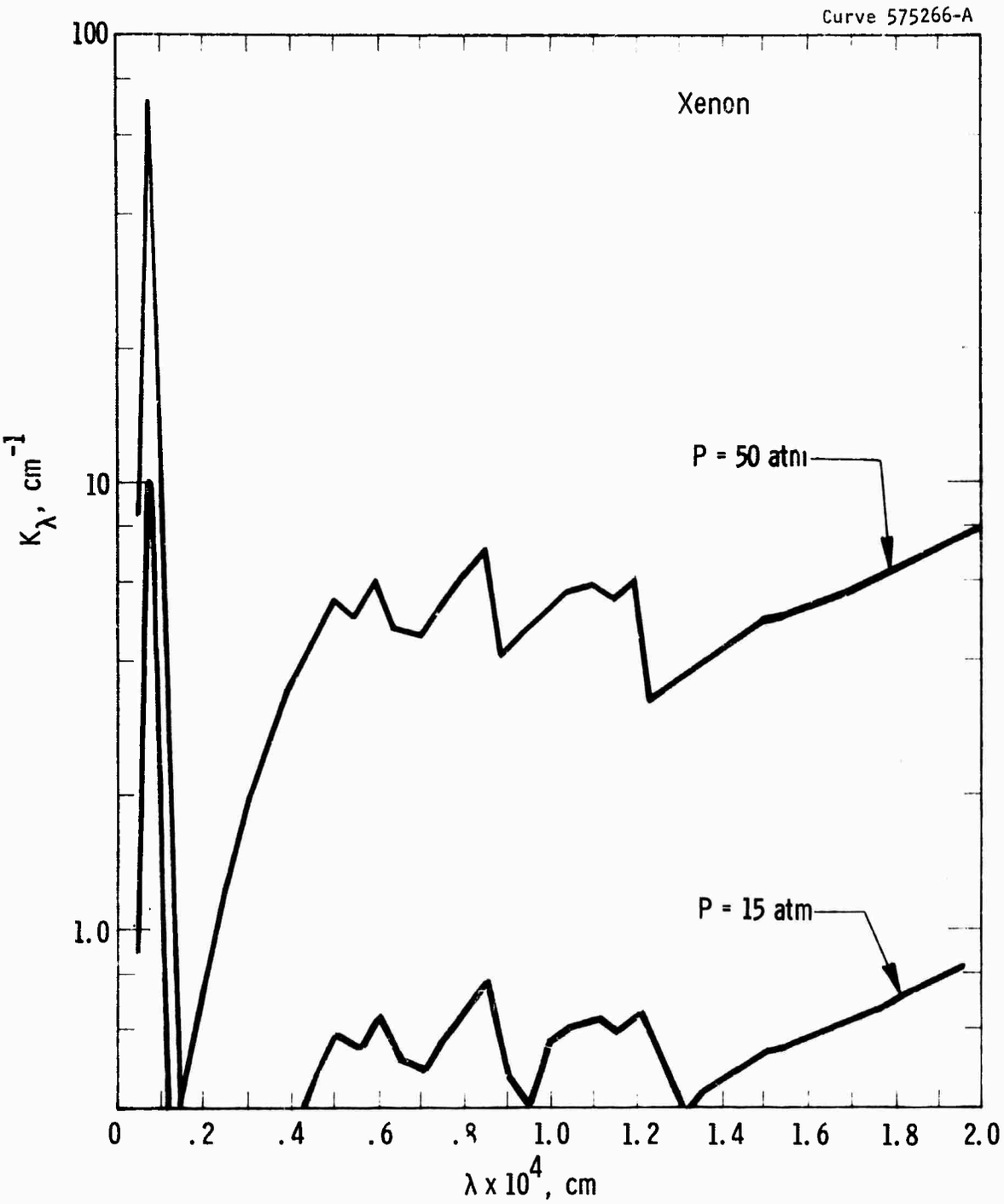

Fig. 6—Absorption coefficient vs wavelength: T = 20000°K

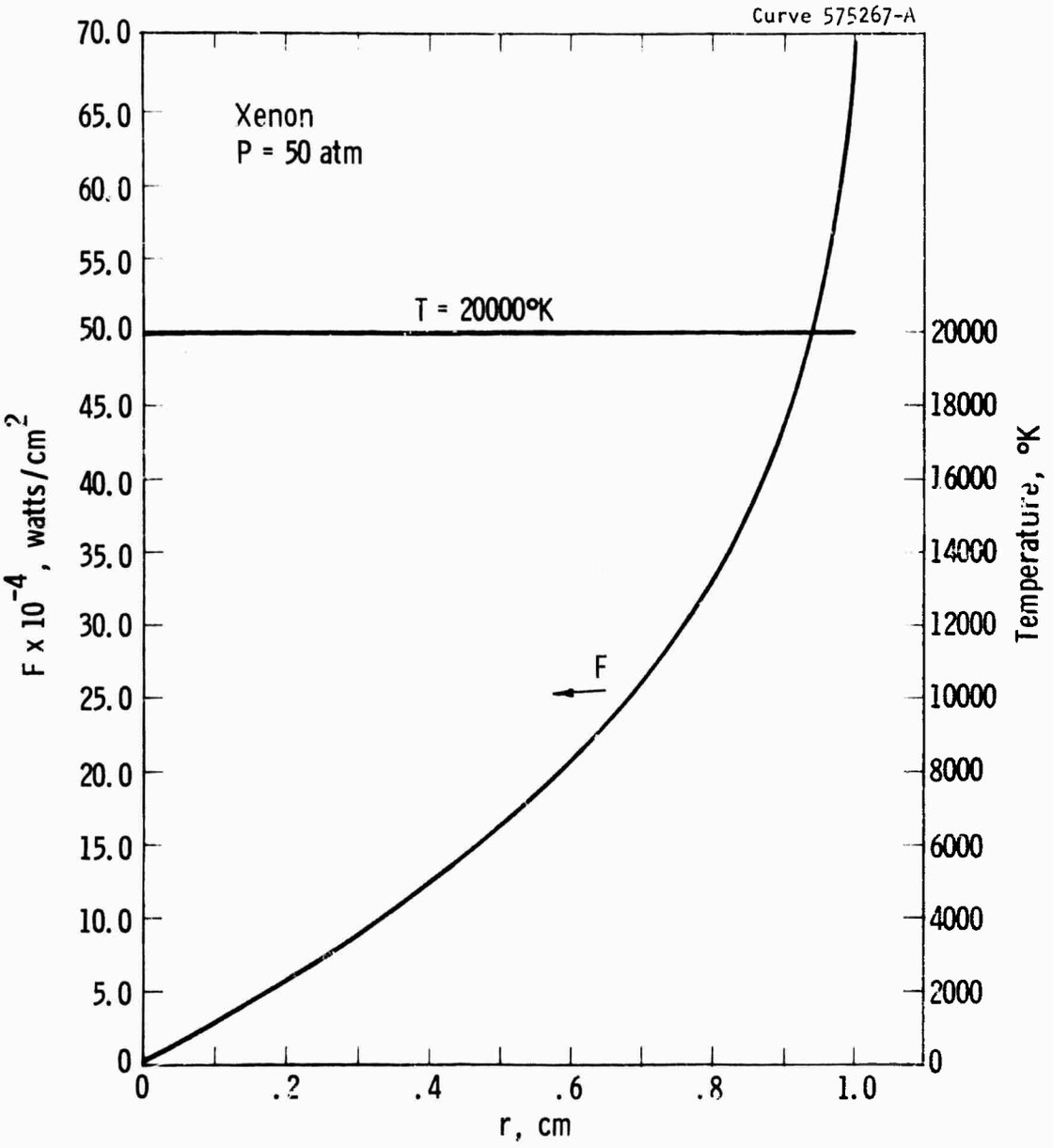

Fig. 7—Flux vs r for an isothermal arc

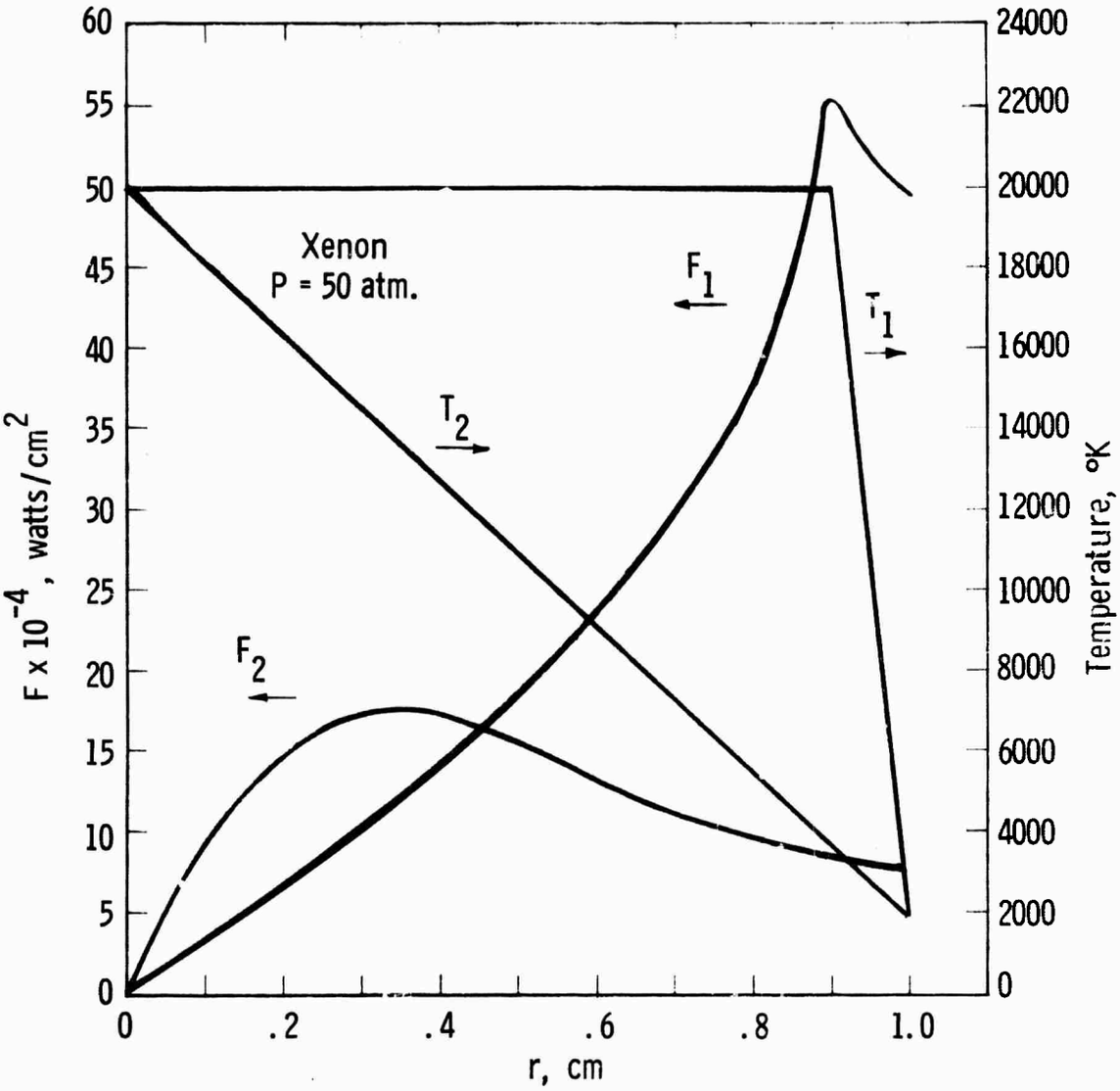

Fig. 8—Arc flux and temperature vs r

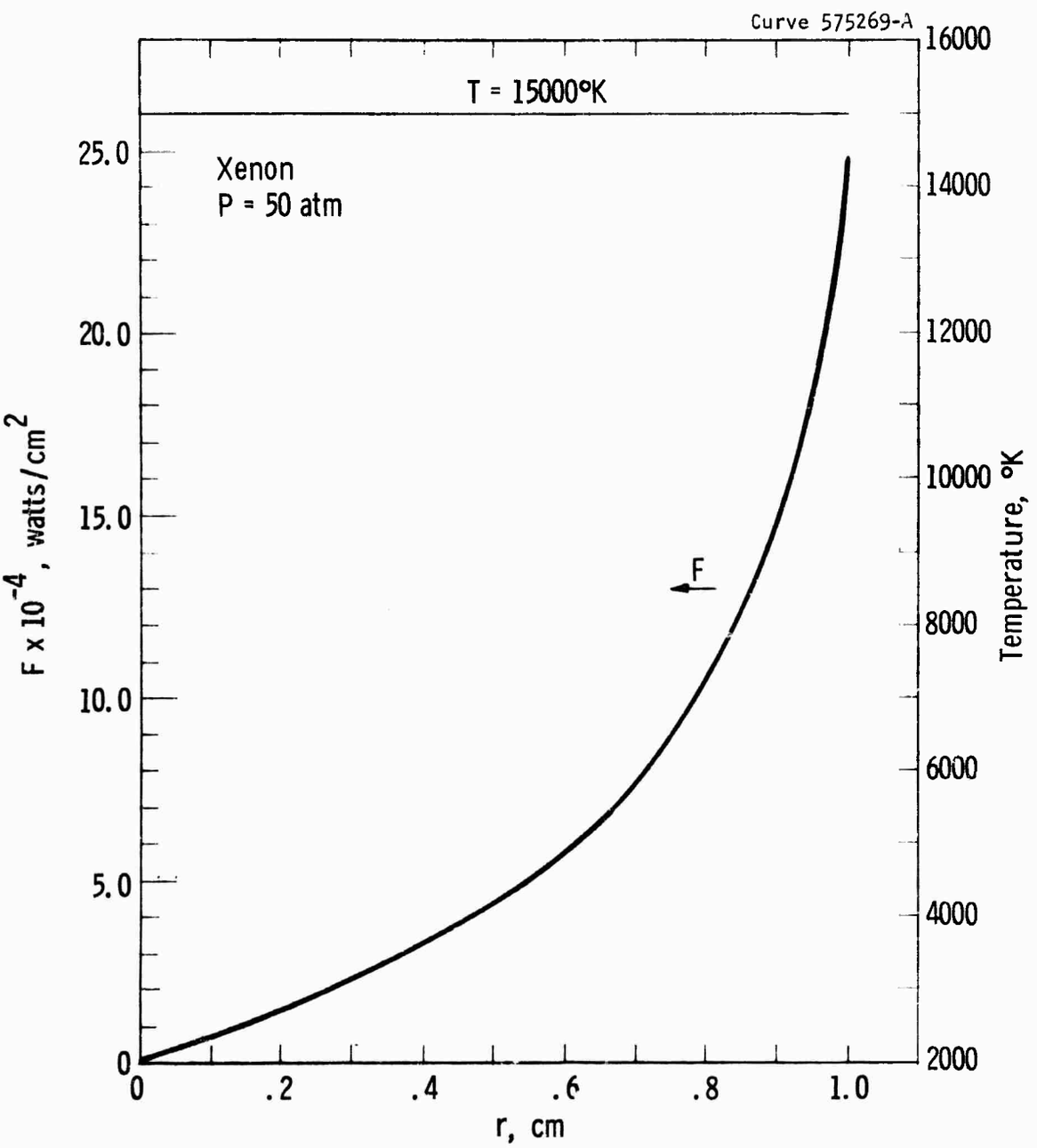

Fig. 9—Flux vs r for an isothermal arc

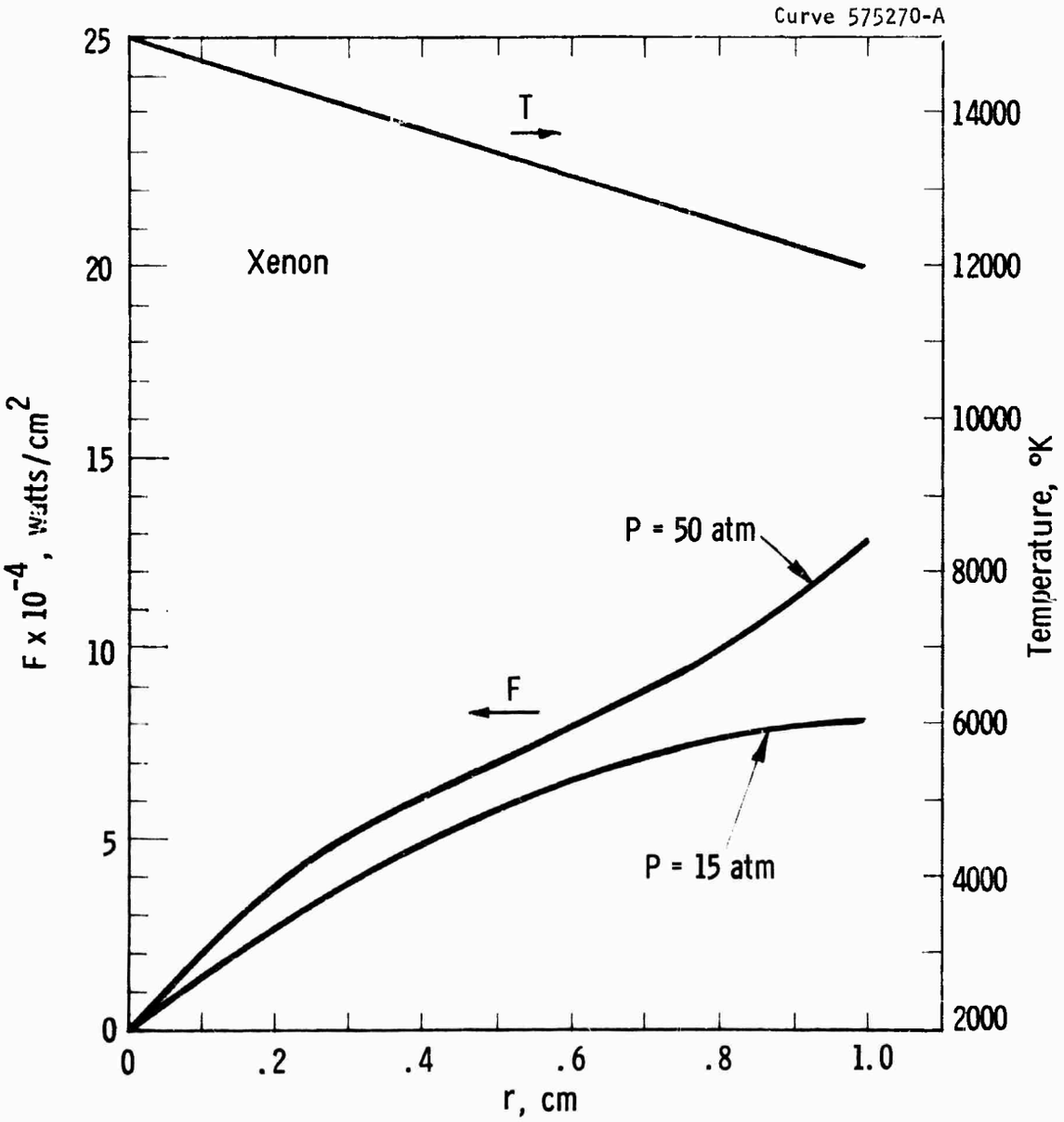

Fig. 10—Arc flux and temperature vs r

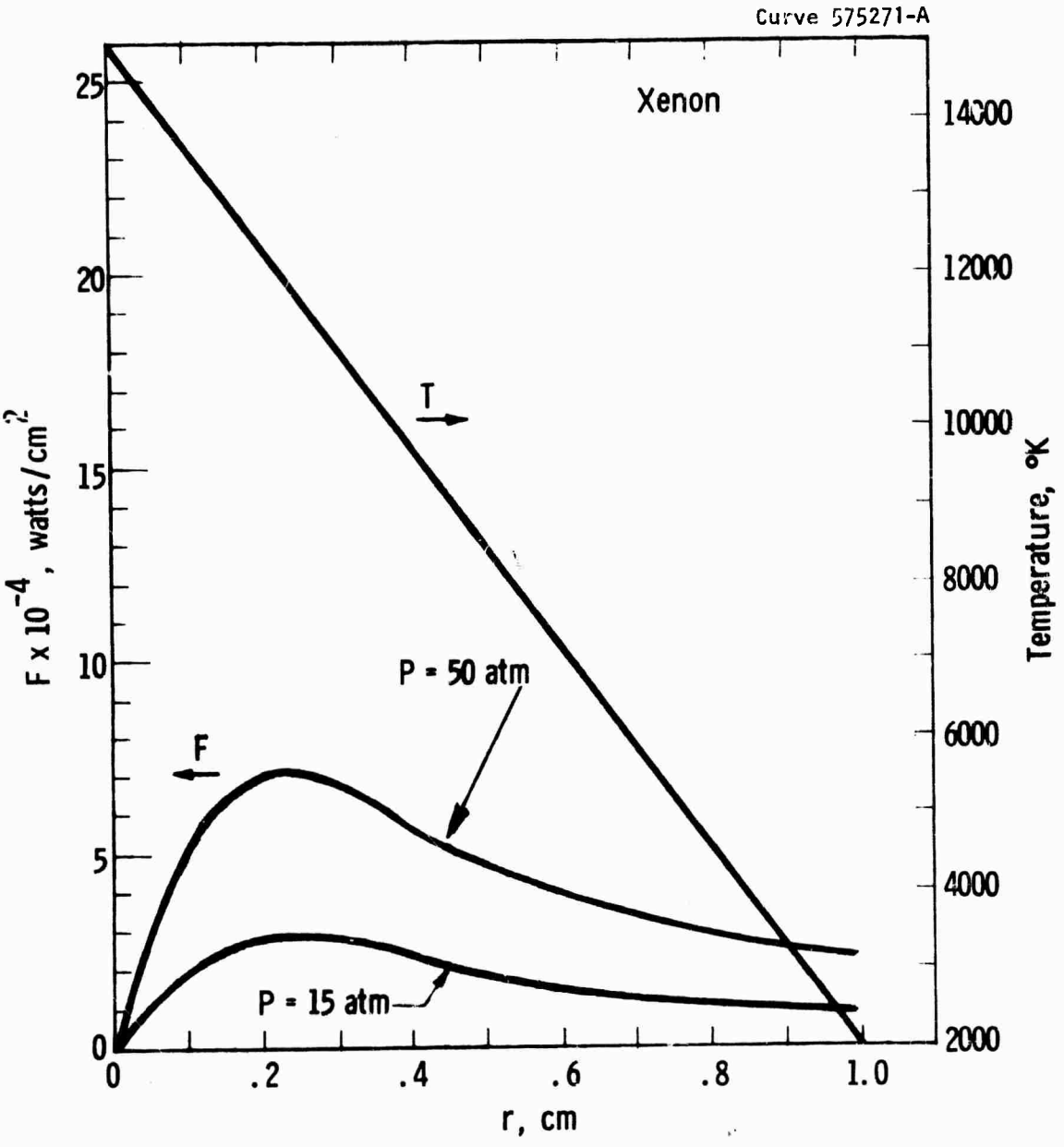

Fig. 11—Arc flux and temperature vs r

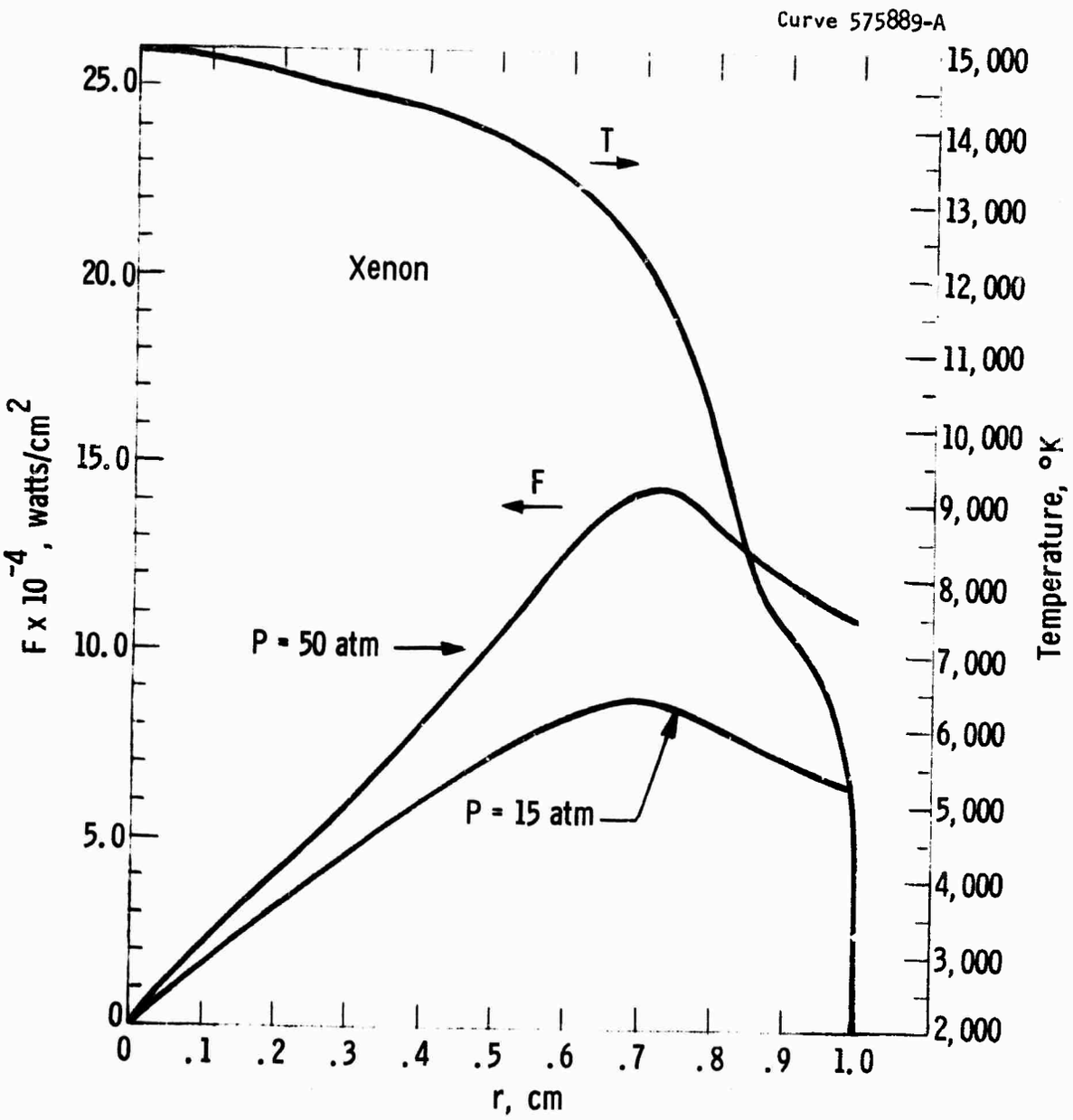

Fig. 12—Arc flux and temperature vs r

APPENDIX B

TRANSITION PROBABILITIES OF XENON I

by

E. G. F. Arnott

TRANSITION PROBABILITIES OF XENON I

by

E. G. F. Arnott

An investigation was made of the possibility of using the Bates-Damgaard[1] method for calculating transition probabilities and oscillator strengths for some of the spectral lines of the rare gases, particularly Xenon. The Bates-Damgaard approximation consists of assuming a Coulomb field for the atom and has given good agreement with experimental results for the simpler systems and for some more complicated systems.

The present work assumes that the approximation may be valid for the rare gases where it is thought that L-S coupling still occurs for some levels. The levels for which this might be expected are given in Moore's[2] tables where such designations are said to be significant for Ne, A and Kr but less so for Xe.

The oscillator strength is given by

$$f_{12} = \frac{304\ S}{g_1 \lambda}$$

where g_1 is the statistical weight of the lower level, λ is the wavelength in Angstrom units and the line strength

$$S = S(M)\ S(L)\ \sigma^2$$

where S(M) is a factor depending on the particular multiplet of the transition array, S(L) is a factor depending on the particular line. These values can be obtained from tables published by Goldberg[3] and White and Eliason[4] respectively. σ is the product of two quantities taken from Bates' and

Damgaard's [1] tables divided by C the excess charge in the nucleus when the active electron is removed. i.e., C=1 for a neutral atom.

$$\sigma = \frac{1}{C} F(n^*_\ell, \ell) I(n^*_{\ell-1}, n^*_\ell, \ell)$$

where $n^* = C/E^{1/2}$, where E is an energy parameter and ℓ is the azimuthal quantum number. A sample calculation is given in the Appendix.

Calculations of f_{12} for the lines of A and Kr given by Moore as having LS coupling were made and the results are shown in Tables I and II compared with the experimental values of Pery-Thorne and Chamberlain[5] for the same spectral lines.

Table I

Absolute f_{12} Values for Argon

Line (Å)	Transition (Paschen)	f(exp) P-T	f(calc) B-D
6965	$s_5 - p_2$	0.04	0.09
7384	$s_4 - p_3$	0.12	0.14
7515	$s_4 - p_5$	0.15	0.12
8015	$s_5 - p_8$	0.09	0.08
8104	$s_4 - p_7$	0.18	0.14
8115	$s_5 - p_9$	0.27	0.45
8425	$s_4 - p_8$	0.19	0.40

Table II

Absolute f_{12} Values for Krypton

Line (Å)	Transition (Paschen)	f(exp) P-T	f(calc) B-D
7601	$s_5 - p_6$	0.14	0.28
7695	$s_5 - p_7$	~0.03	0.006
8104	$s_5 - p_8$	0.07	0.085
8113	$s_5 - p_9$	0.23	0.48
8780	$s_4 - p_8$	0.44	0.42
8929	$s_5 - p_{10}$	0.20	0.104

The correspondence between calculated and observed values is remarkably good for argon and also for krypton except for the 7695A line These results were sufficiently encouraging to suggest that similar calculations be made for Xe for the strong lines which might be expected to have L-S coupling. This was done for 15 of the strongest lines given in the table by Crosswhite and Dieke[6].

As a check on the results three sets of three lines each were chosen:

$1s_4 - 2p_5$	$1s_5 - 2p_8$	$1s_4 - 2p_9$
$1s_4 - 3p_5$	$1s_5 - 3p_8$	$1s_4 - 3p_9$
$1s_4 - 4p_5$	$1s_5 - 4p_8$	$1s_4 - 4p_9$

Following the method of Wilkerson[7] the quantity $\log \frac{I \lambda^3}{g_1 f_{12}}$ where I is the intensity of the line was plotted against E_2, the energy of the upper level. A straight line should result whose slope will give the excitation temperature as given by

$$T^{\circ}K = 5041\ (E_2^n - E_2^m)/\log_{10}\left(\frac{I\lambda^3}{g_1 f_{12}}\right)_m - \log_{10}\left(\frac{I\lambda^3}{g_1 f_{12}}\right)_n$$

The results are shown in the Fig. 1 for a 16 mm pressure microwave discharge. The $1s_4$ - np_9 series does not seem to fall on the same line as the others and gives a slightly lower temperature. However, a temperature of 2850°K was chosen and the values of f_{12} were calculated from Wilkerson's expression

$$f_{12} = f_{12}^{\circ}\left(\frac{I\lambda^3}{g_1}\right)/\left(\frac{I\lambda^3}{g_1}\right)_{\leftarrow o} e^{\frac{-E^{\circ}_2 - E_2}{kT}}$$

A value of 0.117 for f_{12}° was chosen from the Bates-Damgaard calculations as a reasonable value for the strong line at 8280A.

Table III shows the values obtained in this way for 24 strong Xe lines and also gives the values calculated from the Bates-Damgaard approximation.

A more detailed study is necessary to determine the reliability of the values particularly where there are large differences between the two methods.

Curve 575808-A

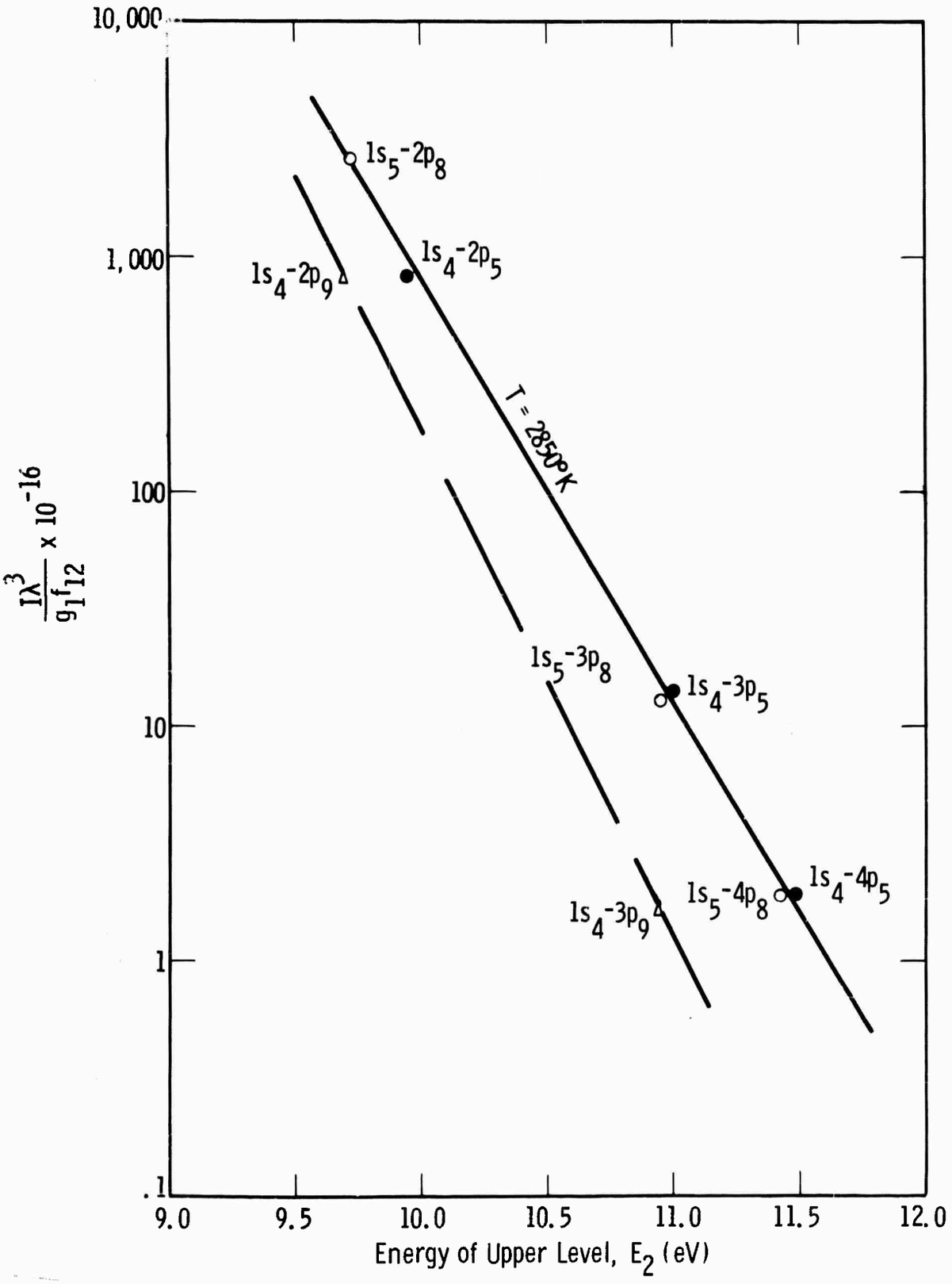

Fig. –1

Table III

Absolute f_{12} Values for Xenon

Line Å	Transition	f_{12}(2850°K)	f(calc) B-D
10838	$1s_4 - 2p_{10}$		.106
9923	$1s_4 - 2p_9$	.152	.434
9800	$1s_5 - 2p_{10}$	.083	.110
9163	$1s_4 - 2p_7$	.145	.140
9045	$1s_5 - 2p_9$	.0034	.086
8952	$1s_4 - 2p_6$	.092	
8819	$1s_5 - 2p_8$	.074	.054
8409	$1s_5 - 2p_7$	.008	.006
8347	$1s_2 - 3p_3$	.151	
8280	$1s_4 - 2p_5$	.117	.117
8267	$1s_2 - 3p_2$	.222	
8232	$1s_5 - 2p_6$	.062	
7641	$1s_3 - 3p_2$	.380	
6318	$2p_8 - 6d_{\frac{1}{4}}$	.035	.140
4932	$1s_4 - 3p_9$	.005	.040
4917	$1s_4 - 3p_4$	.008	
4807	$1s_4 - 3p_5$	.0076	.006
4671	$1s_5 - 3p_8$	.016	.014
4624	$1s_5 - 3p_6$	.0125	
4525	$1s_5 - 3p_3$	.002	
4501	$1s_5 - 3p_2$	.006	
4079	$1s_4 - 4p_5$	.0034	.0032
3968	$1s_5 - 4p_8$	.0038	.0036
3693	$1s_5 - 5p_8$		.0002

Consider the transition $1s_4$ - $2p_5$ in Xe I. From Bacher and Goudsmit[8] the term values are $1s_4$ 29789.34

$2p_5$ 17715.59

Dividing by 109,678 to express these in Rydbergs gives values of E of .2715 and .1615 respectively and therefore values of $C/E^{1/2}$ or n^* for the two levels.

$$n^*_{\ell-1} = 1.92$$

$$n^*_{\ell} = 2.49$$

since C=1 for neutral Xenon. Therefore

$$n^*_{\ell-1} - n^*_{\ell} = -0.57$$

From the tables of Bates and Damgaard with $\ell=1$

$$F(2.49,\ 1) = 4.9$$

$$I(-.57,\ 2.49,\ 1) = 0.65$$

From these values

$$\sigma^2 = (F\ I/C)^2 = 10.2$$

Goldberg's and White and Eliason's tables are reproduced in convenient form in Aller's book[9].

From Aller's Table A-2 for a ps to pp transition

$$S(M) = 9$$

and from Table A-1 for a spin of 1

$$\log \frac{\Sigma s}{s} = 9.95$$

$$S(L) = \frac{s}{\Sigma s} = 0.112$$

So that $S = S(M)S(L) = 9 \times 0.112 \times 10.2 = 10.3$

The oscillator strength

$$f_{12} = \frac{304\ s}{g_1 \lambda} = .117 \text{ for } \lambda = 8280\text{A and } g_1 = 3.$$

REFERENCES

1. D. R. Bates and Agnete Damgaard, Philo. Trans. Roy. Soc. (London), Vol. 242A, 101 (1949).
2. C. E. Moore, "Atomic Energy Levels", Circular of the National Bureau of Standards 467, Vol. I, II and III (1949)(1952)(1958).
3. L. Goldberg, Astrophys. J. 82, 1 (1935).
   L. Goldberg, Astrophys. J. 84, 11 (1936).
4. H. E. White and A. Y. Eliason, Phys. Rev. 44, 753 (1933).
5. A. Pery-Thorne and J. E. Chamberlain, Proc. Phys. Soc. 82, 133 (1963).
6. American Institute of Physics Handbook, 2nd Edition, McGraw-Hill Book Co., New York (1963).
7. T. Wilkerson, Air Force Office of Scientific Research, Air Research and Development Command, Contract No. AF49(638)-439, Washington, D.C.
8. R. Bacher and S. Goudsmit, Atomic Energy States, McGraw-Hill Book Co., New York (1932).
9. L. H. Aller, The Atmospheres of the Sun and Stars, Ronald (1963).

APPENDIX C

COMPUTER PROGRAMS USED IN THIS WORK

by

Esther Geil

COMPUTER PROGRAMS USED IN THIS WORK

by

Esther Geil

The five computer programs written in ALGOL for the Burroughs B-5500 DISK computer used in this work are given in this appendix. The first four programs are preceded by a symbol table and followed by a sample calculation printout. The fifth program whose output is just the radiative flux does not have a sample calculation printout. The five programs are as follows: (The named references are at the end of this appendix)

a) SIMPLIFIED - a calculation for the electron density and spectral absorptivity given the heavy particle density and temperature, based upon the Raizer-Penner model[1-4] for the plasma.

b) DØUBLE - the calculation of the particle densities and then the spectral absorptivity and emissivity using methods similar to Drelliskak[5] et al. and Biberman and Norman[6]. The program is in two parts, particle density calculation, & spectral absorptivity calculation with separate symbol tables.

c) DICSLAB - calculation of the spectral radiance, radiant emittance, and then the balancing current density using the particle densities and spectral absorptivities from DØUBLE and the electrical conductivity calculated according to Spitzer[7,8] et al. DICSLAB is the calculation for a plane parallel slab of homogeneous temperature and pressure.

d) DICKCYL is a calculation of the same quantities in (c) for an infinite cylinder of homogeneous temperature and pressure.

e) Radiative Flux throughout a non-isothermal non-grey cylindrical arc. This program is for the calculation of the radiative flux (radiant emittance) throughout a cylindrical arc of arbitrary spectral absorptivity and radial temperature distribution (the latter must be symmetrical about the center axis of the cylinder in this program). It uses the particle densities and spectral absorptivities calculated by program "DØUBLE".

Program a

Symbol Table for Raizer-Penner Model

Simplified Model for Electron Density and Spectral Absorptivity of Plasma

D = thickness of plasma

I[m] = ionization potential for mth degree of ionization from Penner's model

HNU(i) = $h\nu$ = the energy corresponding to the ith frequency being used.

N = the heavy particle (atom and ion) density of the plasma

THETA = temperature in eV

M = $\bar{m}$ = average number of electrons per atom

IM2 = $I_{(\bar{m} - \frac{1}{2})}$

IM2P = $I_{(\bar{m} + \frac{1}{2})}$

KAPPAPRIME = κ' = absorptivity including stimulated emission

Note: Total number of particles, temperature in degrees K, and pressure in atmospheres are calculated in the write statement following the computation of KAPPAPRIME.

Wavelength, tau = KAPPAPRIME x D, $1 - e^{-\kappa' d}$, B_ν and I_ν for each frequency are calculated within the next write statement.

```
17:26:28 THURSDAY, OCTOBER 21, 1965          WRL ALGOL VERSION OF 9/1/65
        BEGIN                                                                    SC  1:  010
                                                                 START OF SEGMENT ********** 0002
        COMMENT  GEIL,FOR CHURCH,678,F0437,SIMPLIFIED PROBLEM;                   SC  2:  010
        FILE IN READER(2,10); FILE OUT GEIL 6(2,15);                             SC  2:  010
        COMMENT       DABTIME                                                 /  SL  2:  710
            TO OBTAIN LISTING MERGE IN BLANK CARD WITH SEQUENCE NUMBER 00000030; S  SL  2:  710
                                                                 99999999 SC  2:  710
        REAL A,K,N,THETA,COUNT,M,IM2,TEMP,E,MM,KE,TEMP1,J,EPS;                   SC  2:  710
        REAL D;                                                                  SC  2:  710
        REAL IM2P,LITTLEA,AT3,X,HNU1,HNUS,HNUL,NHNU,C1,C2,C2A,C2B,C3;            SC  2:  710
        REAL L,M1,M2,F1,F2;                                                      SC  2:  710
        REAL EXPON,BNU,FACT;                                                     SC  2:  710
        ARRAY I[0:6],DI[0:6];                                                    SC  2:  710
        ARRAY KAPPAPRIME[    0:4000],HNU[0:4000];                                SC  2: 1012
        FORMAT TITLF("NAME OF THE GAS IS READ FROM TITLE CARD"),                  SC  2: 1410
                                                                 START OF SEGMENT ********** 0004
            NTHETA("N=",R9.0,X5,"THETA=",R7.4),                                  SC  4: 1410
            IM("M=",X6,"I(M)"/(I1,F10.3)),                                       SC  4: 1410
            IMS("I(M-1/2)="    ,F8.4,X5,"I(M+1/2)="    ,F8.4),                   SC  4: 1410
            NIS("N=",E10.1),                                                     SC  4: 1410
        TITLEPLOT(X10,"THETA=",F7.4," EV",X7,"NTOTAL=",E9.3,X7,"NDENSITY=",E9.3,  SC  4: 1410
            " PARTICLES/CM3"  //                                                 SC  4: 1410

            X16,"T=",F8.1," DEGREES K.",X7,"P=",E9.3," ATM"  /////               SC  4: 1410
                 " HNU   WAVELENGTH   KAPPA-PRIME        (-TAU)       BNU",      SC  4: 1410
                 X11,"INU" /                                                     SC  4: 1410
                 "  EV    MICRONS         1/CM",X9 ,"1-E "  ,X14,"WATTS/CM STER"/  SC  4: 1410
        ),                                                                       SC  4: 1410
        LISTPLOT(F5.1,E12.3,4E14.3),                                             SC  4: 1410
            MBAR("AFTER",I5," ITERATIONS, MBAR=",F6.3," WHERE M=KE=",F6.4);      SC  4: 1410
                                                                 0004 IS 0122 LONG, NEXT SEG 0002
        DEFINE JOO="FOR J=0 STEP 1 UNTIL 6 DO #,                                 SC  2: 1410
              JOO1="FOR J=1 STEP 1 UNTIL 6 DO #;                                 SC  2: 1410
        LABEL START,EXIT,PRINTIT;                                                SC  2: 1410
        TIMEIT(GEIL`);                                                           SC  2: 1410
        FACT=1,1909E-12*(11605/1,438)**3;                                        SC  2: 1510
        A=3E21;                                                                  SC  2: 1713
        EPS=.001;                                                                SC  2: 1812
        START;                                                                   SC  2: 1911
        READ(READER,TITLE)[EXIT]; WRITE(GEIL[PAGE]); WRITE(GEIL,TITLE);          SC  2: 2010
        READ(READER,/,0);                                                        SC  2: 3011
        READ(READER,/,JOO I[J]);                                                 SC  2: 4213
        WRITE(GEIL,IM,JOO(J,I[J]));                                              SC  2: 5413
        READ(READER,/,FOR J=1 STEP 1 UNTIL 1000 DO HNU[J]);                      SC  2: 6811
        NHNU=J-1;                                                                SC  2: 7913
        CLOSE(READER,RELEASE);                                                   SC  2: 8110
```

```
FOR N:=5*10 DO BEGIN                                                    SC  2:  8212
WRITE(GEIL(PAGE));                                                      SC  2:  8512
FOR THETA:=1 DO BEGIN                                                   SC  2:  8811
WRITE(GEIL,NTHETA,N,THETA);                                             SC  2:  9110
AT3:=A*SQRT(THETA*3);                                                   SC  2: 10111
K:=AT3/N;                                                               SC  2: 10410
J001 DI[J]:=I[J]-I[J-1];                                                SC  2: 10511
DI[0]:=DI[1];                                                           SC  2: 11110
M1:=1/2;                                                                SC  2: 11212
M2:=3/2;                                                                SC  2: 11313
F1:=K*EXP(-I[0]/THETA)-M1;                                              SC  2: 11510
F2:=K*EXP(-I[1]/THETA)-M2;                                              SC  2: 11811
FOR COUNT:=1 STEP 1 UNTIL 1000 OD BEGIN                                 SC  2: 12112
M:=(F2*M1-F1*M2)/(F2-F1);                                               SC  2: 12310
IM2:=I[TEMP:=ENTIER(TEMP1:=M+1/2)]-(TEMP-TEMP1+1)*DI[TEMP];             SC  2: 12611
E:=EXP(-IM2/THETA);                                                     SC  2: 13212
KE:=K*E;                                                                SC  2: 13412
IF ABS(TEMP:=KE-M) < EPS THEN GO PRINTIT;                               SC  2: 13513
F1:=F2;                                                                 SC  2: 13811
F2:=TEMP;                                                               SC  2: 13910
M1:=M2;                                                                 SC  2: 13913
M2:=M;                                                                  SC  2: 14012
END OF COUNT LOOP;                                                      SC  2: 14111


PRINTIT:                                                                SC  2: 14312
WRITE(GEIL,MBAR,COUNT,M,TEMP);                                          SC  2: 14410
LITTLEA:=7.38-16;                                                       SC  2: 15511
IM2P:=I[TEMP:=ENTIER(TEMP1:=M+3/2))]-(TEMP-TEMP1+1)*DI[TEMP];           SC  2: 15610
WRITE(GEIL,IMS,IM2,IM2P);                                               SC  2: 16211
C1:=LITTLEA/THETA*2*(N*2*M/AT3)*(M*2+.25);                              SC  2: 17411
C2:=LITTLEA/THETA*2*N*(M+.5)*2;                                         SC  2: 17912
C2A:=C2*N*M/(2*AT3);                                                    SC  2: 18311
C2B:=C2*IM2/THETA;                                                      SC  2: 18610
C3:=LITTLEA/THETA*3*N*((M+.5)*2*IM2+(M+1.5)*2*IM2P);                    SC  2: 18713
FOR J:=1 STEP 1 UNTIL NHNU OD BEGIN                                     SC  2: 19412
X:=HNU[J]/THETA;                                                        SC  2: 19910
IF X≤IM2 THEN KAPPAPRIME[          J]:=C1*EXP(X)/X*3 ELSE               SC  2: 20012
    IF X≥IM2P THEN KAPPAPRIME[          J]:=C3/X*3 ELSE                 SC  2: 20512
        KAPPAPRIME[          J]:=(C2A*EXP(X)+C2B)/X*3;                  SC  2: 21010
END OF J LOOP;                                                          SC  2: 21413
WRITE(GEIL[PAGE]);                                                      SC  2: 21710
WRITE(GEIL,TITLEPLOT,THETA,TEMP1:=(1+M)*N,N,                            SC  2: 21913
        TEMP:=1165*THETA,TEMP1*TEMP/(2.687E19*273));                    SC  2: 22512
WRITE(GEIL,LISTPLOT,FOR J:=1 STEP 1 UNTIL NHNU OD (TEMP1:=HNU[J],       SC  2: 24211
        1.2397/TEMP1, TEMP:=KAPPAPRIME[  J],                            SC  2: 25013
        EXPON:=1-EXP(-TEMP*D),BNU:=FACT*TEMP1*3/(EXP(TEMP1/THETA        SC  2: 25713
                                                )-1),EXPON*BNU) );      SC  2: 26510
```

```
        WRITE(GE1L[PAGE]);                                                  SC   2: 27511
        END OF THETA LOOP;                                                  SC   2: 27810
        END OF N LOOP;                                                      SC   2: 27812
        TIME1T(GE1L);                                                       SC   2: 27910
        EXIT: END.                                                          SC   2: 28010
                                                                  0002 IS 0283 LONG. NEXT SEG 0001

      EXP          IS SEGMENT NUMBER 0005, PRT ADDRESS IS 0117
      SQRT                    0005                  0116
      OUTPUT(W)               0007                  0034
      BLOCK CONTROL           0008                  0005
      INPUT(W)                0009                  0110
      GO TO SOLVER            0010                  0107
      ALGOL WRITE             0011                  0014
      ALGOL READ              0012                  0015
      ALGOL SELECT            0013                  0016
NUMBER OF ERRORS DETECTED = 000                    LAST CARD WITH ERROR WAS SEQ #
PRT SIZE=0084;    TOTAL SEGMENT SIZE=00593 WORDS;    DISK STORAGE REQ.=00693 WORDS;    NO. SEGS.=0014.
ESTIMATED CORE STORAGE REQUIREMENT = 03522 WORDS.
17:26:48 THURSDAY, OCTOBER 21, 1965    PROCESSOR TIME = 10.28 SECONDS    I/O TIME = 17.20 SECONDS


LABEL  000000000LINE   000652947  COMPILE 1050118 BY GEIL     USING ALGOL                    F0437EG
```

XENON

M	I(M)
0	12.127
1	21.200
2	32.100
3	46.000
4	57.700
5	82.000
6	100.000

N= 5.E+18 THETA= 1.0000
AFTER 6 ITERATIONS, MBAR= 0.111 WHERE M-KE=0.0000
I(M-1/2)= 8.5965 I(M+1/2)= 17.6695

THETA= 1.0000 EV NTOTAL=5.5549+18 NDENSITY=5.000+18 PARTICLES/CM3

T= 11605.0 DEGREES K. P=8.7870+00 ATM

HNU EV	WAVELENGTH MICRONS	KAPPA-PRIME 1/CM	(=TAU 1=E	BNU WATTS/CM	INU STER
0.0	1.240E+03	1.771E+08	1.000E+00	6.256E-07	6.256E-07
0.1	2.479E+01	1.488E+03	1.000E+00	1.526E-03	1.526E-03
0.1	1.240E+01	1.955E+02	1.000E+00	5.952E-03	5.952E-03
0.2	6.265E+00	6.090E+01	1.000E+00	1.305E-02	1.305E-02
0.2	6.199E+00	2.701E+01	1.000E+00	2.262E-02	2.262E-02
0.3	4.959E+00	1.454E+01	1.000E+00	3.443E-02	3.443E-02
0.3	4.132E+00	8.845E+00	9.999E-01	4.831E-02	4.830E-02
0.4	3.542E+00	5.855E+00	9.971E-01	6.404E-02	6.386E-02
0.4	3.099E+00	4.124E+00	9.838E-01	8.145E-02	8.013E-02
0.5	2.755E+00	3.045E+00	9.524E-01	1.004E-01	9.559E-02
0.5	2.479E+00	2.333E+00	9.030E-01	1.206E-01	1.089E-01
0.6	2.066E+00	1.492E+00	7.752E-01	1.645E-01	1.275E-01
0.7	1.771E+00	1.039E+00	6.461E-01	2.118E-01	1.368E-01
0.8	1.550E+00	7.690E-01	5.365E-01	2.615E-01	1.403E-01
0.9	1.377E+00	.969E-01	4.495E-01	3.126E-01	1.405E-01
1.0	1.240E+00	4.809E-01	3.818E-01	3.643E-01	1.391E-01
1.5	8.265E-01	2.349E-01	2.094E-01	6.068E-01	1.270E-01
2.0	6.199E-01	1.634E-01	1.508E-01	7.838E-01	1.182E-01
2.5	4.959E-01	1.379E-01	1.288E-01	8.746E-01	1.127E-01
3.0	4.132E-01	1.316E-01	1.233E-01	8.855E-01	1.092E-01
3.5	3.542E-01	1.366E-01	1.277E-01	8.356E-01	1.067E-01
4.0	3.099E-01	1.509E-01	1.401E-01	7.474E-01	1.047E-01
4.5	2.755E-01	1.748E-01	1.603E-01	6.408E-01	1.027E-01
5.0	2.479E-01	2.101E-01	1.895E-01	5.308E-01	1.006E-01
6.0	2.066E-01	3.304E-01	2.814E-01	3.360E-01	9.454E-02
7.0	1.771E-01	5.656E-01	4.320E-01	1.960E-01	8.465E-02
8.0	1.550E-01	1.030E+00	6.430E-01	1.075E-01	6.915E-02
9.0	1.377E-01	1.746E+01	1.000E+00	5.632E-02	5.632E-02
10.0	1.240E-01	1.448E+01	1.000E+00	2.842E-02	2.842E-02
12.0	1.033E-01	1.863E+01	1.000E+00	6.646E-03	6.646E-03
14.0	8.855E-02	5.942E+01	1.000E+00	1.428E-03	1.428E-03
16.0	7.748E-02	2.759E+02	1.000E+00	2.885E-04	2.885E-04
18.0	6.887E-02	3.070E+01	1.000E+00	5.560E-05	5.560E-05
20.0	6.199E-02	2.238E+01	1.000E+00	1.032E-05	1.032E-05
25.0	4.959E-02	1.146E+01	1.000E+00	1.358E-07	1.358E-07
30.0	4.132E-02	6.632E+00	9.987E-01	1.581E-09	1.579E-09
35.0	3.542E-02	4.176E+00	9.846E-01	1.692E-11	1.666E-11
40.0	3.099E-02	2.798E+00	9.391E-01	1.702E-13	1.598E-13
45.0	2.755E-02	1.965E+00	8.599E-01	1.633E-15	1.404E-15
50.0	2.479E-02	1.433E+00	7.613E-01	1.509E-17	1.149E-17
55.0	2.254E-02	1.076E+00	6.591E-01	1.353E-19	8.921E-20
60.0	2.066E-02	8.290E-01	5.635E-01	1.184E-21	6.672E-22
65.0	1.907E-02	6.520E-01	4.790E-01	1.014E-23	4.858E-24
70.0	1.771E-02	5.221E-01	4.067E-01	8.535E-26	3.471E-26
75.0	1.653E-02	4.244E-01	3.459E-01	7.073E-28	2.446E-28
80.0	1.550E-02	3.497E-01	2.951E-01	5.784E-30	1.707E-30
85.0	1.458E-02	2.916E-01	2.529E-01	4.675E-32	1.182E-32
90.0	1.377E-02	2.456E-01	2.178E-01	3.739E-34	8.143E-35
95.0	1.305E-02	2.089E-01	1.885E-01	2.963E-36	5.585E-37
100.0	1.240E-02	1.791E-01	1.639E-01	2.329E-38	3.818E-39

Program b_1
Symbol Table for DØUBLE
Program to Calculate Spectral Absorptivities and
Emissivities Given Temperature and Pressure

JT1 = initial temperature desired

JTINC = temperature step size desired

JTMAX = maximum temperature desired

JBØLTZ = Boltzmann's constant

NW = input as upper limit, becomes actual value, of number of energy states input for the atom

NW1 = input as upper limit, becomes actual value, of number of energy states input for the first ion

NW2 = input as upper limit, becomes actual value, of number of energy states input for the second ion

NW3 = input as upper limit, becomes actual value, of number of energy states input for the third ion

NW4 = input as upper limit, becomes actual value, of number of energy states input for the fourth ion

JC = a constant used in calculating electron density

IP[i] = ionization potential of the ith species

NP = number of pressures desired

P[i] = the ith pressure, input in atmospheres but converted internally to mm mercury

SVENGA[i] = ith energy level of the atom

SVENG1[i] = ith energy level of the first ion

SVENG2[i] = ith energy level of the second ion

SVENG3[i] = ith energy level of the third ion

SVENG4[i] = ith energy level of the fourth ion

SVØMEGA[i] = total angular momenta for the ith energy level of the atom

SVØMEG1[i] = total angular momenta for the ith energy level of the first ion

SVØMEG2[i] = total angular momenta for the ith energy level of the second ion

SVØMEG3[i] = total angular momenta for the ith energy level of the third ion

SVØMEG4[i] = total angular momenta for the ith energy level of the fourth ion

NLAMBDA = number of wavelengths desired

ALAMBDA[i] = ith wavelength

JELEC = electron density (called NELEC on output sheet)

JT = current value of temperature

JP = current value of pressure

JTØTL = total particle density (called NTØTL on output sheet)

JNQ = cutoff energy for the atom

JN1 = cutoff energy for the first ion

JN2 = cutoff energy for the second ion

JN3 = cutoff energy for the third ion

JN4 = cutoff energy for the fourth ion

JATØM = atomic particle density (called NO on output sheet)

JCHR1 = particle density for the first ion (called N1 on output sheet)

JCHR2 = particle density for the second ion (called N2 on output sheet)

JCHR3 = particle density for the third ion (called N3 on output sheet)

JCHR4 = particle density for the fourth ion (called N4 on output sheet)

JSUMA = internal partition function for the atom (called Q0 on output sheet)

JSUM1 = internal partition function for the first ion (called Q1 on output sheet)

JSUM2 = internal partition function for the second ion (called Q2 on output sheet)

JSUM3 = internal partition function for the third ion (called Q3 on output sheet)

JSUM4 = internal partition function for the fourth ion (called Q4 on output sheet)

JV1 = ionization potential lowering for the atom

Program b_2

Symbol Table for the Spectral Absorptivity Part of DOUBLE

T = temperature

NO = atomic density

QO = internal partition function for the atom

Q1 = internal partition function for the first ion

NU = ν = frequency

KO = total spectral absorptivity for the atom

KOPRIME = effective spectral absorptivity for the atom, including stimulated emission

XI[INU] = the Biberman-Norman factor for the frequency INU x 10^{-14} cycles/sec

H = Planck's constant

K = Boltzmann's constant

V6P = ν_{6p} = ionization frequency from the 6P state

V7P = ν_{7p} = ionization frequency from the 7P state

V5D = ν_{5d} = ionization frequency from the 5D state

V6D = ν_{6d} = ionization frequency from the 6D state

V1MVG = $\nu_1 - \nu_g$ where ν_1 = ionization frequency of lowest level not considered individually, and

ν_g = ionization frequency of the ground state where $h\nu_g$ = ionization potential

GP = degeneracy of each of the p levels

GD = degeneracy of each of the d levels

A6P = cross section of the 6P state

A6D = cross section of the 6D state

A7P = cross section of the 7P state

A7D = cross section of the 7D state

Note: The emission coefficient, ϵ, is calculated within the final write statement.

JV2 = ionization potential lowering for the first ion

JV3 = ionization potential lowering for the second ion

JV4 = ionization potential lowering for the third ion

```
14:59:49 MONDAY, OCTOBER 25, 1965          NRL ALGOL VERSION OF 9/1/65
      BEGIN                                                                       SC    1:    0:0
                                                              START OF SEGMENT ********** 0002
      SAVE FILE PASSKAPPA DISK SERIAL [20:1200](2,60,1200,SAVE 100);              SC    2:    0:0
      FILE IN READER (2,10);                                                      SC    2:    3:2
      FILE OUT PRINT 4" GEIL "" CHURCH"(2,15);                                    SC    2:    7:0
      REAL BISL,BISU,NBSTEPS,BISLNGTH;                                            SC    2:   10:2
      COMMENT        DABTINE                                                  /   SL    2:   10:2
         TO OBTAIN LISTING MERGE IN BLANK CARD WITH SEQUENCE NUMBER 00000030;  S   SL    2:   10:2
                                                                    99999999 SC    2:   12:0
      REAL NLAMBDA,ILAMBDA;                                                       SC    2:   12:0
      ARRAY XI[0:20];                                                             SC    2:   12:0
      ARRAY KARRAY[1:90];                                                         SC    2:   13:3
      ARRAY ALAMBDA[0:90];                                                        SC    2:   15:2
      REAL JT,JATON,JSUNA,JSUM1;                                                  SC    2:   17:1
      DEFINE GEIL=PRINT#;                                                         SC    2:   17:1
      BEGIN                                                                       SC    2:   17:1
      DEFINE STIL=+1 STEP 1 UNTIL #;                                              SC    2:   17:1
                                                              START OF SEGMENT ********** 0004
      REAL TEMP,TEMP1,TEMP2;                                                      SC    4:    0:0
      INTEGER  INDEXI;                                                            SC    4:    0:0
      INTEGER NW,NW1,NW2,NW3,NW4;                                                 SC    4:    0:0
      INTEGER  DXI;                                                               SC    4:    0:0



      REAL XO,YO,XN,YN;                                                           SC    4:    0:0
      REAL KT;                                                                    SC    4:    0:0
          INTEGER JKX, JK1, JK2, JK3, JKC, JK,         JN, JJ;                    SC    4:    0:0
          REAL        JT1, JZEFF,         JTINC, JFXX, JEX1, JEXB, JEXC;          SC    4:    0:0
          INTEGER JN0, JN1, JN2, JN3, JN4, JL, JI, JNY, JNTCHK, JLLL;             SC    4:    0:0
          REAL JTMAX, JBOLTZ, JC, JATWT, JCULE,        JELEC, JP,     JTOTL,      SC    4:    0:0
       JGN, JGN1, JGN2, JGN3, JGN4, JDEL1, JDEL2, JDEL3, JDEL4,                   SC    4:    0:0
      JSUM2, JSUN3, JSUNA, JPOW1, JPOW2, JPOW3, JPOW4, JC1, JC2, JC3, JC4,        SC    4:    0:0
       JR, JRR, JA1, JA2, JA3, JA4, JA5, JA6,        JOPOLA, JAAA, JBBB,          SC    4:    0:0
             JCHR1, JCHR2, JCHR3, JCHR4, JSNCH, JV, JV1, JV2, JV3, JV4,           SC    4:    0:0
       JPP;                                                                       SC    4:    0:0
      ARRAY IP[0:4],        POW[0:4];                                             SC    4:    0:0
      ARRAY DEL[0:4];                                                             SC    4:    3:2
      PROCEDURE BISECT(X, A, B, N, Y) ; REAL X, A, B, N, Y ;             BISECT1  SC    4:    5:1
      % BISECT A < X < B TO ERROR IN X ≤ 2*-N × (B-A) FOR Y = 0.         BISECT2  SC    4:    5:1
      BEGIN REAL D,I,S; X ← B; S ← Y; X ← A; S ← SIGN(Y-S); D ← (B-A)/2; BISECT3  SC    4:    5:1
                                                              START OF SEGMENT ********** 0005
          FOR I ← 0 STEP 1 UNTIL N DO                                    BISECT4  SC    5:    7:2
          BEGIN X ← X + D ; D ← SIGN(Y × S) × ABS(D)/2 ;                 BISECT5  SC    5:    9:3
          END ;                                                          BISECT6  SC    5:   14:3
      END BISECT ;                                                       BISECT8  SC    5:   17:0
                                                              0005 IS 0020 LONG, NEXT SEG 0004
      DEFINE                                                                      SC    4:    5:1
```

b-1

```
     JPOLA=JELEC*(JA1*(JELEC*JELEC))+JELEC*(JA2*JELEC)+JA3*JELEC+JA4+((                SC   41   511
 JA5/JELEC)/JRR)+(1/JELEC)*((JA6/JELEC)/JRR)#  ;                                    SC   41   511
PROCEDURE ORDER2(ENG,OMEG,NW);                                                     SC   41   511
VALUE NW;                                                                          SC   41   511
INTEGER NW;                                                                        SC   41   511
ARRAY ENG,OMEG[0];                                                                 SC   41   511
BEGIN                                                                              SC   41   511
INTEGER I,J;                                                                       SC   41   511
                                                        START OF SEGMENT ********** 0006
FOR I:=1 STEP 1 UNTIL NW DO BEGIN                                                  SC   61   010
TEMP:=ENG[I];                                                                      SC   61   110
TEMP1:=I;                                                                          SC   61   210
FOR J:=I+1 STEP 1 UNTIL NW DO                                                      SC   61   213
IF TEMP2:=ENG[J] < TEMP THEN BEGIN TEMP:=TEMP2; TEMP1:=J  END;                     SC   61   911
DOUBLE(ENG[TEMP1],ENG[I],=:,ENG[I],ENG[TEMP1]);                                    SC   61   1311
DOUBLE(OMEG[TEMP1],OMEG[I],=:,OMEG[I],OMEG[TEMP1]);                                SC   61   1610
END OF I LOOP;                                                                     SC   61   1813
END OF PROCEDURE ORDER2;                                                           SC   61   2110
                                                        0006 IS 0024 LONG, NEXT SEG 0004
PROCEDURE FIND(SVENG,ENER,NW,NQ);                                                  SC   41   511
VALUE ENER;                                                                        SC   41   511
ARRAY SVENG[0];                                                                    SC   41   511
INTEGER NW,NQ;                                                                     SC   41   511


REAL ENER;                                                                         SC   41   511
BEGIN                                                                              SC   41   511
LABEL RETURN;                                                                      SC   41   511
                                                        START OF SEGMENT ********** 0007
FOR NQ:=NW STEP -1 UNTIL 1 DO                                                      SC   71   010
IF ENER > SVENG[NQ ] THEN GO RETURN;                                               SC   71   110
RETURN; END;                                                                       SC   71   511
                                                        0007 IS 0007 LONG, NEXT SEG 0004
REAL  Q,X9R;                                                                       SC   41   511
INTEGER COUNT,COUNTT,NP,II;                                                        SC   41   511
INTEGER  K;                                                                        SC   41   511
LABEL EXIT;                                                                        SC   41   511
FORMAT FLF(5E20.12);                                                               SC   41   511
                                                        START OF SEGMENT ********** 0008
                                                        0008 IS 0004 LONG, NEXT SEG 0004
FORMAT                                                                             SC   41   511
TITLE1("OUTPUT OF PROGRAM 1"),                                                     SC   41   511
                                                        START OF SEGMENT ********** 0009
FL216(6E16.8);                                                                     SC   91   511
                                                        0009 IS 0011 LONG, NEXT SEG 0004
BEGIN                                                                              SC   41   511
ARRAY P,NELEC[0:20];                                                               SC   41   511
                                                        START OF SEGMENT ********** 0010
```

```
LIST LIST0(JT1,JTINC,JTMAX,      JROLTZ,NW,NW1,NW2,NW3,NW4,                    SC  10:   2:0
          JC,IP(1),IP(2),IP(3),IP(4),NP,                                      SC  10:  14:3
    FOR INDEX1:1 STEP 1 UNTIL NP DO P(INDEX1));                               SC  10:  23:1
FORMAT CONSTANTS("JT1,JTINC,JTMAX,"     "JROLTZ,NW,NW1,NW2,NW3,NW4,"          SC  10:  30:2
                                                                  START OF SEGMENT ********** 0011
    "JC,IP(1),IP(2),IP(3),IP(4),"          "NP,FOR...P(NP)"                   SC  11:  30:2
   /(5R20,5));                                                                SC  11:  30:2
                                                                  0011 IS 0024 LONG, NEXT SEG 0010
COMMENT  VERIFY INPUT TO PARTITION SERIES PROGRAM ;                           SC  10:  30:2
FORMAT OUT  EFORM(7E15.7),  IFORM(10I4) ;                                     SC  10:  30:2
                                                                  START OF SEGMENT ********** 0012
                                                                  0012 IS 0008 LONG, NEXT SEG 0010
TIMEIT(PRIN1);                                                                SC  10:  30:2
READ(READER,/,LIST0 )(EXIT);                                                  SC  10:  31:2
WRITE(GE1L,CONSTANTS,LIST0);                                                  SC  10:  3A:0
WRITE(PRINT[0BL]);                                                            SC  10:  39:1
FOR DX1 ← 1 STEP 1 UNTIL                                                      SC  10:  42:0
     NP DO PIOX:]←PIOX1]×760;                                                 SC  10:  42:0
BEGIN                                                                         SC  10:  47:1
LABEL      L508,L516,L517,L608,L615,L708,L715,L808,L815,L908,L915;            SC  10:  47:1
                                                                  START OF SEGMENT ********** 0013
REAL ARRAY   SVENGA[0:NW ],  SVENG1[0:NW1],  SVENG2[0:NW2],                   SC  13:   0:0
  SVENG3[0:NW3],  SVENG4[0:NW4],  SVOMEGAI0:NW ),  SVOMEG1[0:NW1],            SC  13:   8:2


  SVOMEG2[0:NW2],  SVOMEG3[0:NW3],  SVOMEG4[0:NW4],  SVSUMA[0:NW],            SC  13:  19:2
  SVS1[0:NW1], SVS2[0:NW2],  SVS3[0:NW3],  SVS4[0:NW4],                       SC  13:  30:2
               SVSI0:NW];                                                     SC  13:  41:2
LIST LIST1(FOR DX1←1 STEP 1 UNTIL NW  DO SVENGA [DX1]);                       SC  13:  44:0
LIST LIST2(FOR DX1←1 STEP 1 UNTIL NW  DO SVOMEGA[DX1]);                       SC  13:  53:2
LIST LIST3(FOR DX1←1 STEP 1 UNTIL N41 DO SVENG1 [DX1]);                       SC  13:  62:2
LIST LIST4(FOR DX1←1 STEP 1 UNTIL NW1 DO SVOMEG1IDX1]);                       SC  13:  71:2
LIST LIST5(FOR  X1←1 STEP 1 UNTIL NW2 DO SVENG2 [DX1]);                       SC  13:  80:2
LIST LIST6(FOR DX1←1 STEP 1 UNTIL NW2 DO SVOMEG2[DX1]);                       SC  13:  89:2
LIST LIST7(FOR DX1←1 STEP 1 UNTIL NW3 DO SVENG3 IDX1]);                       SC  13:  98:2
LIST LIST8(FOR DX1←1 STEP 1 UNTIL NW3 DO SVOMEG3[DX1]);                       SC  13: 107:2
LIST LIST9(FOR DX1←1 STEP 1 UNTIL NW4 DO SVENG4 [DX1]);                       SC  13: 116:2
LIST LIST10(FOR DX1←1 STEP 1 UNTIL NW4 DO SVOMEG4[DX1]);                      SC  13: 125:2
LIST LIST11(FOR INDEX1←1 STEP 1 UNTIL NW  DO SVS[INDEX1],FOR INDEX1←1         SC  13: 134:2
STEP 1 UNTIL NW1 DO SVS1[INDEX1], FOR INDEX1←1 STEP 1 UNTIL NW2 DO SVS2[      SC  13: 140:3
 INDEX1],FOR INDEX1←1 STEP 1 UNTIL NW3 DO SVS3IINDEX1],FOR INDEX1←1           SC  13: 147:3
 STEP 1 UNTIL NW4 DO SVS4IINDEX1],JT);                                        SC  13: 155:3
READ(READER, / ,LIST1);                                                       SC  13: 165:2
NW ←DX1-1;                                                                    SC  13: 169:0
READ(READER, / ,LIST2);                                                       SC  13: 170:1
READ(READER, / ,LIST3);                                                       SC  13: 173:3
NW1←DX1-1;                                                                    SC  13: 177:1
READ(READER,/,LIST4 );                                                        SC  13: 178:2
```

```
READ(READER, / ,LIST5));                                                    SC  131 18210
NW2←0X1-1;                                                                  SC  131 18512
READ(READER,/,LIST6 ));                                                     SC  131 18813
READ(READER, / ,LIST7);                                                     SC  131 19011
NW3←0X1-1;                                                                  SC  131 19313
READ(READER,/,LIST8 ));                                                     SC  131 19510
READ(READER, / ,LIST9));                                                    SC  131 19812
NW4←0X1-1;                                                                  SC  131 20210
READ(READER,/,LIST10));                                                     SC  131 20311
READ(READER,/,NLAMBDA,FOR 0X1←I STEP 1 UNTIL NLAMBDA DO ALAMBDA[0X1]));     SC  131 20613
READ(READER,/,NUSTEPS));                                                    SC  131 21913
CLOSE(READER,RELEASE));                                                     SC  131 22713
WRITE(PASSKAPPA,*,JT1,JINC,JTMAX));                                         SC  131 22912
WRITE(PASSKAPPA,*,NLAMBDA));                                                SC  131 24011
WRITE(PASSKAPPA,NLAMBDA+1,ALAMBDA[*]));                                     SC  131 24711
ORDER2(SVENGA,SVOMEGA,NW));                                                 SC  131 25013
ORDER2(SVENG1,SVOMEG1,NW1));                                                SC  131 25310
ORDER2(SVENG2,SVOMEG2,NW2));                                                SC  131 25511
ORDER2(SVENG3,SVOMEG3,NW3));                                                SC  131 25712
ORDER2(SVENG4,SVOMEG4,NW4));                                                SC  131 25913
FOR 0XI ← 1 STEP I UNTIL                                                    SC  131 26210
    NW DO SVOMEGA[0X1]←2*SVOMEGA[0X1]+I;                                    SC  131 26210
FOR 0XI ← 1 STEP 1 UNTIL                                                    SC  131 26713

    NW1 DO SVOMEG1[0X1]←2*SVOMEG1[0XI]+1;                                   SC  131 26713
FOR 0X1 ← 1 STEP 1 UNTIL                                                    SC  131 27313
    NW2 DO SVOMEG2[0X1]←2*SVOMEG2[0X1]+1;                                   SC  131 27313
FOR 0XI ← 1 STEP I UNTIL                                                    SC  131 27913
    NW3 DO SVOMEG3[0X1]←2*SVOMEG3[0X1]+I;                                   SC  131 27913
FOR 0XI ← 1 STEP I UNTIL                                                    SC  131 28513
    NW4 DO SVOMEG4[0X1]←2*SVOMEG4[0X'  1.                                   SC  131 28513
FIND(SVENGA,IP[I],NW,NW));                                                  SC  131 29113
IF FALSE THEN BEGIN                                                         SC  131 29410
    WRITE(PRINT, EFORM, LIST1) ;                                            SC  131 29413
    WRITE(PRINT[DBL]) ;                                                     SC  131 29810
    WRITE(PRINT, EFORM, LIST2] ;                                            SC  131 30013
    WRITE(PRINT[DBL]) ;                                                     SC  131 30410
    WRITE(PRINT, EFORM, LIST3) ;                                            SC  131 30613
    WRITE(PRINT[DBL)] ;                                                     SC  131 31010
WRITE(PRINT,EFORM,LIST4 ));                                                 SC  131 31213
WRITE(PRINT[DBL]));                                                         SC  131 31610
    WRITE(PRINT, EFORM, LIST5) ;                                            SC  131 318 )
    WRITE(PRINT[DBL]) ;                                                     SC  131 32210
WRITE(PRINT,EFORM,LIST6 ));                                                 SC  131 32413
WRITE(PRINT[DBL]));                                                         SC  131 32810
    WRITE(PRINT, EFORM, LIST7) ;                                            SC  131 33013
    WRITE(PRINT[DBL]) ;                                                     SC  131 33410
```

```
WRITE(PRINT,EFORM,LIST8 );                                          SC  131 33613
WRITE(PRINT[DBL]);                                                  SC  131 34010
    WRITE(PRINT, EFORM, LIST9) ;                                    SC  131 34213
    WRITE(PRINT[DBL]) ;                                             SC  131 34610
WRITE(PRINT,EFORM,LIST10);                                          SC  131 34813
WRITE(PRINT[DBL]);                                                  SC  131 35210
END OF IF FALSE;                                                    SC  131 35413
KT←JBOLTZ×JT1;                                                      SC  131 35413
TEMP ←      JC×SQRT(JT1)+3×SVOMEG1[1]/                              SC  131 35610
        (SVOMEGA[1]                    )×EXP(-(P[1]/KT));           SC  131 35910
FOR DX1 ← 1 STEP 1 UNTIL                                            SC  131 36211
     NP DO                                                          SC  131 36211
BEGIN                                                               SC  131 36310
NELEC[DX1]←SQRT((TEMP×(TEMP+P[DX1]×6.712818/KT))-TEMP);             SC  131 36310
NELEC[DX1]←NELEC[DX1]×.1;                                           SC  131 36712
END;                                                                SC  131 36912
TIME1T(PRINT);                                                      SC  131 37113
FOR JT←JT1 STEP JTINC UNTIL JTMAX DO BEGIN                          SC  131 37213
KT←JBOLTZ×JT;                                                       SC  131 37610
SVS[1]←SVOMEGA[1]×EXP(-SVENGA[1]/KT);                               SC  131 37711
JJ←2;                                                               SC  131 38013
DO BEGIN                                                            SC  131 38112
L516:SVS[JJ]←SVS[JJ-1]+SVOMEGA[JJ]×EXP(-SVENGA[JJ]/KT);             SC  131 38112

L517: END UNTIL JJ←JJ+1 > NW;                                       SC  131 38613
SVS1[1]←SVOMEG1[1]×EXP(-SVENG1[1]/KT);                              SC  131 38911
JJ←2;                                                               SC  131 39213
DO BEGIN                                                            SC  131 39312
SVS1[JJ]←SVS1[JJ-1]+SVOMEG1[JJ]×EXP(-SVENG1[JJ]/KT);                SC  131 39312
L615: END UNTIL JJ←JJ+1 > NW1;                                      SC  131 39811
SVS2[1]←SVOMEG2[1]×EXP(-SVENG2[1]/KT);                              SC  131 40111
JJ←2;                                                               SC  131 40413
DO BEGIN                                                            SC  131 40512
SVS2[JJ]←SVS2[JJ-1]+SVOMEG2[JJ]×EXP(-SVENG2[JJ]/KT);                SC  131 40512
L715: END UNTIL JJ←JJ+1 > NW2;                                      SC  131 41011
SVS3[1]←SVOMEG3[1]×EXP(-SVENG3[1]/KT);                              SC  131 41311
JJ←2;                                                               SC  131 41613
DO BEGIN                                                            SC  131 41712
SVS3[JJ]←SVS3[JJ-1]+SVOMEG3[JJ]×EXP(-SVENG3[JJ]/KT);                SC  131 41712
L815: END UNTIL JJ←JJ+1 > NW3;                                      SC  131 42211
SVS4[1]←SVOMEGA[1]×EXP(-SVENG4[1]/KT);                              SC  131 42511
JJ←2;                                                               SC  131 42813
DO BEGIN                                                            SC  131 42912
SVS4[JJ]←SVS4[JJ-1]+SVOMEG4[JJ]×EXP(-SVENGA[JJ]/KT);                SC  131 42912
L915: END UNTIL JJ←JJ+1 > NW4;                                      SC  131 43411

                                                                    SC  131 43711
BEGIN                                                               SC  131 43711
```

```
COMMENT  SECOND MAJOR PORTION OF PROGRAM;                                  SC  13: 4371
FORMAT F3("PARTITION FUNCTIONS"/                                           SC  13: 4371
                                                        START OF SEGMENT ********** 0014
                                                        START OF SEGMENT ********** 0015
          "Q0=",E16.8,X5,"Q1=",E16.8,X5,"Q2=",F16.8,X5/                    SC  15:  010
          "Q3=",E16.8,X5,"Q4=",E16.8/),                                    SC  15:  010
FORBISECT("NUMBER OF BISECTING STEPS TAKEN=",16),                          SC  15:  010
        F4("DENSITIES IN INVERSE CM3"/                                     SC  15:  010
          "N0=",E16.8,X5,"N1=",E16.8,X5,"N2=",E16.8,X5/                    SC  15:  010
          "N3=",E16.8,X5,"N4=",E16.8,X5,/                                  SC  15:  010
          "NELEC=",E16.8,X5,"NTOTL=",E16.8/),                              SC  15:  010
        F6("IONIZATION POTENTIAL LOWERINGS IN INVERSE CM FOR"/             SC  15:  010
        "ATOM=",E16.8,X3,"ION1=",E16.8,X3,"ION2=",E16.8,X3,                SC  15:  010
           "ION3=",E16.8/),                                                SC  15:  010
      FTP("TEMP=",16," DEGREES K.",X5,"PRESSURE=",E16.8," ATMOSPHERES"));  SC  15:  010
LIST LIST3(JSUMA,JSUM1,JSUM2,JSUM3,JSUM4       ));                         SC  15:  010
                                                        0015 IS 0102 LONG, NEXT SEG 0014
LIST LIST4(JATOM,JCHR1,JCHR2,JCHR3,JCHR4,JELEC,JTOTL    ));                SC  14:  1012
LIST LIST6(   JV1,JV2,JV3,JV4    ));                                       SC  14:  2312
BEGIN                                                                      SC  14:  3212
LABEL       L10,    L51,L52,L55,L56,L59,L60,L66,L71,L72,L74,L81,L84,       SC  14:  3212
                                                        START OF SEGMENT ********** 0016
 L87,L90,L101,L118;                                                        SC  16:  010



TIMEIT(GEIL);                                                              SC  16:  010
WRITE(GEIL));                                                              SC  16:  110
FOR II←1 STEP 1 UNTIL NP DO BEGIN                                          SC  16:  313
WRITE(GEIL[PAGE]));                                                        SC  16:  510
JP←P[II];                                                                  SC  16:  713
JELEC←NELEC[II];                                                           SC  16:  813
WRITE(GEIL,FORBISECT,NBSTEPS);                                             SC  16:  913
JTOTL←JP×6.712E15/(JBOLTZ×JT);                                             SC  16:  1711
JPOW1←SVENGA[NW]/KT;                                                       SC  16:  1912
JPOW2←SVENG1[NW1]/KT←JPOW1;                                                SC  16:  2110
JPOW3←SVENG2[NW2]/KT←JPOW2;                                                SC  16:  2310
JPOW4←SVENG3[NW3]/KT←JPOW3;                                                SC  16:  2510
JN0←NW;                                                                    SC  16:  2710
JN1←NW1;                                                                   SC  16:  2713
JN2←NW2;                                                                   SC  16:  2812
JN3←NW3;                                                                   SC  16:  2911
JN4←NW4;                                                                   SC  16:  3010
L10:                                                                       SC  16:  3013
JSUMA←SVS [JN0];                                                           SC  16:  3110
JSUM1←SVS1[JN1];                                                           SC  16:  3210
JSUM2←SVS2[JN2];                                                           SC  16:  3310
JSUM3←SVS3[JN3];                                                           SC  16:  3410
JSUM4←SVS4[JN4];                                                           SC  16:  3510
```

```
JC1←JC×(JT*1.5)×EXP(-JPOW1)×(JSUM1/JSUMA);                          SC 161 3610
JC2←JC×(JT*1.5)×EXP(-JPOW2+JPOW1)×(JSUM2/JSUM1);                    SC 161 4112
COMMENT                                                             SC 161 4712
IF (5995>JT) THEN GO TO L51;                                        SC 161 4712
JC3←JC×(JT*1.5)×EXP(-JPOW3+JPOW2)×(JSUM3/JSUM2);                    SC 161 4712
GO TO L52;                                                          SC 161 5312
L51: JC3←0;                                                         SC 161 5610
L52:                                                                SC 161 5613
COMMENT                                                             SC 161 5710
     IF (8995>JT) THEN GO TO L55;                                   SC 161 5710
JC4←JC×(JT*1.5)×EXP(-JPOW4+JPOW3)×(JSUM4/JSUM3);                    SC 161 5710
GO TO L56;                                                          SC 161 6310
L55: JC4←0;                                                         SC 161 6510
L56: IF (12995≤JT) THEN GO TO L59;                                  SC 161 6513
JR←10-15;                                                           SC 161 6711
JRR←1;                                                              SC 161 6810
GO TO L60;                                                          SC 161 6813
L59: JR←10-35;                                                      SC 161 7210
JRR←10-20;                                                          SC 161 7213
L60: JA1←JR;                                                        SC 161 7312
JA2←2×JC1×JR;                                                       SC 161 7413
JA3←3×(JC2×(JC1×JR))-JC1×(JTOTL×JR);                                SC 161 7412
JA4←4×(JC3×(JC2×(JC1×JR)))-2×(JTOTL×(JC2×(JC1×JR)));                SC 161 8011

JA5←5×(JC4×JRR)×(JC3×(JC2×(JC1×JR)))-3×(JTOTL×JRR)×(JC3×(JC2×(JC1×JR)));   SC 161 8512
JA6←-4×(JTOTL×JRR)×(JC4×(JC3×(JC2×(JC1×JR))));                      SC 161 9113
L66:                                                                SC 161 9711
BISECT(JELEC,100,5020,NBSTEPS,JPOLA);                               SC 161 9810
JAAA←JC1+(2×JC1×(JC2/JELEC))+(3×JC1×JC2×(JC3/(JELEC*2)));           SC 161 11410
JBBB←4×(JC1/JELEC)×(JC2/JELEC)×(JC3/JELEC)×JC4;                     SC 161 11913
JATOM←(JELEC*2)/(JAAA+JBBB);                                        SC 161 12410
JCHR1←JC1×JATOM/JELEC;                                              SC 161 12611
IF (JCHR1≥1) THEN GO TO L81;                                        SC 161 12810
JCHR1←0;                                                            SC 161 12911
L81: JCHR2←JC2×JCHR1/JELEC;                                         SC 161 13010
IF (JCHR2≥1) THEN GO TO L84;                                        SC 161 13113
JCHR2←0;                                                            SC 161 13310
L84: JCHR3←JC3×JCHR2/JELEC;                                         SC 161 13313
IF (JCHR3≥1) THEN GO TO L87;                                        SC 161 13513
JCHR3←0;                                                            SC 161 13710
L87: JCHR4←JC4×JCHR3/JELEC;                                         SC 161 13713
IF (JCHR4≥1) THEN GO TO L90;                                        SC 161 13913
JCHR4←0;                                                            SC 161 14110
L90:                                                                SC 161 14113
JV1←2×3.95792359@-5×SQRT((3.1415926536/KT)×(JELEC+JCHR1+4×JCHR2+    SC 161 14310
     9×JCHR3+16×JCHR4));                                            SC 161 14512
JV2←2×JV1;                                                          SC 161 14813
```

```
JV3←3×JV1;
JV4←4×JV1;                                                    SC 16: 150:0
IF IP[1]-JPOW1×KT< JV1 THEN                                   SC 16: 151:1
BEGIN                                                         SC 16: 152:2
TEMP←IP[1]-JV1;                                               SC 16: 154:2
FIND(SVENGA,TEMP      ,NW,JNQ);                               SC 16: 155:0
JPOW1←SVENGA[JNQ]/KT;                                         SC 16: 156:2
TEMP←IP[2]-JV2;                                               SC 16: 158:2
FIND(SVENG1,TEMP      ,NW1,JN1);                              SC 16: 160:0
JPOW2←SVENG1[JN1]/KT+JPOW1;                                   SC 16: 161:2
TEMP←IP[3]-JV3;                                               SC 16: 163:2
JPOW3←SVENG2[JN2]/KT+JPOW2;                                   SC 16: 165:2
TEMP←IP[4]-JV4;                                               SC 16: 167:0
FIND(SVENG2,TEMP      ,NW2,JN2);                              SC 16: 169:0
FIND(SVENG3,TEMP      ,NW3,JN3);                              SC 16: 170:2
JPOW4←SVENG3[JN3]/KT+JPOW3;                                   SC 16: 172:2
GO TO L10;                                                    SC 16: 174:2
END;                                                          SC 16: 176:2
WRITE(GEIL[DBL],FTP,JT,JP/760);                               SC 16: 179:0
WRITE(GEIL,F3,LIST3);                                         SC 16: 179:0
WRITE(GEIL,F4,LIST4);                                         SC 16: 189:1
WRITE(GEIL,F6,LIST6);                                         SC 16: 192:2
NELEC[II]←JELEC;                                              SC 16: 195:3
                                                              SC 16: 199:0

BEGIN
COMMENT GEIL,ABSORPTION COEFFICIENT FOR THE XENON ATOM,SCHLECHT,576;   SC 16: 200:1
REAL LITTLECOEF,BIGCOEF;                                      SC 16: 200:1
                                                              SC 16: 200:1
                                    START OF SEGMENT ********** 0017
REAL V6P,V7P,V5D,V6D,
TEMP,                                                         SC 17:   0:0
    GP,GD,V1MVG,I,                                            SC 17:   0:0
    COEF,C1,     H,K,                                         SC 17:   0:0
    DNU2,                                                     SC 17:   0:0
EV1MVG,EV6P,EV6D,EV7P,EV5D,                                   SC 17:   0:0
HOK,C12,                                                      SC 17:   0:0
E6P,E6D,E7P,E5D,                                              SC 17:   0:0
     NU        ,XNU,                                          SC 17:   0:0
   KO,KOPRIME,                                                SC 17:   0:0
   AGS1,AGS2,A6P,A6D,A7P,A5D,ACOEF;                           SC 17:   0:0
DEFINE T=JT#,NO=JATOM#,Q0=JSUMA#,Q1=JSUM1#;                   SC 17:   0:0
FORMAT INPUT("T=",I6," DEGREES K",X6,"NO=",E10.3,X6,          SC 17:   0:0
                                                              SC 17:   0:0
                                    START OF SEGMENT ********** 0018
   "Q0=",E10.3,X6,"Q1=",E10.3),
OUTPUT(4E15.3),                                               SC 18:   0:0
TITLEOUT(/                                                    SC 18:   0:0
"         NU           LAMBDA  "                              SC 18:   0:0
"    KAPPAPRIME    EMISSION COEF"                             SC 18:   0:0
                                                              SC 18:   0:0
```

```
/                                                                                    SC  18!   010
"     CYCLES/SEC        MICRONS "                                                    SC  18!   010
"     INVERSE CM    WATTS/CM3 STER SEC-1"                                          SC  18!   010
/                                                                                    SC  18!   010
))                                                                                   SC  18!   010
                                                                  0018 IS 0049 LONG, NEXT SEG 0017
REAL PROCEDURE LAG ( X , XO , DX , Y , N ) ;                          LAG   1  SC  17!   010
COMMENT ORDER 3 LAGRANGE INTERPOLATION. EQUAL INDEPENDENT STEP.       LAG   2  SC  17!   010
SINGLE DEPENDENT,INDEPENDENT VARIABLE.EXTRAPOLATE IF NOT XO≤X≤XO+N×DX.  LAG   3  SC  17!   010
X  = DESIRED INDEPENDENT VALUE                                        LAG   4  SC  17!   010
XO = FIRST INDEPENDENT VALUE OF Y TABLE (FOR Y(0))                    LAG   5  SC  17!   010
DX = TABLE STEP FOR INDEPENDENT                                       LAG   6  SC  17!   010
Y  = NAME,DEPENDENT VARIABLE VALUE TABLE (MUST BE SINGLE SUBSCRIPT)   LAG   7  SC  17!   010
N  = MAX INDEX OF Y TABLE ( ≥ 4 ) ;                                   LAG   8  SC  17!   010
    VALUE X , XO , DX , N ;                                           LAG   9  SC  17!   010
    REAL X , XO , DX ; INTEGER N ; ARRAY  Y[0] ;                      LAG  10  SC  17!   010
    BEGIN                                                             LAG  11  SC  17!   010
        INTEGER I ; REAL S ;                                          LAG  12  SC  17!   010
                                                                  START OF SEGMENT ********** 0019
        IF (I ← ENTIER((X - XO)/DX - I)) < 0 THEN I ← 0 ELSE          LAG  13  SC  19!   010
            IF I ← 3 > N THEN I ← N - 3 ;                             LAG  14  SC  19!   510
        S ← (X - XO)/DX - I ;                                         LAG  15  SC  19!  1010
        LAG ← ((Y[I + 3] × S - Y[I] × (S - 3)) × ((S - 3) × S + 2)/3  LAG  16  SC  19!  12!1


            + (Y[I + 1] × (S - 2) - Y[I + 2] × (S - 1)) × (S - 3) × S)/2   LAG  17  SC  19!  17!2
    END LAG ;                                                         LAG  18  SC  19!  2410
                                                                  0019 IS 0028 LONG, NEXT SEG 0017
LABEL START,EXIT;                                                                    SC  17!   010
FILL X1[*] WITH 1,.6,.5,1,2.25,2.8,3,3.1,    3,                                      SC  17!   010
                                                                  START OF SEGMENT ********** 0020
    2.9,2.8,2.6,2.4,2.1,1.8,1.6,1.4,1.25,                                            SC  17!   113
    1.2,1.1,1;                                                                       SC  17!   113
                                                                  0020 IS 0021 LONG, NEXT SEG 0017
H←6.625176-27;                                                                       SC  17!   113
K←1.380446-16;                                                                       SC  17!   212
HOK←H/K;                                                                             SC  17!   311
 V6P←2.35536@15;                                                                     SC  17!   412
 V7P←2.65419@15;                                                                     SC  17!   511
 V5D←2.43618@15;                                                                     SC  17!   610
 V6O←2.67309@15;                                                                     SC  17!   613
V1MVG←2.7252@15;                                                                     SC  17!   712
EV1MVG←HOK×V1MVG;                                                                    SC  17!   811
EV6P←HOK×V6P;                                                                        SC  17!   912
EV6D←HOK×V6D;                                                                        SC  17!  1013
EV7P←HOK×V7P;                                                                        SC  17!  1210
EV5D←HOK×V5D;                                                                        SC  17!  1311
GP←24;                                                                               SC  17!  1412
```

```
GD←4D;                                                          SC 17: 1511
ACOEF ←1,20423×2@13;                                            SC 17: 1610
AGS2←2.59@-32;                                                  SC 17: 1711
AGS1←9@-17+AGS2×2,93@15;                                        SC 17: 1810
A6P←ACOEF×.072×GP;                                              SC 17: 1913
A6D←ACOEF×.025×GD;                                              SC 17: 2112
A7P←ACOEF×.021×GP;                                              SC 17: 2311
A5D←ACOEF×.076×GD;                                              SC 17: 2510
C1←.89@2@;                                                      SC 17: 2613
C12←C1×2;                                                       SC 17: 2712
START:                                                          SC 17: 2813
WRITE(GEIL[DBL ]);                                              SC 17: 2910
WRITE(GEIL[DBL],INPUT,T,NO,QD,Q1);                              SC 17: 3113
WRITE(GEIL     ,TITLEOUT);                                      SC 17: 6011
LITTLECOEF←C12×Q1×T;                                            SC 17: 6311
BIGCOEF←LITTLECOEF×EXP(-EV1NVG/T);                              SC 17: 6510
E6P←A6P×EXP(-EV6P/T);                                           SC 17: 6712
E6D←A6D×EXP(-EV6D/T);                                           SC 17: 7010
E7P←A7P×EXP(-EV7P/T);                                           SC 17: 7212
E5D←A5D×EXP(-EV5D/T);                                           SC 17: 7510
FOR ILAMBDA←1 STEP 1 UNTIL NLAMBDA DO BEGIN                     SC 17: 7712
NU←3@14/ALAMBDA[ILAMBDA];                                       SC 17: 7910
INU←NU×@-14;                                                    SC 17: 8012


IF NU<2@14 THEN COEF←LITTLECOEF×EXP(HOK×(NU-2.935@15)/T) ELSE   SC 17: 8113
COEF←BIGCOEF;                                                   SC 17: 8611
ONU2←1.0/NU   *2;                                               SC 17: 9113
KO   ←NO/QO × (COEF/NU    *3 ×                                  SC 17: 9312
  (IF INU≥20 THEN 1 ELSE IF INU≥2 THEN XI[INU] ELSE LAG(INU,0,1,X1,40))+   SC 17: 9610
     ( IF NU   ≥2.93@15 THEN AGS1-AGS2×NU     ELSE 0)+          SC 17: 10212
            ( IF NU   ≥5.7966@14 THEN E6P×ONU2 ELSE 0)+         SC 17: 10611
            ( IF NU   ≥2.6193@14 THEN E6D×ONU2 ELSE 0)+         SC 17: 10911
            ( IF NU   ≥2.8083@14 THEN E7P×ONU2 ELSE 0)+         SC 17: 11211
            ( IF NU   ≥4.9884@14 THEN E5D×ONU2 ELSE 0));        SC 17: 11511
KOPRIME←KO×(1-EXP(-H×NU/(K×T)));                                SC 17: 11910
KARRAY[ILAMBDA]←KOPRIME;                                        SC 17: 12310
WRITE(GEIL,OUTPUT,NU,3@14/NU,KOPRIME,IF TEMP←HOK×NU/T>15 THEN   SC 17: 12413
        EXP(LN (KOPRIME×2×H×NU*3)-64.36715-TEMP) ELSE           SC 17: 14411
                               KOPRIME×2×H×NU*3/(9@27×          SC 17: 15010
      (EXP(HOK×NU/T)-1))));                                     SC 17: 15310
END OF INU;                                                     SC 17: 16211
WRITE(PASSKAPPA,NLAMBDA,KARRAY[*]);                             SC 17: 16412
EXIT:END;                                                       SC 17: 16712
                                            0017 IS 0169 LONG, NEXT SEG 0016
WRITE(PASSKAPPA,*,JP);                                          SC 16: 20110
END OF JP LOOP;                                                 SC 16: 20811
END  END;                                                       SC 16: 21012
```

```
                                                                    0016 IS 0211 LONG, NEXT SEG 0014
                                                                    0014 IS 0034 LONG, NEXT SEG 0013
      WRITE(PASSKAPPA,**,JELEC,JTOTL);                                        SC  13: 4BA10
      END OF JT LOOP;                                                         SC  13: 44711
        GO TO EXIT;                                                           SC  13: 45012
      END OF DYNAMIC ARRAYS;                                                  SC  13: 45213
                                                                    0013 IS 0456 LONG, NEXT SEG 0010
      END;                                                                    SC  10: 6A10
                                                                    0010 IS 0051 LONG, NEXT SEG 0004
      EXIT:                                                                   SC   4: 6A0
      WRITE(GEIL);                                                            SC   4: 6A0
      TIMEIT (PRINT);                                                         SC   4: 8A3
      END OF ORELLISHAK;                                                      SC   4: 9A3
                                                                    0004 IS 0013 LONG, NEXT SEG 0002
      END.                                                                    SC   2: 1A10
                                                                    0002 IS 0021 LONG, NEXT SEG 0001

    EXP          IS SEGMENT NUMBER 0021, PRT ADDRESS IS 0277
    LN                          0022                 0307
    SQRT                        0023                 0276
    OUTPUT(W)                   0024                 0041
    BLOCK CONTROL               0025                 0005
    INPUT(W)                    0026                 0235
    X TO THE I                  0027                 0310


    GO TO SOLVER                0028                 0234
    ALGOL WRITE                 0029                 0014
    ALGOL READ                  0030                 0015
    ALGOL SELECT                0031                 0016
NUMBER OF ERRORS DETECTED = 000                    LAST CARD WITH ERROR WAS SEG #
PRT SIZE=0254;    TOTAL SEGMENT SIZE=01431 WORDS;    DISK STORAGE REQ.=01733 WORDS;    NO. SEGS.=0032.
ESTIMATED CORE STORAGE REQUIREMENT = 06689 WORDS.
15:00:29 MONDAY, OCTOBER 25, 1965    PROCESSOR TIME = 22.75 SECONDS    I/O TIME = 52.48 SECONDS
```

15:00:33 MONDAY, OCTOBER 25, 1965

JTI,JTFNC,JTMAX,JBOLTZ,NW,NW1,NW2,NW3,NW4,JC,IP(1),IP(2),IP(3),IP(4),NP,FOR...,PINP)

9000.00000	1000.00000	10000.00000	0.69502	400.00000
200.00000	150.00000	100.00000	2.00000	4.83000E+15
97834.40000	171068.40000	259089.00000	371037.00000	1.00000
1.00000				

15:01:04 MONDAY, OCTOBER 25, 1965 PROCESSOR TIME = 18.80 SECONDS I/O TIME = 28.47 SECONDS

15:01:05 MONDAY, OCTOBER 25, 1965 PROCESSOR TIME = 19.47 SECONDS I/O TIME = 28.58 SECONDS

NUMBER OF BISECTING STEPS TAKEN= 75
TEMP= 9000 DEGREES K. PRESSURE= 1.00000000E+00 ATMOSPHERES

PARTITION FUNCTIONS
Q0= 1.00082966E+00 Q1= 4.37106237E+00 Q2= 6.22667678E+00
Q3= 4.87216147E+00 Q4= 1.00000000E+00

DENSITIES IN INVERSE CM3
N0= 7.19930480E+17 N1= 4.77863084E+16 N2= 7.13042656E+10
N3= 6.21119317E+01 N4= 0.00000000E+00
NELEC= 4.77864511E+16 NTOTL= 8.15503311E+17

IONIZATION POTENTIAL LOWERINGS IN INVERSE CM FOR
ATOM= 5.48428661E+02 ION1= 1.09685732E+03 ION2= 1.64528598E+03 ION3= 2.19371464E+03

T= 9000 DEGREES K N0= 7.199E+17 Q0= 1.001E+00 Q1= 4.371E+00

NU CYCLES/SEC	LAMBDA MICRONS	KAPPAPRIME INVERSE CM	EMISSION COEF WATTS/CM3 STER SEC-1
6.000E+15	5.000E-02	7.544E+00	3.052E-20
5.455E+15	5.500E-02	1.771E+01	9.865E-19
5.000E+15	6.000E-02	2.617E+01	1.268E-17
4.615E+15	6.500E-02	3.334E+01	9.879E-17
4.286E+15	7.000E-02	3.948E+01	5.433E-16
4.000E+15	7.500E-02	4.481E+01	2.300E-15
3.750E+15	8.000E-02	4.946E+01	7.937E-15
3.333E+15	9.000E-02	5.723E+01	5.949E-14
3.000E+15	1.000E-01	6.344E+01	2.844E-13
2.857E+15	1.050E-01	1.348E-04	1.118E-16
2.000E+15	1.500E-01	2.759E-04	7.587E-17
1.500E+15	2.000E-01	4.966E-04	8.290E-16
1.200E+15	2.500E-01	7.908E-04	3.352E-15
1.000E+15	3.000E-01	1.155E-03	8.254E-15
8.571E+14	3.500E-01	1.582E-03	1.534E-14
7.500E+14	4.000E-01	2.082E-03	2.414E-14
6.667E+14	4.500E-01	2.636E-03	3.383E-14
6.000E+14	5.000E-01	3.236E-03	4.375E-14
5.455E+14	5.500E-01	2.368E-03	3.264E-14
5.000E+14	6.000E-01	2.816E-03	3.871E-14
4.615E+14	6.500E-01	9.768E-04	1.319E-14
4.286E+14	7.000E-01	1.014E-03	1.331E-14

4.000E+14	7.500E-01	1.194E-03	1.512E-14
3.750E+14	8.000E-01	1.389E-03	1.688E-14
3.529E+14	8.500E-01	1.600E-03	1.860E-14
3.333E+14	9.000E-01	1.137E-03	1.262E-14
3.158E+14	9.500E-01	1.275E-03	1.388E-14
3.000E+14	1.000E+00	1.421E-03	1.430E-14
2.857E+14	1.050E+00	1.575E-03	1.507E-14
2.727E+14	1.100E+00	1.447E-03	1.317E-14
2.609E+14	1.150E+00	1.041E-03	9.010E-15
2.500E+14	1.200E+00	1.150E-03	9.547E-15
2.400E+14	1.250E+00	6.422E-04	5.035E-15
2.308E+14	1.300E+00	7.084E-04	5.289E-15
2.222E+14	1.350E+00	7.780E-04	5.536E-15
2.143E+14	1.400E+00	8.512E-04	5.775E-15
2.069E+14	1.450E+00	9.279E-04	6.007E-15
2.000E+14	1.500E+00	1.008E-03	6.232E-15
1.935E+14	1.550E+00	9.444E-04	5.815E-15
1.875E+14	1.600E+00	1.017E-03	5.747E-15
1.818E+14	1.650E+00	1.055E-03	5.706E-15
1.765E+14	1.700E+00	1.098E-03	5.686E-15
1.714E+14	1.750E+00	1.145E-03	5.688E-15
1.667E+14	1.800E+00	1.197E-03	5.696E-15
1.622E+14	1.850E+00	1.252E-03	5.720E-15
1.579E+14	1.900E+00	1.311E-03	5.753E-15
1.538E+14	1.950E+00	1.374E-03	5.794E-15
1.500E+14	2.000E+00	1.440E-03	5.841E-15
6.000E+13	5.000E+00	1.039E-02	8.763E-15
3.000E+13	1.000E+01	4.473E-02	1.025E-14
1.500E+13	2.000E+01	1.849E-01	1.103E-14
6.000E+12	5.000E+01	1.177E+00	1.151E-14
3.000E+12	1.000E+02	4.734E+00	1.167E-14

15:01:08 MONDAY, OCTOBER 25, 1965 PROCESSOR TIME = 21.55 SECONDS I/O TIME = 29.52 SECONDS

NUMBER OF BISECTING STEPS TAKEN= 75
TEMP= 10000 DEGREES K. PRESSURE= 1.000000000E+00 ATMOSPHERES

PARTITION FUNCTIONS
Q0= 1.002866800E+00 Q1= 4.439197890E+00 Q2= 6.474966870E+00
Q3= 5.120920000E+00 Q4= 1.000000000E+00

DENSITIES IN INVERSE CM3
N0= 5.356691300E+17 N1= 9.914034130E+16 N2= 1.055829660E+12
N3= 1.285052950E+04 N4= 0.000000000E+00
NELEC= 9.914245290E+16 NTOTL= 7.339529800E+17

IONIZATION POTENTIAL LOWERINGS IN INVERSE CM FOR
ATOM= 7.494123170E+02 ION1= 1.498824630E+03 ION2= 2.248236950E+03 ION3= 2.997649270E+03

T= 10000 DEGREES K N0= 5.357E+17 Q0= 1.003E+00 Q1= 4.439E+00

NU CYCLES/SEC	LAMBDA MICRONS	KAPPAPRIME INVERSE CM	EMISSION COEF WATTS/CM3 STER SEC-1
6.000E+15	5.000E-02	5.601E+00	5.556E-19
5.455E+15	5.500E-02	1.315E+01	1.343E-17
5.000E+15	6.000E-02	1.944E+01	1.355E-16
4.615E+15	6.500E-02	2.476E+01	8.596E-16
4.286E+15	7.000E-02	2.932E+01	3.966E-15
4.000E+15	7.500E-02	3.327E+01	1.442E-14
3.750E+15	8.000E-02	3.673E+01	4.353E-14
3.333E+15	9.000E-02	4.249E+01	2.613E-13
3.000E+15	1.000E-01	4.710E+01	1.046E-12
2.857E+15	1.050E-01	3.645E-04	1.388E-17
2.000E+15	1.500E-01	7.472E-04	5.969E-16
1.500E+15	2.000E-01	1.350E-03	5.015E-15
1.200E+15	2.500E-01	2.161E-03	1.739E-14
1.000E+15	3.000E-01	3.165E-03	3.870E-14
8.571E+14	3.500E-01	4.342E-03	6.690E-14
7.500E+14	4.000E-01	5.722E-03	9.969E-14
6.667E+14	4.500E-01	7.240E-03	1.3[illegible]E-13
6.000E+14	5.000E-01	8.876E-03	1.679E-13
5.455E+14	5.500E-01	6.745E-03	1.268E-13
5.000E+14	6.000E-01	8.022E-03	1.474E-13
4.615E+14	6.500E-01	3.244E-03	5.753E-14
4.286E+14	7.000E-01	3.341E-03	5.677E-14

4.000E+14	7.500E-01	3.929E-03	6.362E-14
3.750E+14	8.000E-01	4.569E-03	7.027E-14
3.529E+14	8.500E-01	5.260E-03	7.668E-14
3.333E+14	9.000E-01	3.630E-03	5.008E-14
3.158E+14	9.500E-01	4.069E-03	5.311E-14
3.000E+14	1.000E+00	4.533E-03	5.597E-14
2.857E+14	1.050E+00	5.022E-03	5.865E-14
2.727E+14	1.100E+00	4.695E-03	5.189E-14
2.609E+14	1.150E+00	3.545E-03	3.711E-14
2.500E+14	1.200E+00	3.942E-03	3.909E-14
2.400E+14	1.250E+00	2.180E-03	2.051E-14
2.308E+14	1.300E+00	2.401E-03	2.144E-14
2.222E+14	1.350E+00	2.634E-03	2.233E-14
2.143E+14	1.400E+00	2.877E-03	2.320E-14
2.069E+14	1.450E+00	3.133E-03	2.404E-14
2.000E+14	1.500E+00	3.399E-03	2.485E-14
1.935E+14	1.550E+00	3.344E-03	2.331E-14
1.875E+14	1.600E+00	3.444E-03	2.303E-14
1.818E+14	1.650E+00	3.600E-03	2.287E-14
1.765E+14	1.700E+00	3.753E-03	2.279E-14
1.714E+14	1.750E+00	3.921E-03	2.278E-14
1.667E+14	1.800E+00	4.104E-03	2.283E-14
1.622E+14	1.850E+00	4.300E-03	2.292E-14
1.579E+14	1.900E+00	4.510E-03	2.306E-14
1.538E+14	1.950E+00	4.732E-03	2.322E-14
1.500E+14	2.000E+00	4.967E-03	2.341E-14
6.000E+13	5.000E+00	3.686E-02	3.512E-14
3.000E+13	1.000E+01	1.600E-01	4.107E-14
1.500E+13	2.000E+01	6.643E-01	4.422E-14
6.000E+12	5.000E+01	4.238E+00	4.613E-14
3.000E+12	1.000E+02	1.706E+01	4.677E-14

15:01:10 MONDAY, OCTOBER 25, 1965 PROCESSOR TIME = 22.93 SECONDS I/O TIME = 30.27 SECONDS

LABEL 0 GEIL 0 CHURCH000652987 EXECUTE DOUBLE/GEIL R0636EQ

Symbol Table for DICSLAB (c) and DICKCYL (d)

ZBAR = $\bar{Z}$ = mean ionic charge

DELTE[i] = δ_{T_ϵ} for the ith given value of $\bar{Z}$. A correction factor to the electrical conductivity σ.

DELTK[i] = δ_{T_k} for the ith given value of $\bar{Z}$. A correction factor to the thermal conductivity.

Z[i] = the ith integral value of $\bar{Z}$, at which δ_{T_ϵ} and δ_{T_k} are tabulated

KAPPA[t,λ] = κ, for temperature t and wavelength λ

D = thickness of plasma

NT = number of temperatures to be solved for (they must be in equal increments)

NLAMBDA = number of wavelengths to be solved for

P = pressure

HNU[j] = input as jth wavelength, changed within program to jth energy $h\nu$

BT = lowest temperature desired

DT = temperature step size

ET = maximum temperature desired

T = current temperature

THETA = temperature in eV

KAPPAPRIME[j] = κ' at jth frequency and current temperature

NE = electron density

NTOTL = total particle density

N = heavy particle density

M = average number of electrons per heavy particle

SIGMA = electrical conductivity

KK = thermal conductivity

TAU = $\kappa' D$

E1 = approximation to exponential integral $\int_1^\infty \frac{e^{-\tau u}}{u}\,du$

FNU[j] = $F_\nu(j)$ = spectral radiant emittance corresponding to jth given energy $h\nu(j)$

BNU[j] = the Planck function for the jth given energy

FNUDNU = radiant emittance between energies bounding optically thick or thin regions ($\tau > 3$ or $\tau < 3$ respectively)

SUM = total radiant emittance = $\int_0^\infty F_\nu d\nu$

EXPON = $1 - e^{-\kappa' D}$

Note: The electric field, E, and current density, J, are calculated within the write statement following the printout of SUM. The quantities $h\nu$, λ, κ', τ, $1 - e^{-\tau}$, B_ν, the spectral radiance I_ν, and F_ν are printed out in the final write statement, and λ, τ, and I_ν are calculated there.

Procedure CHOP prints out $\int_{\lambda_1}^{\lambda_2} F_\nu d\nu$ where λ_1 and λ_2 are the bounds of an optically thick or thin region

Procedure INTERP does a linear interpolation to find the value of δ_{T_ϵ} or δ_{T_k} corresponding to a given value of $\bar{Z}$.

Procedure SIMPSON performs a numerical integration (used in DICKCYL only)

LPHI = minimum ϕ value at which integral will be calculated during integration.

MPHI = maximum ϕ value at which integral will be calculated during integration.

LENGTH = length of ray from point R_i to cylinder wall in PHI direction

N = maximum number of intervals into which ray may be divided (input).

NDS = actual number of intervals into which a particular ray is divided.

DS = step size along a particular ray.

APPRØXDS = approximate step size (input)

$DS = \frac{LENGTH}{\min(NDS,N)}$ where NDS is an integer such that $NDS \geq \frac{LENGTH}{APPR\phi XDS} > NDS-1$.

S = point along ray at which integrand is numerically evaluated.

LS = minimum value of S along a particular ray.

MS = maximum value of S along a particular ray.

RSMXY = radial distance from axis of cylinder to point S.

TM = temperature at the radial distance RSMXY.

KLM = interpolated value of KAPPA at ILAMBDAth wavelength and temperature TM.

IBB = Planck function = amount of radiation emitted by a black body as a function of frequency and temperature.

YMT = value of the integrand (without multiplier DLAMBDA [ILAMBDA] x DS x CØS(ϕ) x DPHI x (-4)).

SUMF = total flux at point R_i (output).

```
17:11:22 MONDAY, OCTOBER 25, 1965          XRL ALGOL VERSION OF 9/1/65
        COMMENT  INPUT P AND T  USES DICKS KAPPAS AND NE AND NT IN HOMO T,                    SC  1:  010
              PLANE PARALLEL SLAB;                                                           SC  1:  010
        BEGIN                                                                                SC  1:  010
                                                                  START OF SEGMENT ********** 0002
        COMMENT  GEIL,FOR CHURCH,678,F0A37,SIMPLIFIED PROBLEM;                               SC  2:  010
        FILE IN PASSKAPPA DISK SERIAL (2,60,1200);                                           SC  2:  010
        FILE IN READER(2,10);  FILE OUT GEIL 6(2,15);                                        SC  2:  312
        COMMENT       DABTIME                                                          /     SL  2:  1212
            TO OBTAIN LISTING MERGE IN BLANK CARD WITH SEQUENCE NUMBER 00000030;        S     SL  2:  1212
                                                                  99999999 SC  2:  1210
        REAL A,K,N,THETA,COUNT,M,IM2,TEMP,E,MM,KE,TEMP1,J,EPS;                               SC  2:  1210
        REAL O;                                                                              SC  2:  1210
        REAL IM2P,LITTLEA,AT3,X,HNU1,HNUS,HNUL,NHNU,C1,C2,C2A,C2B,C3;                        SC  2:  1210
        REAL L,M1,M2,F1,F2;                                                                  SC  2:  1210
        REAL EXPON,    FACT;                                                                 SC  2:  1210
        REAL E1,TEST,DNU,D3,SUM;                                                             SC  2:  1210
        REAL PRINT,SIGMA,SBTHETA,DTE,DTK,KK,DENOM,TAU,FNUDNU;                                SC  2:  1210
          REAL ILAMBDA,T;                                                                    SC  2:  1210
        REAL NLAMBDA,BT,ET,DT,NT;                                                            SC  2:  1210
          REAL IT,NE,NTDTL,P;                                                                SC  2:  1210
        INTEGER LOW;                                                                         SC  2:  1210
        REAL ZBAR,TKTN;                                                                      SC  2:  1210

        INTEGER NOTHETA,NN,JTHETA,JN;                                                        SC  2:  1210
        ARRAY ATHETA,AN[0:30];                                                               SC  2:  1210
        ARRAY DELTE,DELTK,Z[0:5];                                                            SC  2:  1410
        ARRAY HNU[0:800];                                                                    SC  2:  1611
        ARRAY I[0:6],DI[0:6];                                                                SC  2:  1910
        ARRAY KAPPA[0:23,1:90];                                                              SC  2:  2112
        FORMAT DEBUG(5E20.8);                                                                SC  2:  2312
                                                                  START OF SEGMENT ********** 0004
                                                                  0004 IS 0004 LONG, NEXT SEG 0002
        FORMAT SN(   "FROM NU=",F6.3," TO NU=",F7.3," THE VALUE OF THE INTEGRAL              SC  2:  2312
                                                                  START OF SEGMENT ********** 0005
         OF FNU IS=",E10.3," WATTS/CM2",X5,A6),                                              SC  5:  2312
            SIGMAK("LN LAMBDA =",E11.3/                                                      SC  5:  2312
           "ELECTRICAL CONDUCTIVITY SIGMA=",E11.3 ," INVERSE OHMS INVERSE CM"/               SC  5:  2312
            "THERMAL CONDUCTIVITY K=",E11.3 ," WATTS/CM DEGREES"),                           SC  5:  2312
            EJ("ELECTRIC FIELD E=",E11.3 ," VOLTS/CM "/                                      SC  5:  2312
                       "CURRENT DENSITY J=",E11.3 ," AMP/CM2"),                              SC  5:  2312
            FINAL(/"RADIANT EMITTANCE F=",E11.3 ," WATTS/CM2"));                             SC  5:  2312
                                                                  0005 IS 0073 LONG, NEXT SEG 0002
        FORMAT TITLE("NAME OF THE GAS IS READ FROM TITLE CARD"),                             SC  2:  2312
                                                                  START OF SEGMENT ********** 0006
        DP("D=",F5.2,X5,"P=", F7.2," ATM"),                                                  SC  6:  2312
        WRITET("T=",I6," DEGREES"),
```

```
DESCRIPTION("PLANE PARALLEL SLAB FOR HOMOGENEOUS TEMPERATURE"                    SC  61  2312
    ", NEGLECTING THERMAL CONDUCTIVITY"),                                       SC  61  2312
  NTHETA("N=",R9.0,X5,"THETA=",R5.2," EV"),                                     SC  61  2312
  IM("M=",X6,"I[M]="/(11,F10.3)),                                               SC  61  2312
  IMS("I(M-1/2)="   ,F8.4,X5,"I(M+1/2)="   ,F8.4),                              SC  61  2312
  NIS("N=",E10.1),                                                              SC  61  2312
TITLEPLOT(X10,"THETA=",F4.2," EV",X7,"NTOTAL=",E9.3,X7,"NDENSITY=",E9.3,        SC  61  2312
  " PARTICLES/CM3"  /                                                           SC  61  2312
  X16,"T=",F8.1," DEGREES K.",X7,"P=",E9.3," ATM"  ///                          SC  61  2312
    "   MNU   WAVELENGTH   KAPPA-PRIME"                                         SC  61  2312
                        "        TAU            ("TAU)        BNU",             SC  61  2312
      X11,"INU" ,X11,"FNU" /                                                    SC  61  2312
    "    EV    MICRONS         1/CM",X23,"1-E " ,X14 ,"WATTS/CM STER",          SC  61  2312
  X11,"WATTS/CM"  /                                                             SC  61  2312
  );                                                                            SC  61  2312
LISTPLOT(F7.3,E12.3,6E14.3),                                                    SC  61  2312
  MBAR("AFTER",I5," ITERATIONS, MBAR=",E10.3," WHERE M=KE=",E10.3);             SC  61  2312

                                                  0006 IS 0161 LONG, NEXT SEG 0002
DEFINE JOD=FOR J=0 STEP 1 UNTIL 6 DO #,                                         SC  21  2312
    JOD1=FOR J=1 STEP 1 UNTIL 6 DO #;                                           SC  21  2312
PROCEDURE CHOP; BEGIN                                                           SC  21  2312
WRITE(GEIL,SN,MNU[LOW],MNU[J-1],ABS(FNUONU),TKTN);                              SC  21  2312
IF TKTN="THICK" THEN TKTN=" THIN " ELSE TKTN=" THICK";                          SC  21  3711


SUM=SUM+FNUONU;                                                                 SC  21  4213
FNUONU=0;                                                                       SC  21  4410
LOW=J;                                                                          SC  21  4413
END OF PROCEDURE CHOP;                                                          SC  21  4512
PROCEDURE INTERP(DT,DELT); REAL DT; ARRAY DELT[0];                              SC  21  4710
BEGIN                                                                           SC  21  4710
LABEL JUMP;                                                                     SC  21  4710
                                                  START OF SEGMENT ********** 0007
JOD1
IF ZBAR<TEMP=Z[J] THEN  BEGIN                                                   SC  71  010
                    DT=DELT[J]-(DELT[J]-DELT[J-1])*(TEMP-ZBAR)/                 SC  71  110
                  (TEMP-Z[J-1]) ; GO JUMP  END;                                 SC  71  710
JUMP;                                                                           SC  71  612
END OF PROCEDURE INTERP;                                                        SC  71  1113
                                                                                SC  71  1210
                                                  0007 IS 0013 LONG, NEXT SEG 0002
LABEL START,EXIT;                                                               SC  21  4710
TIMEIT(GEIL);                                                                   SC  21  4710
FILL DELTE(*) WITH 0,.5816,.6833,.7849,.9225,1;                                 SC  21  4810
                                                  START OF SEGMENT ********** 0008
                                                  0008 IS 0006 LONG, NEXT SEG 0002
FILL DELTK(*) WITH 0,.225,.356,.513,.791,1;                                     SC  21  4913
                                                  START OF SEGMENT ********** 0009
                                                  0009 IS 0006 LONG, NEXT SEG 0002
```

```
FILL Z   [*] WITH 0,1,2,4,16,100;                                    SC   2:  5112
                                          START OF SEGMENT ********** 0010
                                          0010 IS 0006 LONG, NEXT SEG 0002
FACT+1.1909**-12×(11605/1.438)*3;                                    SC   2:  5311
READ(PASSKAPPA,*,BT,DT,ET);                                          SC   2:  5610
WRITE(SEIL,DEBUG,BT,DT,ET);                                          SC   2:  6913
NT+(ET-BT)/DT;                                                       SC   2:  8011
READ(PASSKAPPA,*,NLAMBDA);                                           SC   2:  8210
WRITE(SEIL,DEBUG,NLAMBDA);                                           SC   2:  8913
READ(PASSKAPPA,NLAMBDA+1,HNU[*]);                                    SC   2:  9711
WRITE(SEIL,DEBUG,FOR IT+0 STEP 1 UNTIL NLAMBDA DO HNU[IT]);          SC   2: 10111
READ(READER,TITLE)[EXIT]; WRITE(SEIL[PAGE]); WRITE(SEIL,TITLE);      SC   2: 11311
WRITE(SEIL,DESCRIPTION);                                             SC   2: 12312
READ(READER,/,D);                                                    SC   2: 12612
[illegible]                                                          SC   2: 13413
NHNU+NLAMBDA;                                                        SC   2: 13612
FOR J+1 STEP 1 UNTIL NLAMBDA DO HNU[J]+1.2397/HNU[J];                SC   2: 13[illegible]
HNU[NLAMBDA+1]+0;                                                    SC   2: 14211
BEGIN                                                                SC   2: 14410
ARRAY GNU,KAPPAPRIME,ENU[0:NHNU];                                    SC   2: 14410
                                          START OF SEGMENT ********** 0011
  IT+-1;                                                             SC  11:   311
FOR T+BT STEP DT UNTIL ET DO BEGIN                                   SC  11:   411

[illegible]                                                          SC  11:   510
IT+IT+1;                                                             SC  11:  1211
THETA+T/11605;                                                       SC  11:  1312
[illegible]                                                          SC  11:  1413
READ(PASSKAPPA,NLAMBDA,KAPPA[IT,*]);                                 SC  11:  1610
WRITE(SEIL,DEBUG,FOR J +1 STEP 1 UNTIL NLAMBDA DO KAPPA[IT,J]);      SC  11:  1913
READ(PASSKAPPA,*,P);                                                 SC  11:  3011
WRITE(SEIL,DEBUG,P);                                                 SC  11:  4113
P+P/760;                                                             SC  11:  4911
[illegible]                                                          SC  11:  5012
WRITE(SEIL[PAGE]);                                                   SC  11:  6011
FOR J+1 STEP 1 UNTIL NLAMBDA DO KAPPAPRIME[J]+KAPPA[IT,J];           SC  11:  6310
READ(PASSKAPPA,*,NE,NTOTL);                                          SC  11:  6910
WRITE(SEIL,DEBUG,NE,NTOTL);                                          SC  11:  7813
N+NTOTL-NE;                                                          SC  11:  8811
M+NE/N;                                                              SC  11:  8912
IF M≤.3 THEN ZBAR+1 ELSE                                             SC  11:  9013
ZBAR+M+.25/M;                                                        SC  11:  9213
INTERP(DTE,DELTE);                                                   SC  11:  9413
INTERP(DTK,DELTK);                                                   SC  11:  9811
DENOM+ZBAR×.434294481903×    ( PRINT+          LN(2.401*20×THETA*3/  SC  11:  9913
        (ZBAR+2×M×(1+ZBAR)×N)));                                     SC  11: 10212
SIGMA+286×SQTHETA*3×DTE/DENOM;                                       SC  11: 10710
```

```
KK←.2465×SQTHETA×5×DTK/DENOM;
WRITE(GEIL      );
WRITE(GEIL,SIGMAK,PRINT,SIGMA,KK);
FOR J←1 STEP 1 UNTIL NHNU DO BEGIN
TAU←KAPPAPRIME[J]×D;
IF TAU≤1 THEN
E1←-.57721566+TAU×(.99999193+TAU×(-.24991055+TAU×(.05519968+TAU×
     (-.00976004+TAU×(.00107857))))) ELSE
E1←EXP(-TAU)/TAU×(TAU*2+8.334733×TAU+.250621)/
                              (TAU*2+3.330657×TAU+1.681534);
                    BNU[J]←FACT×(TEMP1←HNU[J]) *3/(EXP(TEMP1/THETA )-1);
FNU[J]←[illegible]×BNU[J]    ×(1+(TAU-1)×EXP(-TAU)-TAU*2×E1);
END OF J LOOP;
WRITE(GEIL,[illegible]);
[illegible]
SUM←0;
LOW←1;
TEMP←SIGN(KAPPAPRIME[1]-D);
FNUONU←FNU[1]×(HNU[1]-HNU[2]);
IF TEMP[illegible] THEN [illegible] ELSE
[illegible]
FOR J←2 STEP 1 UNTIL NHNU DO BEGIN
IF TEMP≠ TEMP←SIGN(KAPPAPRIME[J]-D))         THEN CHOP;

[illegible]
FNUONU←FNUONU+TEMP  ×FNU[J]×DNU;
END OF J LOOP;
CHOP:
WRITE(GEIL,FINAL,SUM);
WRITE(GEIL,EJ,TEMP←SQRT(2×SUM/(SIGMA×D)),SIGMA×TEMP);
WRITE(GEIL,[illegible]);
WRITE(GEIL,TITLEPLOT,THETA,TEMP1←(1+N)×N,N,
      TEMP←11605×THETA,TEMP1×TEMP/(2.687@19×273));
WRITE(GEIL,LISTPLOT,FOR J←1 STEP 1 UNTIL NHNU DO [TEMP1←HNU[J],
      1.2397/TEMP1, TEMP←KAPPAPRIME[  J], TEMP×D,
      EXPON←1-EXP(-TEMP×D),BNU[J] ,EXPON×BNU[J],FNU[J]]);
WRITE(GEIL[PAGE]);
END OF THETA LOOP;
TIMEIT(GEIL);
END DYNAMIC HNU;
                                                  0011 IS 0299 LONG, NEXT SEG 0002
EXIT: END.
                                                  0002 IS 0150 LONG, NEXT SEG 0001
EXP        IS SEGMENT NUMBER 0012, PRT ADDRESS IS 0207
LN                           0013                 0205
SQRT                         0014                 0176
OUTPUT(W)                    0015                 0035
```

```
      BLOCK CONTROL                0016              0005
      INPUT(#)                     0017              0161
      GO TO SOLVER                 0018              0167
      ALGOL WRITE                  0019              0014
      ALGOL READ                   0020              0015
      ALGOL SELECT                 0021              0016
NUMBER OF ERRORS DETECTED = 000                      LAST CARD WITH ERROR WAS SEQ #
PNT SIZE=0141)    TOTAL SEGMENT SIZE=00896 WORDS)    DISK STORAGE REQ.=01075 WORDS)    NO. SEGS.=0022.
ESTIMATED CORE STORAGE REQUIREMENT = 06298 WORDS.
17:11:49 MONDAY, OCTOBER 25, 1965    PROCESSOR TIME = 13.00 SECONDS    I/O TIME = 33.73 SECONDS
```

```
LABEL  000000000LINE  000052987 COMPILE DICSLAB BY GEIL IN ALGOL TO LIBRARY                R0630EG
```

LABEL 000000000GEIL 000652947 EXECUTE DICSLAB BY GEIL

R0636EG

17:11:54 MONDAY, OCTOBER 29, 1985

9.00000000E+03	1.00000000E+03	1.00000000E+04		
5.30000000E+01				
0.00000000E+00	5.00000000E-02	5.50000000E-02	6.00000000E-02	6.50000000E-02
7.00000000E-02	7.50000000E-02	8.00000000E-02	9.00000000E-02	1.00000000E-01
1.05000000E-01	1.50000000E-01	2.00000000E-01	2.50000000E-01	3.00000000E-01
3.50000000E-01	4.00000000E-01	4.50000000E-01	5.00000000E-01	5.50000000E-01
6.00000000E-01	6.50000000E-01	7.00000000E-01	7.50000000E-01	8.00000000E-01
8.50000000E-01	9.00000000E-01	9.50000000E-01	1.00000000E+00	1.05000000E+00
1.10000000E+00	1.15000000E+00	1.20000000E+00	1.25000000E+00	1.30000000E+00
1.35000000E+00	1.40000000E+00	1.45000000E+00	1.50000000E+00	1.55000000E+00
1.60000000E+00	1.65000000E+00	1.70000000E+00	1.75000000E+00	1.80000000E+00
1.85000000E+00	1.90000000E+00	1.95000000E+00	2.00000000E+00	5.00000000E+00
1.00000000E+01	2.00000000E+01	5.00000000E+01	1.00000000E+02	

XENON
PLANE PARALLEL SLAB FOR HOMOGENEOUS TEMPERATURE, NEGLECTING THERMAL CONDUCTIVITY
T= 9000 DEGREES

7.54388274E+00	1.77059122E+01	2.61748385E+01	3.33401163E+01	3.94821275E+01
4.48052055E+01	4.94629005E+01	5.72257297E+01	6.34359943E+01	1.34765653E-04
2.75947924E-04	4.96613294E-04	7.90843507E-04	1.15478213E-03	1.58239780E-03
2.08234173E-03	2.63571139E-03	3.23603340E-03	2.36754133E-03	2.81570271E-03
9.76847882E-04	1.01436196E-03	1.19355069E-03	1.38868653E-03	1.59982723E-03
1.13726209E-03	1.27532877E-03	1.42116045E-03	1.57471939E-03	1.44725091E-03
1.04078576E-03	1.15913371E-03	6.42226420E-04	7.08376527E-04	7.78030431E-04
8.51199913E-04	9.27895476E-04	1.00812651E-03	9.84352931E-04	1.01736340E-03
1.05542135E-03	1.09818762E-03	1.14537670E-03	1.19674673E-03	1.25209163E-03
1.31123483E-03	1.37402428E-03	1.44032842E-03	1.03909118E-02	4.47280091E-02
1.84908575E-01	1.17681574E+00	4.73435401E+00		
7.60000000E+02				

D= 1.00   P= 1.00 ATM

4.778045112E+16   8.155033210E+17

LN LAMBDA = 7.086E+00
ELECTRICAL CONDUCTIVITY SIGMA= 3.702E+01 INVERSE OHMS INVERSE CM
THERMAL CONDUCTIVITY K= 9.572E-03 WATTS/CM DEGREES

FROM NU=24.794 TO NU= 12.397 THE VALUE OF THE INTEGRAL OF FNU IS 3.412E+00 WATTS/CM2   THICK
FROM NU=11.807 TO NU= 0.025 THE VALUE OF THE INTEGRAL OF FNU IS 1.137E+02 WATTS/CM2   THIN
FROM NU= 0.012 TO NU= 0.012 THE VALUE OF THE INTEGRAL OF FNU IS 2.319E-02 WATTS/CM2   THICK

RADIANT EMITTANCE F= 1.172E+02 WATTS/CM2
ELECTRIC FIELD E= 2.510E+00 VOLTS/CM
CURRENT DENSITY J= 9.310E+01 AMP/CM2

THETA=0.78 EV   NTOTAL=8.155E+17   NDENSITY=7.677E+17 PARTICLES/CM3
T= 9000.0 DEGREES K.   P=1.001E+00 ATM

WNU EV	WAVELENGTH MICRONS	KAPPA-PRIME 1/CM	TAU	1-E(-TAU)	BNU WATTS/CM STER	INU WATTS/CM STER	FNU WATTS/CM
24.794	5.000E-02	7.544E+00	7.544E+00	9.995E-01	1.244E-10	1.244E-10	3.153E-06
22.540	5.500E-02	1.771E+01	1.771E+01	1.000E+00	1.710E-09	1.710E-09	4.333E-05
20.662	6.000E-02	2.617E+01	2.617E+01	1.000E+00	1.484E-08	1.484E-08	3.761E-04
19.072	6.500E-02	3.334E+01	3.334E+01	1.000E+00	9.063E-08	9.063E-08	2.297E-03
17.710	7.000E-02	3.948E+01	3.948E+01	1.000E+00	4.204E-07	4.204E-07	1.065E-02
16.529	7.500E-02	4.481E+01	4.481E+01	1.000E+00	1.566E-06	1.566E-06	3.969E-02
15.496	8.000E-02	4.946E+01	4.946E+01	1.000E+00	4.890E-06	4.890E-06	1.239E-01
13.776	9.000E-02	5.723E+01	5.723E+01	1.000E+00	3.163E-05	3.163E-05	8.015E-01
12.397	1.000E-01	6.344E+01	6.344E+01	1.000E+00	1.362E-04	1.362E-04	3.451E+00
11.807	1.050E-01	1.348E-04	1.348E-04	1.348E-04	2.519E-04	3.394E-08	1.720E-03
8.265	1.500E-01	2.759E-04	2.759E-04	2.759E-04	5.318E-03	2.295E-06	1.163E-01
6.199	2.000E-01	4.966E-04	4.966E-04	4.965E-04	5.040E-02	2.502E-05	1.268E+00
4.959	2.500E-01	7.908E-04	7.908E-04	7.905E-04	1.278E-01	1.010E-04	5.120E+00
4.132	3.000E-01	1.155E-03	1.155E-03	1.154E-03	2.153E-01	2.485E-04	1.260E+01
3.542	3.500E-01	1.582E-03	1.582E-03	1.581E-03	2.919E-01	4.616E-04	2.340E+01
3.099	4.000E-01	2.082E-03	2.082E-03	2.080E-03	3.490E-01	7.259E-04	3.679E+01
2.753	4.500E-01	2.636E-03	2.636E-03	2.632E-03	3.851E-01	1.016E-03	5.152E+01
2.479	5.000E-01	3.236E-03	3.236E-03	3.231E-03	4.067E-01	1.314E-03	6.660E+01
2.254	5.500E-01	2.368E-03	2.368E-03	2.365E-03	4.145E-01	9.803E-04	4.969E+01
2.066	6.000E-01	2.816E-03	2.816E-03	2.812E-03	4.134E-01	1.162E-03	5.891E+01
1.907	6.500E-01	9.768E-04	9.768E-04	9.764E-04	4.060E-01	3.964E-04	2.009E+01
1.771	7.000E-01	1.014E-03	1.014E-03	1.014E-03	3.946E-01	4.000E-04	2.027E+01

1.453	7.500E-01	1.194E-03	1.194E-03	1.193E-03	3.806E-01	4.541E-04	2.301E+01
1.550	8.000E-01	1.369E-03	1.369E-03	1.368E-03	3.653E-01	5.075E-04	2.575E+01
1.458	8.500E-01	1.600E-03	1.600E-03	1.599E-03	3.494E-01	5.586E-04	2.831E+01
1.377	9.000E-01	1.137E-03	1.137E-03	1.137E-03	3.334E-01	3.789E-04	1.920E+01
1.305	9.500E-01	1.275E-03	1.275E-03	1.275E-03	3.176E-01	4.048E-04	2.051E+01
1.241	1.000E+00	1.421E-03	1.421E-03	1.420E-03	3.022E-01	4.292E-04	2.175E+01
1.181	1.050E+00	1.575E-03	1.575E-03	1.573E-03	2.875E-01	4.524E-04	2.293E+01
1.127	1.100E+00	1.447E-03	1.447E-03	1.446E-03	2.734E-01	3.954E-04	2.004E+01
1.078	1.150E+00	1.041E-03	1.041E-03	1.040E-03	2.601E-01	2.705E-04	1.371E+01
1.033	1.200E+00	1.159E-03	1.159E-03	1.158E-03	2.475E-01	2.867E-04	1.453E+01
0.992	1.250E+00	6.422E-04	6.422E-04	6.420E-04	2.355E-01	1.512E-04	7.664E+00
0.954	1.300E+00	7.084E-04	7.084E-04	7.081E-04	2.243E-01	1.588E-04	8.050E+00
0.919	1.350E+00	7.780E-04	7.780E-04	7.777E-04	2.137E-01	1.662E-04	8.425E+00
0.886	1.400E+00	8.512E-04	8.512E-04	8.508E-04	2.038E-01	1.734E-04	8.789E+00
0.855	1.450E+00	9.279E-04	9.279E-04	9.275E-04	1.945E-01	1.804E-04	9.141E+00
0.826	1.500E+00	1.008E-03	1.008E-03	1.008E-03	1.857E-01	1.871E-04	9.483E+00
0.800	1.550E+00	9.844E-04	9.844E-04	9.839E-04	1.775E-01	1.746E-04	8.848E+00
0.775	1.600E+00	1.017E-03	1.017E-03	1.017E-03	1.697E-01	1.726E-04	8.745E+00
0.751	1.650E+00	1.055E-03	1.055E-03	1.055E-03	1.624E-01	1.713E-04	8.682E+00
0.729	1.700E+00	1.098E-03	1.098E-03	1.098E-03	1.555E-01	1.707E-04	8.652E+00
0.708	1.750E+00	1.145E-03	1.145E-03	1.145E-03	1.491E-01	1.706E-04	8.648E+00
0.689	1.800E+00	1.197E-03	1.197E-03	1.196E-03	1.430E-01	1.710E-04	8.666E+00
0.670	1.850E+00	1.252E-03	1.252E-03	1.251E-03	1.372E-01	1.717E-04	8.701E+00
0.652	1.900E+00	1.311E-03	1.311E-03	1.310E-03	1.318E-01	1.727E-04	8.752E+00
0.636	1.950E+00	1.374E-03	1.374E-03	1.373E-03	1.266E-01	1.739E-04	8.814E+00
0.620	2.000E+00	1.440E-03	1.440E-03	1.439E-03	1.218E-01	1.753E-04	8.885E+00
0.248	5.000E+00	1.039E-02	1.039E-02	1.034E-02	2.533E-02	2.618E-04	1.327E+01
0.124	1.000E+01	4.473E-02	4.473E-02	4.374E-02	6.880E-03	3.009E-04	1.527E+01
0.062	2.000E+01	1.849E-01	1.849E-01	1.808E-01	1.788E-03	3.025E-04	1.526E+01
0.025	5.000E+01	1.177E+00	1.177E+00	6.917E-01	2.037E-04	2.091E-04	6.154E+00
0.012	1.000E+02	4.734E+00	4.734E+00	9.912E-01	7.401E-05	7.336E-05	1.871E+00

T= 10000 DEGREES

5.60141841E+00	1.31671212E+01	1.94335115E+01	2.67559078E+01	2.93165093E+01
3.32600351E+01	3.07276995E+01	4.24916189E+01	4.71029107E+01	3.64515233E-04
7.47164119E-04	1.34857127E-03	2.16057607E-03	3.16530231E-03	4.34192888E-03
5.72203867E-03	7.24014922E-03	8.87604714E-03	6.74481466E-03	9.02248167E-03
3.24382229E-03	3.34125402E-03	3.92927136E-03	4.56868346E-03	5.26031188E-03
3.62967234E-03	4.00922812E-03	4.53345379E-03	5.02225851E-03	4.69483336E-03
3.54529328E-03	3.98174576E-03	2.16342258E-03	2.40133873E-03	2.63854319E-03
3.87739966E-03	3.13280184E-03	3.39928487E-03	3.34410800E-03	3.46357410E-03
3.60024052E-03	3.75304458E-03	3.92108749E-03	4.10360444E-03	4.29994097E-03
4.50953410E-03	4.73189711E-03	4.96660730E-03	3.68553866E-02	1.60016295E-01
6.64269920E-01	4.23785782E+00	1.70631389E+01		
7.60000000E+02				

D= 1.00 P= 1.00 ATM

9.914245298+15 7.339+29808+17

LN LAMBDA = 6.653E+00
ELECTRICAL CONDUCTIVITY SIGMA= 4.6C5E+01 INVERSE OHMS INVERSE CM
THERMAL CONDUCTIVITY K= 1.323E-02 WATTS/CM DEGREES

FROM NU=24.794 TO NU= 12.397 THE VALUE OF THE INTEGRAL OF ENU IS 1.869E+01 WATTS/CM2 THICK
FROM NU=11.807 TO NU= C.042 THE VALUE OF THE INTEGRAL OF ENU IS 4.695E+02 WATTS/CM2 THIN
FROM NU= 0.025 TO NU= 0.012 THE VALUE OF THE INTEGRAL OF ENU IS 1.281E-01 WATTS/CM2 THICK

RADIANT EMITTANCE F= 0.893E+02 WATTS/CM2
ELECTRIC FIELD E= 4.605E+00 VOLTS/CM
CURRENT DENSITY J= 2.121E+02 AMP/CM2

THETA=0.86 EV NTOTAL=7.340E+17 NDENSITY=6.348E+17 PARTICLES/CM3
T= 10000.0 DEGREES K. P=1.001E+00 ATM

HNU EV	WAVELENGTH MICRONS	KAPPA-PRIME 1/CM	TAU	(-TAU) 1-E	BNU WATTS/CM	INU STER	ENU WATTS/CM
24.794	5.000E-02	5.601E+00	5.601E+00	9.963E-01	3.044E-09	3.033E-09	7.706E-05
22.540	5.500E-02	1.315E+01	1.315E+01	1.000E+00	3.128E-08	3.128E-08	7.925E-04
20.662	6.000E-02	1.944E+01	1.944E+01	1.000E+00	2.131E-07	2.131E-07	5.400E-03
19.072	6.500E-02	2.476E+01	2.476E+01	1.000E+00	1.060E-06	1.060E-06	2.686E-02
17.710	7.000E-02	2.932E+01	2.932E+01	1.000E+00	4.125E-06	4.125E-06	1.045E-01
16.529	7.500E-02	3.327E+01	3.327E+01	1.000E+00	1.320E-05	1.320E-05	3.345E-01
15.496	8.000E-02	3.673E+01	3.673E+01	1.000E+00	3.607E-05	3.607E-05	9.140E-01
13.774	9.000E-02	4.240E+01	4.240E+01	1.000E+00	1.568E-04	1.568E-04	4.730E+00
12.397	1.000E-01	4.710E+01	4.710E+01	1.000E+00	6.736E-04	6.736E-04	1.707E+01
11.807	1.050E-01	3.645E+04	3.645E+04	3.644E+04	1.154E-03	4.207E-07	2.132E-02
8.265	1.500E-01	7.472E+04	7.469E+04	2.415E-02	1.803E-05	1.803E-05	9.140E-01
6.199	2.000E-01	1.350E-03	1.350E-03	1.349E-03	1.121E-01	1.121E-04	7.664E-00
4.960	2.500E-01	2.161E-03	2.161E-03	2.158E-03	2.428E-01	5.235E-04	2.653E+01
4.132	3.000E-01	3.165E-03	3.165E-03	3.160E-03	3.682E-01	1.163E-03	5.897E+01
3.542	3.500E-01	4.342E-03	4.342E-03	4.333E-03	4.638E-01	2.009E-03	1.018E+02
3.099	4.000E-01	5.722E-03	5.722E-03	5.706E-03	5.252E-01	2.997E-03	1.519E+02
2.755	4.500E-01	7.240E-03	7.240E-03	7.214E-03	5.578E-01	4.024E-03	2.040E+02
2.479	5.000E-01	8.876E-03	8.876E-03	8.837E-03	5.690E-01	5.028E-03	2.549E+02
2.254	5.500E-01	6.745E-03	6.745E-03	6.722E-03	5.658E-01	3.801E-03	1.927E+02
2.066	6.000E-01	8.022E-03	8.022E-03	7.990E-03	5.522E-01	4.412E-03	2.237E+02
1.907	6.500E-01	3.244E-03	3.244E-03	3.239E-03	5.331E-01	1.726E-03	8.750E+01
1.771	7.000E-01	3.341E-03	3.341E-03	3.336E-03	5.106E-01	1.703E-03	8.634E+01

1.653	7.500E-01	3.929E-03	3.929E-03	3.922E-03	4.806E-01	1.908E-03	9.673E+01
1.550	8.000E-01	4.569E-03	4.569E-03	4.558E-03	4.622E-01	2.107E-03	1.068E+02
1.459	8.500E-01	5.280E-03	5.280E-03	5.247E-03	4.380E-01	2.298E-03	1.165E+02
1.377	9.000E-01	3.630E-03	3.630E-03	3.623E-03	4.146E-01	1.502E-03	7.614E+01
1.305	9.500E-01	4.069E-03	4.069E-03	4.061E-03	3.922E-01	1.593E-03	8.073E+01
1.240	1.000E+00	4.533E-03	4.533E-03	4.523E-03	3.709E-01	1.678E-03	8.504E+01
1.181	1.050E+00	5.022E-03	5.022E-03	5.010E-03	3.509E-01	1.758E-03	8.910E+01
1.127	1.100E+00	4.695E-03	4.695E-03	4.684E-03	3.321E-01	1.555E-03	7.884E+01
1.078	1.150E+00	3.545E-03	3.545E-03	3.539E-03	3.144E-01	1.113E-03	5.640E+01
1.033	1.200E+00	3.949E-03	3.949E-03	3.944E-03	2.979E-01	1.172E-03	5.941E+01
0.992	1.250E+00	2.180E-03	2.180E-03	2.178E-03	2.825E-01	6.154E-04	3.119E+01
0.954	1.300E+00	2.401E-03	2.401E-03	2.398E-03	2.682E-01	6.432E-04	3.260E+01
0.918	1.350E+00	2.634E-03	2.634E-03	2.630E-03	2.547E-01	6.700E-04	3.396E+01
0.886	1.400E+00	2.877E-03	2.877E-03	2.873E-03	2.422E-01	6.959E-04	3.527E+01
0.855	1.450E+00	3.133E-03	3.133E-03	3.128E-03	2.305E-01	7.209E-04	3.654E+01
0.826	1.500E+00	3.399E-03	3.399E-03	3.394E-03	2.196E-01	7.451E-04	3.777E+01
0.800	1.550E+00	3.344E-03	3.344E-03	3.339E-03	2.093E-01	6.988E-04	3.542E+01
0.775	1.600E+00	3.468E-03	3.464E-03	3.458E-03	1.998E-01	6.907E-04	3.501E+01
0.751	1.650E+00	3.600E-03	3.600E-03	3.594E-03	1.908E-01	6.856E-04	3.475E+01
0.729	1.700E+00	3.753E-03	3.753E-03	3.746E-03	1.824E-01	6.832E-04	3.463E+01
0.708	1.750E+00	3.921E-03	3.921E-03	3.913E-03	1.745E-01	6.829E-04	3.461E+01
0.689	1.800E+00	4.104E-03	4.104E-03	4.095E-03	1.671E-01	6.842E-04	3.468E+01
0.670	1.850E+00	4.300E-03	4.300E-03	4.291E-03	1.601E-01	6.870E-04	3.482E+01
0.652	1.900E+00	4.510E-03	4.510E-03	4.499E-03	1.536E-01	6.909E-04	3.502E+01
0.636	1.950E+00	4.732E-03	4.732E-03	4.721E-03	1.474E-01	6.957E-04	3.527E+01
0.620	2.000E+00	4.967E-03	4.967E-03	4.958E-03	1.416E-01	7.013E-04	3.555E+01
0.248	5.000E+00	3.668E-02	3.684E-02	3.618E-02	2.862E-02	1.035E-03	5.253E+01
0.124	1.000E+01	1.600E-01	1.600E-01	1.479E-01	7.707E-03	1.144E-03	5.763E+01
0.042	2.000E+01	5.643E-01	5.643E-01	4.854E-01	1.909E-03	9.791E-04	4.209E+01
0.025	5.000E+01	4.238E+00	4.238E+00	9.856E-01	3.268E-04	3.221E-04	8.247E+00
0.012	1.000E+02	1.706E+01	1.706E+01	1.000E+00	8.230E-05	8.230E-05	2.068E+00

```
17:41:02 MONDAY, OCTOBER 25, 19A.          NRL ALGOL VERSION OF 9/1/65
      COMMENT  INPUT P AND T  USES DICKS KAPPAS AND NE AND NT IN HOMO T,                    SC  1:  0:0
            CYLINDER;                                                                       SC  1:  0:0
      BEGIN                                                                                 SC  1:  0:0
                                                                        START OF SEGMENT ********** 0002
      COMMENT  GEIL,FOR CHURCH,67A,F0437,SIMPLIFIED PROBLEM;                                SC  2:  0:0
      FILE IN PASSKAPPA DISK SERIAL (2,60,1200);                                            SC  2:  0:0
      FILE IN READER(2,10);  FILE OUT GEIL 4(2,15);                                         SC  2:  3:2
      COMMENT       TIMEIT                                                                / SL  2:  10:2
          TO OBTAIN LISTING MERGE IN BLANK CARD WITH SEQUENCE NUMBER 00000D30;           S SL  2:  10:2
                                                                        99999999 SC  2:  15:0
      INTEGER LOW;                                                                          SC  2:  15:0
      REAL IT,NE,N1,P;                                                                      SC  2:  15:0
      REAL ILAMBDA,T;                                                                       SC  2:  15:0
      REAL NLAMBDA,BT,DT,ET,NTOTL;                                                          SC  2:  15:0
      REAL A,K,N,THETA,COUNT,M,IM2,TEMP,E,MM,KE,TEMP1,J,EPS;                                SC  2:  15:0
      REAL D;                                                                               SC  2:  15:0
      REAL IM2P,LITTLEA,AT3,X,HNU1,HNUS,HNUL,NHNU,C1,C2,C2A,C2B,C3;                         SC  2:  15:0
      REAL L,M1,M2,F1,F2;                                                                   SC  2:  15:0
      REAL EXPON,    FACT;                                                                  SC  2:  15:0
      REAL E1,TEST,DNU,O3,SUM;                                                              SC  2:  15:0
      REAL PRINT,SIGMA,SQTHETA,DTE,DTK,KK,DENOM,TAU,FNUDNU;                                 SC  2:  15:0
      REAL ZBAR,TKTN;                                                                       SC  2:  15:0
      REAL UDIV,VDIV;                                                                       SC  2:  15:0
      REAL DV;                                                                              SC  2:  15:0
      REAL U,V,U2;                                                                          SC  2:  15:0
      REAL MTHETA,JTHETA,MN,JN;                                                             SC  2:  15:0
      ARRAY KAPPA[0:23,1:9D];                                                               SC  2:  15:0
      ARRAY ATHETA,AN[0:40];                                                                SC  2:  17:0
      SAVE ARRAY SINV[0:4];                                                                 SC  2:  19:0
      ARRAY DELTE,DELTK,Z[0:5];                                                             SC  2:  20:3
      ARRAY HNU[0:4DD];                                                                     SC  2:  23:0
      ARRAY I[D:6],DI[0:6];                                                                 SC  2:  24:3
      FORMAT DEBUG(/"THE DOUBLE INTEGRAL IS",E10.3);                                        SC  2:  28:1
                                                                        START OF SEGMENT ********** 0007
                                                                        0007 IS 0009 LONG, NEXT SEG 0002
      FORMAT SN(   "FROM NU=",F6.3," TO NU=",F7.3," THE VALUE OF THE INTEGRAL               SC  2:  28:1
                                                                        START OF SEGMENT ********** 0008
       OF FNU IS",E10.3," WATTS/CM2",X5,A6),                                            SC  8:  28:1
          SIGMAK("LN LAMBDA =",E11.3/                                                   SC  8:  28:1
         "ELECTRICAL CONDUCTIVITY SIGMA=",E11.3 ," INVERSE OHMS INVERSE CM"/            SC  8:  28:1
          "THERMAL CONDUCTIVITY K=",E11.3 ," WATTS/CM DEGREES"),                        SC  8:  28:1
          EJ("ELECTRIC FIELD E=",E11.3 ," VOLTS/CM "/                                   SC  8:  28:1
                       "CURRENT DENSITY J=",E11.3 ," AMP/CM2"),                         SC  8:  28:1
          FINAL(/"RADIANT EMITTANCE F=",E11.3 ," WATTS/CM2");                           SC  8:  28:1
                                                                        0008 IS 0073 LONG, NEXT SEG 0002
```

```
FORMAT FORGOT("SIMPSON REQUIRED EVEN NUMBER OF POINTS");                    SC  2:  2811
                                                                  START OF SEGMENT ********** 0009
                                                                  0009 IS 0010 LONG, NEXT SEG 0002
FORMAT TITLE("NAME OF THE GAS IS READ FROM TITLE CARD"),                    SC  2:  2811
                                                                  START OF SEGMENT ********** 0010
DP("D=",F5.2,X5,"P=", F7.2," ATM"),                                         SC 10:  2811
WRITET("T=",I6," DEGREES").                                                 SC 10:  2811
DESCRIPTION("CYLINDER            FOR HOMOGENEOUS TEMPERATURE"               SC 10:  2811
      ", NEGLECTING THERMAL CONDUCTIVITY"),                                 SC 10:  2811
    DOUT("D=",R9.4),                                                        SC 10:  2811
    NTHETA["N=",R9.0,X5,"THETA=",R5.2," EV"),                               SC 10:  2811
    IM("N=",X6,"I[M]="/[11,F10.3)),                                         SC 10:  2811
    IMS("I[M+1/2)="    ,F8.4,X5,"I(M+1/2)="    ,F8.4),                      SC 10:  2811
    NIS["N=",E10.1),                                                        SC 10:  2811
TITLEPLOT(X10,"THETA=",F4.2," EV",X7,"NTOTAL=",E9.3,X7,"DENSITY=",E9.3,     SC 10:  2811
    " PARTICLES/CM3" ·/                                                     SC 10:  2811
    X16,"T=",F8.1," DEGREES K.",X7,"P=",E9.3," ATM"  ///                    SC 10:  2811
       "   WNU   WAVELENGTH   KAPPA-PRIME"                                  SC 10:  2811
                          "        TAU            ("TAU)       BNU",       SC 10:  2811
         X11,"INU" ,X11,"FNU" /                                             SC 10:  2811
       "    EV    MICRONS        1/CM",X23,"1-E " ,X14 ,"WATTS/CM STER",    SC 10:  2811
    X11,"WATTS/CM"  /                                                       SC 10:  2811
);                                                                          SC 10:  2811


LISTPLOT[F7.3,E12.3,6E14.3),                                                SC 10:  2811
    MBAR["AFTER",I5," ITERATIONS, MBAR=",E10.3," WHERE M=KE=",E10.3));      SC 10:  2811
                                                                  0010 IS 0166 LONG, NEXT SEG 0002
DEFINE JOO="FOR J←0 STEP 1 UNTIL 6 DO #,                                    SC  2:  2811
      JOO1="FOR J←1 STEP 1 UNTIL 6 DO #;                                    SC  2:  2811
PROCEDURE CHOP; BEGIN                                                       SC  2:  2811
WRITE(GEIL,SN,HNU[LOW],HNU[J-1],ABS(FNUONU),TKTN);                          SC  2:  2811
IF TKTN="  THICK" THEN TKTN←" THIN " ELSE TKTN←" THICK";                    SC  2:  4211
SUM←SUM+FNUONU;                                                             SC  2:  4713
FNUONU←0;                                                                   SC  2:  4910
LOW←J;                                                                      SC  2:  4913
END OF PROCEDURE CHOP;                                                      SC  2:  5012
PROCEDURE INTERP(DT,DELT); REAL DT; ARRAY DELT[0];                          SC  2:  5210
BEGIN                                                                       SC  2:  5210
LABEL JUMP;                                                                 SC  2:  5210
                                                                  START OF SEGMENT ********** 0011
JOO1                                                                        SC 11:   010
IF ZBAR<TEMP←Z[J] THEN  BEGIN                                               SC 11:   110
                        DT←DELT[J]←(DELT[J]-DELT[J-1])×(TEMP-ZBAR)/         SC 11:   310
                    (TEMP-Z[J-1]) ; GO JUMP  END;                           SC 11:   612
JUMP;                                                                       SC 11:  1113
END OF PROCEDURE INTERP;                                                    SC 11:  1210
                                                                  0011 IS 0013 LONG, NEXT SEG 0002
```

```
REAL                                                                    SC   2:  52:D
PROCEDURE SIMPSON(A,B,X,Y,N);                                           SC   2:  52:D
COMMENT N MUST BE EVEN;                                                 SC   2:  52:0
VALUE A,B,N;                                                            SC   2:  52:0
REAL A,B,N,X,Y;                                                         SC   2:  52:D
BEGIN                                                                   SC   2:  52:0
REAL DX,DX2,SUM2,SUM4,BB,SUM;                                           SC   2:  52:D
                                                        START OF SEGMENT ********** 0012
IF N MOD 2 = 0 THEN BEGIN                                               SC  12:   0:D
SUM2←SUM4←SUM←0;                                                        SC  12:   1:3
DX←(B-A)/(N  );                                                         SC  12:   3:2
DX2←DX←DX; BB←B-DX←DX/3;                                                SC  12:   5:1
FOR X←A←DX2 STEP DX2 UNTIL BB DO                                        SC  12:   8:3
SUM2←SUM2←Y;                                                            SC  12:  14:D
FOR X←A←DX STEP DX2 UNTIL BB DO                                         SC  12:  17:3
SUM4←SUM4←Y;                                                            SC  12:  25:0
FOR X←A,B DO                                                            SC  12:  28:3
SUM←SUM←Y;                                                              SC  12:  31:3
SIMPSON←(SUM←2×SUM2←4×SUM4)×DX/3;                                       SC  12:  33:2
END ELSE WRITE(GEIL,FORGOT);                                            SC  12:  37:1
END OF PROCEDURE SIMPSON;                                               SC  12:  40:3
                                                        0012 IS 0046 LONG, NEXT SEG 0002
LABEL START,EXIT;                                                       SC   2:  52:D


TIMEIT(GEIL);                                                           SC   2:  52:D
FILL DELTE[*] WITH 0,.5816,.6833,.7849,.9225,1;                         SC   2:  53:D
                                                        START OF SEGMENT ********** 0013
                                                        0013 IS 0006 LONG, NEXT SEG 0002
FILL DELTK[*] WITH 0,.225,.356,.513,.791,1;                             SC   2:  54:3
                                                        START OF SEGMENT ********** 0014
                                                        0014 IS 0006 LONG, NEXT SEG 0002
FILL Z   [*] WITH 0,1,2,4,16,100;                                       SC   2:  56:2
                                                        START OF SEGMENT ********** 0015
                                                        0015 IS 0006 LONG, NEXT SEG 0002
FACT←1.1909←12×(1165/1.438)←3;                                          SC   2:  58:1
VDIV←4;                                                                 SC   2:  61:D
DV←1.5707963268/(VDIV  );                                               SC   2:  61:3
V←DV×.9999999;                                                          SC   2:  63:D
FOR TEMP←0 STEP 1 UNTIL VDIV DO                                         SC   2:  64:2
SINV[TEMP]←SIN(V←V←DV)←2;                                               SC   2:  71:0
READ(PASSKAPPA,*,BT,DT,ET);                                             SC   2:  76:2
NT←(ET-BT)/DT;                                                          SC   2:  87:3
READ(PASSKAPPA,*,NLAMBDA);                                              SC   2:  89:2
READ(PASSKAPPA,NLAMBDA←1,HNU[*]);                                       SC   2:  97:3
START;                                                                  SC   2: 101:3
READ(READER,TITLE)[EXIT]; WRITE(GEIL[PAGE]); WRITE(GEIL,TITLE);         SC   2: 102:0
READ(READER,/,D);                                                       SC   2: 112:1
```

```
WRITE(GEIL,DESCRIPTION);                                                SC  2: 11913
NHNU←NLAMBDA;                                                           SC  2: 12213
FOR J←1 STEP 1 UNTIL NLAMBDA DO HNU[J]←1.2397/HNU[J];                   SC  2: 12312
HNU[NLAMBDA+1]←0;                                                       SC  2: 12911
BEGIN                                                                   SC  2: 13110
ARRAY BNU,KAPPAPRIME,FNU[0:NHNU];                                       SC  2: 13110
                                                    START OF SEGMENT ********** 0016
IT←-1;                                                                  SC 16:  311
FOR T←BT STEP DT UNTIL ET DO BEGIN                                      SC 16:  411
WRITE(GEIL,WRITET,T);                                                   SC 16:  510
IT←IT+1;                                                                SC 16:  1211
READ(PASSKAPPA,NLAMBDA,KAPPA[IT,*]);                                    SC 16:  1312
READ(PASSKAPPA,**,P);                                                   SC 16:  1711
WRITE(GEIL,DP,D,P);                                                     SC 16:  2413
WRITE(GEIL[PAGE]);                                                      SC 16:  3411
FOR J←1 STEP 1 UNTIL NLAMBDA DO KAPPAPRIME[J]←KAPPA[IT,J];              SC 16:  3710
READ(PASSKAPPA,**,NE,NTOTL);                                            SC 16:  4310
N←NTOTL-NE;                                                             SC 16:  5213
M←NE/N;                                                                 SC 16:  5410
THETA←T/11605;                                                          SC 16:  5511
SQTHETA←SQRT(THETA);                                                    SC 16:  5612
IF M≤.5 THEN ZBAR←1 ELSE                                                SC 16:  5713
ZBAR←M+.25/M;                                                           SC 16:  5913


INTERP(DTE,DELTE);                                                      SC 16:  6413
INTERP(DTK,DELTK);                                                      SC 16:  6611
DENOM←ZBAR×.43429448190З×    ( PRINT←              LN(2.4D1Ø20×THETA+3/  SC 16:  6713
      (ZBAR+2×M×(1+ZBAR)×N)));                                          SC 16:  7012
SIGMA←286×SQTHETA+3×DTE/DENOM;                                          SC 16:  7510
KK←.2465×SQTHETA+5×DTK/DENOM;                                           SC 16:  7811
WRITE(GEIL     );                                                       SC 16:  8210
WRITE(GEIL,SIGMAK,PRINT,SIGMA,KK);                                      SC 16:  8413
FOR J←1 STEP 1 UNTIL NHNU DO BEGIN                                      SC 16:  9911
TAU←KAPPAPRIME[J]×D;                                                    SC 16: 10010
            BNU[J]←FACT×(TEMP1+HNU[J]) *3/(EXP(TEMP1/THETA )-1);        SC 16: 10112
UDIV←ENTIER(TAU×1.5);                                                   SC 16: 10710
IF UDIV MOD 2≠0 THEN UDIV←UDIV+1;                                       SC 16: 10911
IF UDIV<2 THEN UDIV←2;                                                  SC 16: 11211
FNU[J]←          8066×BNU[J]×(3.1415926536-4×                           SC 16: 11411
TEMP←                                                                   SC 16: 11611
(                                                                       SC 16: 11611
IF UDIV>100 THEN 0 ELSE                                                 SC 16: 11611
SIMPSON(0,1   ,U,SIMPSON(0,VDIV,V,EXP(-TAU×U/((U2←U↑2)+(1-U2)×SINV(V))),SC 16: 11811
          VDIV)×U,UDIV  .5707963268/VDIV                                SC 16: 13012
)                                                                       SC 16: 13613
));                                                                     SC 16: 13613
END OF J LOOP;                                                          SC 16: 13910
```

```
        WRITE(GEIL[DBL]);                                                    SC  16: 14111
        D3←3/D;                                                              SC  16: 14410
        SUM←0;                                                               SC  16: 14510
        LO←1;                                                                SC  16: 14610
        TEMP←SIGN(KAPPAPRIME[1]-D3);                                         SC  16: 14613
        FNUDNU←FNU[1]×(HNU[1]-HNU[2]);                                       SC  16: 15010
        IF TEMP<0 THEN TKTN←" THIN " ELSE                                    SC  16: 15212
        TKTN←" THICK";                                                       SC  16: 15412
        FOR J←2 STEP 1 UNTIL NHNU DO BEGIN                                   SC  16: 15713
        IF TEMP≠ TEMP←SIGN(KAPPAPRIME[J]-D3)          THEN CHOP;             SC  16: 16010
        DNU←HNU[J-1]-HNU[J+1];                                               SC  16: 16413
        FNUDNU←FNUDNU+TEMP1←FNU[J-1]×DNU;                                    SC  16: 16710
        END OF J LOOP;                                                       SC  16: 16912
        CHOP;                                                                SC  16: 17113
        WRITE(GEIL,FINAL,SUM);                                               SC  16: 17211
        WRITE(GEIL,EJ,TEMP←SQRT(4×SUM/(SIGMA×DI),SIGMA×TEMP);                SC  16: 18011
        WRITE(GEIL[DBL]);                                                    SC  16: 19411
        WRITE(GEIL,TITLEPLOT,THETA,TEMP1←(1+M)×N,N,                          SC  16: 19710
              TEMP←11605×THETA,TEMP1×TEMP/(2.667E19×273));                   SC  16: 20612
        WRITE(GEIL,LISTPLOT,FOR J←1 STEP 1 UNTIL NHNU DO [TEMP1←HNU[J],      SC  16: 21911
              1.2397/TEMP1, TEMP←KAPPAPRIME[ JI, TEMP×D,                     SC  16: 22713
              EXPON←1-EXP(-TEMP×DI,BNU[J] ,EXPON×ANU[J],FNU[J]]]);           SC  16: 23711
        WRITE(GEIL[PAGE]);                                                   SC  16: 25211


        END OF THETA LOOP;                                                   SC  16: 25510
        TIMEIT(GEIL);                                                        SC  16: 25811
        END DYNAMIC HNU;                                                     SC  16: 25911


        EXIT: END.                                                  0016 IS 0263 LONG, NEXT SEG 0002
                                                                             SC   2: 13310
                                                                    0002 IS 0136 LONG, NEXT SEG 0001

EXP             IS SEGMENT NUMBER 0017, PRT ADDRESS IS 0213
LN                      0018                    0211
SIN                     0019                    0171
SQRT                    0020                    0210
OUTPUT(W)               0021                    0034
BLOCK CONTROL           0022                    0005
INPUT(W)                0023                    0173
GO TO SOLVER            0024                    0176
ALGOL WRITE             0025                    0014
ALGOL READ              0026                    0015
ALGOL SELECT            0027                    0016
NUMBER OF ERRORS DETECTED = 000                 LAST CARD WITH ERROR HAS SEQ #
PRT SIZE=0147;    TOTAL SEGMENT SIZE=00937 WORDS;    DISK STORAGE REQ.=01128 WORDS;    NO. SEGS.=0028.
ESTIMATED CORE STORAGE REQUIREMENT = 06331 WORDS.
17:41:38 MONDAY, OCTOBER 25, 1965    PROCESSOR TIME = 15.18 SECONDS    I/O TIME = 50.82 SECONDS
```

RUN DATE	RUN TIME	PROCESSOR TIME	I/O TIME
OCT.25,1965	5:41PM	1 SEC.	11 SEC.

XENON
CYLINDER FOR HOMOGENEOUS TEMPERATURE, NEGLECTING THERMAL CONDUCTIVITY
T= 9000 DEGREES
D= 1.00 P= 760.00 ATM

LN LAMBDA = 7.066E+00
ELECTRICAL CONDUCTIVITY SIGMA= 3.702E+01 INVERSE OHMS INVERSE C
THERMAL CONDUCTIVITY K= 9.572E-03 WATTS/CM DEGREES

FROM NU=24.794 TO NU= 12.397 THE VALUE OF THE INTEGRAL OF FNU IS 3.412E+00 WATTS/CM2 THICK
FROM NU=11.807 TO NU= 0.025 THE VALUE OF THE INTEGRAL OF FNU IS 5.658E+01 WATTS/CM2 THIN
FROM NU= 0.012 TO NU= 0.012 THE VALUE OF THE INTEGRAL OF FNU IS 2.238E-02 WATTS/CM2 THICK

RADIANT EMITTANCE F= 6.001E+01 WATTS/CM2
ELECTRIC FIELD E= 2.546E+00 VOLTS/CM
CURRENT DENSITY J= 9.427E+01 AMP/CM2

THETA=0.78 EV NTOTAL=8.155E+17 NDENSITY=7.677E+17 PARTICLES/CM3
T= 9000.0 DEGREES K. P=1.001E+00 ATM

HNU EV	WAVELENGTH MICRONS	KAPPA-PRIME 1/CM	TAU	(-TAU) 1-E	BNU WATTS/CM	INU STER	FNU WATTS/CM
24.794	5.000E-02	7.544E+00	7.544E+00	9.995E-01	1.244E-10	1.244E-10	3.110E-06
22.540	5.500E-02	1.771E+01	1.771E+01	1.000E+00	1.710E-09	1.710E-09	4.323E-05
20.662	6.000E-02	2.617E+01	2.617E+01	1.000E+00	1.484E-08	1.484E-08	3.757E-04
19.072	6.500E-02	3.334E+01	3.334E+01	1.000E+00	9.063E-08	9.063E-08	2.295E-03
17.710	7.000E-02	3.948E+01	3.948E+01	1.000E+00	4.204E-07	4.204E-07	1.065E-02
16.529	7.500E-02	4.481E+01	4.481E+01	1.000E+00	1.566E-06	1.566E-06	3.968E-02
15.496	8.000E-02	4.946E+01	4.946E+01	1.000E+00	4.890E-06	4.890E-06	1.239E-01
13.774	9.000E-02	5.723E+01	5.723E+01	1.000E+00	3.163E-05	3.163E-05	8.013E-01
12.397	1.000E-01	6.344E+01	6.344E+01	1.000E+00	1.362E-04	1.362E-04	3.451E+00
11.807	1.050E-01	1.348E-04	1.348E-04	1.348E-04	2.519E-04	3.394E-08	8.556E-04
8.265	1.500E-01	2.759E-04	2.759E-04	2.759E-04	8.318E-03	2.295E-06	5.785E-02
6.199	2.000E-01	4.966E-04	4.966E-04	4.965E-04	5.040E-02	2.502E-05	6.307E-01
4.959	2.500E-01	7.908E-04	7.908E-04	7.905E-04	1.278E-01	1.010E-04	2.546E+00
4.132	3.000E-01	1.155E-03	1.155E-03	1.154E-03	2.153E-01	2.485E-04	6.264E+00
3.542	3.500E-01	1.582E-03	1.582E-03	1.581E-03	2.919E-01	4.616E-04	1.163E+01
3.099	4.000E-01	2.082E-03	2.082E-03	2.080E-03	3.490E-01	7.259E-04	1.829E+01
2.755	4.500E-01	2.636E-03	2.636E-03	2.632E-03	3.861E-01	1.016E-03	2.561E+01
2.479	5.000E-01	3.236E-03	3.236E-03	3.231E-03	4.067E-01	1.314E-03	3.311E+01
2.254	5.500E-01	2.368E-03	2.368E-03	2.365E-03	4.145E-01	9.803E-04	2.471E+01
2.066	6.000E-01	2.816E-03	2.816E-03	2.812E-03	4.134E-01	1.162E-03	2.929E+01
1.907	6.500E-01	9.768E-04	9.768E-04	9.764E-04	4.060E-01	3.964E-04	9.991E+00
1.771	7.000E-01	1.014E-03	1.014E-03	1.014E-03	3.946E-01	4.000E-04	1.008E+01
1.653	7.500E-01	1.194E-03	1.194E-03	1.193E-03	3.806E-01	4.541E-04	1.144E+01
1.550	8.000E-01	1.389E-03	1.389E-03	1.388E-03	3.653E-01	5.070E-04	1.278E+01
1.458	8.500E-01	1.600E-03	1.600E-03	1.599E-03	3.494E-01	5.586E-04	1.408E+01
1.377	9.000E-01	1.137E-03	1.137E-03	1.137E-03	3.334E-01	3.789E-04	9.550E+00
1.305	9.500E-01	1.275E-03	1.275E-03	1.275E-03	3.176E-01	4.048E-04	1.020E+01
1.240	1.000E+00	1.421E-03	1.421E-03	1.420E-03	3.022E-01	4.292E-04	1.082E+01
1.181	1.050E+00	1.575E-03	1.575E-03	1.573E-03	2.875E-01	4.524E-04	1.140E+01
1.127	1.100E+00	1.447E-03	1.447E-03	1.446E-03	2.734E-01	3.954E-04	9.967E+00
1.078	1.150E+00	1.041E-03	1.041E-03	1.040E-03	2.601E-01	2.705E-04	6.819E+00
1.033	1.200E+00	1.159E-03	1.159E-03	1.158E-03	2.475E-01	2.867E-04	7.225E+00
0.992	1.250E+00	6.422E-04	6.422E-04	6.420E-04	2.355E-01	1.512E-04	3.811E+00
0.954	1.300E+00	7.084E-04	7.084E-04	7.081E-04	2.243E-01	1.588E-04	4.003E+00
0.918	1.350E+00	7.780E-04	7.780E-04	7.777E-04	2.137E-01	1.642E-04	4.140E+00
0.886	1.400E+00	8.512E-04	8.512E-04	8.508E-04	2.038E-01	1.734E-04	4.371E+00
0.855	1.450E+00	9.279E-04	9.279E-04	9.275E-04	1.945E-01	1.804E-04	4.546E+00
0.826	1.500E+00	1.008E-03	1.008E-03	1.008E-03	1.857E-01	1.871E-04	4.716E+00
0.800	1.550E+00	9.844E-04	9.844E-04	9.839E-04	1.775E-01	1.746E-04	4.400E+00
0.775	1.600E+00	1.017E-03	1.017E-03	1.017E-03	1.697E-01	1.726E-04	4.349E+00
0.751	1.650E+00	1.055E-03	1.055E-03	1.055E-03	1.624E-01	1.713E-04	4.318E+00
0.729	1.700E+00	1.098E-03	1.098E-03	1.098E-03	1.555E-01	1.707E-04	4.302E+00
0.708	1.750E+00	1.145E-03	1.145E-03	1.145E-03	1.491E-01	1.706E-04	4.300E+00
0.689	1.800E+00	1.197E-03	1.197E-03	1.196E-03	1.430E-01	1.710E-04	4.309E+00
0.670	1.850E+00	1.252E-03	1.252E-03	1.251E-03	1.372E-01	1.717E-04	4.327E+00
0.652	1.900E+00	1.311E-03	1.311E-03	1.310E-03	1.318E-01	1.727E-04	4.352E+00
0.636	1.950E+00	1.374E-03	1.374E-03	1.373E-03	1.266E-01	1.739E-04	4.383E+00
0.620	2.000E+00	1.440E-03	1.440E-03	1.439E-03	1.218E-01	1.753E-04	4.418E+00
0.248	5.000E+00	1.039E-02	1.039E-02	1.034E-02	2.533E-02	2.615E-04	6.594E+00
0.124	1.000E+01	4.473E-02	4.473E-02	4.374E-02	6.880E-03	3.009E-04	7.562E+00
0.062	2.000E+01	1.849E-01	1.849E-01	1.688E-01	1.792E-03	3.025E-04	7.532E+00
0.025	5.000E+01	1.177E+00	1.177E+00	6.917E-01	2.937E-04	2.031E-04	4.910E+00
0.012	1.000E+02	4.734E+00	4.734E+00	9.912E-01	7.401E-05	7.336E-05	1.805E+00

T= 10000 DEGREES
0= 1.00 P= 760.00 ATM

LN LAMBDA = 6.653@+00
ELECTRICAL CONDUCTIVITY SIGMA= 4.605@+01 INVERSE OHMS INVERSE CM
THERMAL CONDUCTIVITY K= 1.323@-02 WATTS/CM DEGREES

FROM NU=24.794 TO NU= 12.397 THE VALUE OF THE INTEGRAL OF FNU IS 1.868@+01 WATTS/CM2 THICK
FROM NU=11.807 TO NU= 0.062 THE VALUE OF THE INTEGRAL OF FNU IS 2.334@+02 WATTS/CM2 THIN
FROM NU= 0.025 TO NU= 0.012 THE VALUE OF THE INTEGRAL OF FNU IS 1.236@-01 WATTS/CM2 THICK

RADIANT EMITTANCE F= 2.522@+02 WATTS/CM2
ELECTRIC FIELD E= 4.681@+00 VOLTS/CM
CURRENT DENSITY J= 2.156@+02 AMP/CM2

THETA=0.86 EV NTOTAL=7.340@+17 NDENSITY=6.348@+17 PARTICLES/CM3
T= 10000.0 DEGREES K. P=1.001@+00 ATM

HNU EV	WAVELENGTH MICRONS	KAPPA-PRIME 1/CM	TAU	(-TAU) 1-E	BNU WATTS/CM	INU STER	FNU WATTS/CM
24.794	5.000@-02	5.601@+00	5.601@+00	9.963@-01	3.044@-09	3.033@-09	7.514@-05
22.540	5.500@-02	1.315@+01	1.315@+01	1.000@+00	3.128@-08	3.128@-08	7.892@-04
20.662	6.000@-02	1.944@+01	1.944@+01	1.000@+00	2.131@-07	2.131@-07	5.389@-03
19.072	6.500@-02	2.476@+01	2.476@+01	1.000@+00	1.060@-06	1.060@-06	2.683@-02
17.710	7.000@-02	2.932@+01	2.932@+01	1.000@+00	4.125@-06	4.125@-06	1.044@-01
16.529	7.500@-02	3.327@+01	3.327@+01	1.000@+00	1.320@-05	1.320@-05	3.342@-01
15.496	8.000@-02	3.673@+01	3.673@+01	1.000@+00	3.607@-05	3.607@-05	9.135@-01
13.774	9.000@-02	4.249@+01	4.249@+01	1.000@+00	1.868@-04	1.868@-04	4.732@+00
12.397	1.000@-01	4.710@+01	4.710@+01	1.000@+00	6.736@-04	6.736@-04	1.706@+01
11.807	1.050@-01	3.645@-04	3.645@-04	3.644@-04	1.154@-03	4.207@-07	1.060@-02
8.265	1.500@-01	7.472@-04	7.472@-04	7.469@-04	2.415@-02	1.803@-05	4.546@-01
6.199	2.000@-01	1.350@-03	1.350@-03	1.349@-03	1.121@-01	1.512@-04	3.811@+00
4.959	2.500@-01	2.161@-03	2.161@-03	2.158@-03	2.424@-01	5.235@-04	1.319@+01
4.132	3.000@-01	3.165@-03	3.165@-03	3.160@-03	3.682@-01	1.163@-03	2.932@+01
3.542	3.500@-01	4.342@-03	4.342@-03	4.333@-03	4.638@-01	2.009@-03	5.063@+01
3.099	4.000@-01	5.722@-03	5.722@-03	5.706@-03	5.252@-01	2.997@-03	7.551@+01
2.755	4.500@-01	7.240@-03	7.240@-03	7.214@-03	5.578@-01	4.024@-03	1.014@+02
2.479	5.000@-01	8.876@-03	8.876@-03	8.837@-03	5.690@-01	5.028@-03	1.267@+02
2.254	5.500@-01	6.745@-03	6.745@-03	6.722@-03	5.654@-01	3.801@-03	9.575@+01
2.066	6.000@-01	8.022@-03	8.022@-03	7.990@-03	5.522@-01	4.412@-03	1.111@+02
1.907	6.500@-01	3.244@-03	3.244@-03	3.239@-03	5.331@-01	1.726@-03	4.351@+01
1.771	7.000@-01	3.341@-03	3.341@-03	3.336@-03	5.106@-01	1.703@-03	4.292@+01
1.653	7.500@-01	3.929@-03	3.929@-03	3.922@-03	4.866@-01	1.908@-03	4.809@+01

1.350	8.000E-01	4.569E-03	4.569E-03	4.558E-03	4.622E-01	2.107E-03	5.309E+01
1.458	8.500E-01	5.240E-03	5.260E-03	5.247E-03	4.380E-01	2.209E-03	5.790E+01
1.377	9.000E-01	3.633E-03	3.630E-03	3.623E-03	4.146E-01	1.503E-03	3.785E+01
1.305	9.500E-01	4.064E-03	4.064E-03	4.061E-03	3.922E-01	1.593E-03	4.013E+01
1.240	1.000E+00	4.533E-03	4.533E-03	4.523E-03	3.709E-01	1.678E-03	4.228E+01
1.181	1.050E+00	5.022E-03	5.022E-03	5.010E-03	3.509E-01	1.758E-03	4.429E+01
1.127	1.100E+00	4.605E-03	4.605E-03	4.584E-03	3.321E-01	1.555E-03	3.919E+01
1.079	1.150E+00	3.545E-03	3.545E-03	3.539E-03	3.144E-01	1.113E-03	2.804E+01
1.033	1.200E+00	3.942E-03	3.942E-03	3.934E-03	2.979E-01	1.172E-03	2.953E+01
0.992	1.250E+00	2.180E-03	2.180E-03	2.178E-03	2.825E-01	6.154E-04	1.551E+01
0.954	1.300E+00	2.401E-03	2.401E-03	2.398E-03	2.682E-01	6.432E-04	1.621E+01
0.918	1.350E+00	2.634E-03	2.634E-03	2.630E-03	2.547E-01	6.700E-04	1.688E+01
0.886	1.400E+00	2.877E-03	2.877E-03	2.873E-03	2.422E-01	6.959E-04	1.754E+01
0.855	1.450E+00	3.133E-03	3.133E-03	3.128E-03	2.305E-01	7.209E-04	1.817E+01
0.826	1.500E+00	3.399E-03	3.399E-03	3.394E-03	2.196E-01	7.451E-04	1.878E+01
0.800	1.550E+00	3.344E-03	3.344E-03	3.339E-03	2.093E-01	6.988E-04	1.761E+01
0.775	1.600E+00	3.464E-03	3.464E-03	3.458E-03	1.998E-01	6.907E-04	1.740E+01
0.751	1.650E+00	3.600E-03	3.600E-03	3.594E-03	1.908E-01	6.856E-04	1.728E+01
0.729	1.700E+00	3.753E-03	3.753E-03	3.746E-03	1.824E-01	6.832E-04	1.722E+01
0.708	1.750E+00	3.921E-03	3.921E-03	3.913E-03	1.745E-01	6.828E-04	1.721E+01
0.689	1.800E+00	4.104E-03	4.104E-03	4.095E-03	1.671E-01	6.842E-04	1.724E+01
0.670	1.850E+00	4.300E-03	4.300E-03	4.291E-03	1.601E-01	6.870E-04	1.731E+01
0.652	1.900E+00	4.510E-03	4.510E-03	4.499E-03	1.536E-01	6.909E-04	1.741E+01
0.636	1.950E+00	4.732E-03	4.732E-03	4.721E-03	1.474E-01	6.957E-04	1.753E+01
0.620	2.000E+00	4.967E-03	4.967E-03	4.954E-03	1.416E-01	7.013E-04	1.767E+01
0.248	5.000E+00	3.686E-02	3.686E-02	3.618E-02	2.862E-02	1.035E-03	2.603E+01
0.124	1.000E+01	1.600E-01	1.600E-01	1.479E-01	7.707E-03	1.140E-03	2.842E+01
0.062	2.000E+01	6.643E-01	6.643E-01	4.854E-01	1.999E-03	9.701E-04	2.367E+01
0.025	5.000E+01	4.238E+00	4.238E+00	9.856E-01	3.269E-04	3.221E-04	7.894E+00
0.012	1.000E+02	1.706E+01	1.706E+01	1.000E+00	8.230E-05	8.230E-05	2.080E+00

Program e
Symbol Table for Radiation Flux

R = radius of the cylinder (input)

KAPPA [ILAMBDA, IT] = effective absorption coefficient (including stimulated emission) at the ILAMBDAth wavelength and ITth temperature (input from DOUBLE).

BT = minimum temperature at which the KAPPA's have been calculated (input from DOUBLE).

DT = temperature step size (input from DOUBLE).

ET = maximum temperature at which the KAPPA's have been calculated (input from DOUBLE).

NLAMBDA = number of wavelengths at which KAPPA has been calculated (input from DOUBLE).

ALAMBDA [ILAMBDA] = ILAMBDAth wavelength (input from DOUBLE).

NR = number of equidistant radial distances (of the cylinder) at which the temperature will be input. These points will be at equal intervals from 0 to R along the radial direction (input).

T[IR] = temperature at point $\frac{IR}{NR}$ R along the radius (input).

$G[x] = \int_0^{\pi/2} e^{-\frac{x}{\sin\theta}} \sin\theta d\theta$ (tabulated at intervals of .1 from x = 0 to x = 30)

NPHI = number of ϕ values at which intergrand will be evaluated during numerical integration (input)

DPHI = ϕ step size

DLAMBDA [ILAMBDA] = ALAMBDA [ILAMBDA] - ALAMBDA [ILAMBDA - 1]

ARI [I] = Ith value of R_i at which flux is to be found (input).

NRI = number of R_i's at which flux is to be found.

REFERENCES

1. Yu. P. Raizer, "A Simple Method of Calculating the Degree of Ionization and Thermodynamic Functions of a Multiply Ionized Ideal Gas," Sov. Phys.-J.E.T.P. 9, 1124-1125 (1959).
2. Yu. R. Raizer, "Simple Method for Computing the Mean Range of Radiation in Ionized Gases at High Temperatures," Sov. Phys.-J.E.T.P. 10, 769 (1960).
3. R. A. Pappert and S. S. Penner, "Approximate Opacity Calculations for Polyelectronic Atoms at High Temperatures," J. Quant. Spect. Rad. Transfer 1, 259-268, (1961).
4. S. S. Penner and M. Thomas, "Approximate Theoretical Calculation of Continuum Opacities", A.I.A.A. Journ. 2, 1572-1575 (1964).
5. K. Drelliskak, C. Knopp, and A. B. Cambel, "Partition Functions and Thermodynamic Properties of Argon Plasmas", Phys. Fluids 6, 1280-1288 (1963).
6. L. Biberman and G. Norman, "Plasma Radiation due to Recombination and Bremstrahlung Processes", J. Quant. Spect. Rad. Transfer 3, 221-245 (1963) General Atomics-San Diego Translation GA tr 4943.
7. R. S. Cohen, L. Spitzer, Jr. and P. Routly, "The Electrical Conductivity of an Ionized Gas," Phys. Rev. 80, 230-238 (1950).
8. L. Spitzer, Jr. and R. Härm, "Transport Phenomena in a Completely Ionized Gas", Phys. Rev. 89, 977-981 (1953).

```
09:19:59 TUESDAY, NOVEMBER 9, 1965

BEGIN
COMMENT FLUX;
COMMENT  GEIL,BRUCE SWANSON,220,F0437;
   FILE IN PASSG DISK SERIAL(1, 330);
   FILE IN PASSKAPPA DISK SERIAL(2, 60, 1200);
   FILE IN READER(2, 10);
   FILE OUT GEIL 4(2, 15);
COMMENT DOLLAR OR DOUBLE DOLLAR CARD GOES HERE **********************;     00000000
   ARRAY ARI[0:20];                                                      00000000
   INTEGER J;
   REAL I, NRI;
   REAL R, RI, NPHI, NTHETA, DS, NLAMBDA, N, BLAMBDA, ELAMBDA, HT, DT,
    ET, NT, IN, IT, NR, COSPHI, SUMF, PROPS, THETA, TANPHI, INLAMBDA,
    INS, INTHETA, INPHI, COUNTS, DPHI, TI, ILAMBDA, LAMBDA, LPHI, MPHI,
    TAN2PHI, SINPHI, COSALPH, SINALPH, PHI, Z, LENGTH, PROP, NDS,
    APPROXOS, LS, MS, VM, S, RSMXY, TM, IBM, ZM, KLM, I88, TEMP, YMT,
    EPS, SUM;
   REAL X;
   ARRAY SAVEHR[0:12, 0:5, 0:14];
   ARRAY GI0:300];
   ARRAY TI0:40], DLAMBDA, EXPARGI0:50], KAPPAI0:50, 0:35], ALAMBDA[0:
    50];
   FORMAT
      INPUT("R=",E15.8,X5,"RI=",E15.8,X5,"NPHI=",E15.8,X5,/"APPROXOS=",
       E15.8,X5,"NLAMBDA=",E15.8,X5,"N=",E15.8,X5,"EPS=",E15.8),
      LAMBDAALONE(/"ALAMBDA"/(6E18.8)),
      TIMES("TOTAL TIME IN LAMBDA=",F9.3," SECONDS"/
       "TOTAL TIME IN S      =",F9.3," SECONDS"/
       "TOTAL NUMBER OF $ VALUES=",I9/"TOTAL TIME IN THETA =",F9.3,
       " SECONDS"/"TOTAL TIME IN PHI    =",F9.3," SECONDS"/
       "TOTAL PROCESSOR TIME=",F9.3," SECONDS"/"TOTAL I/O        TIME=",
       F9.3," SECONDS"),
      RRI("NR=",E15.8,X10,"(IIR) ARRAY FOLLOWS"/(6E18.8)),
      TT("BT=",E15.8,X5,"DT=",E15.8,X5,"ET=",E15.8),
      TITLEKAPPAI"KAPPA ARRAY FROM DISK FILE"),
      PRINTKAPPAI/"FROM ILAMBDA=",E11.3/(6E16.4)),
      DCLOCKI"TIME FOR 300 INTEGRATIONS USING ROMBERG OF ORDER 6 IS",F8
       .3),
      OUTGI"G(",F5.1,")=",E20.11),
      INPUT1("R=",E15.8,X5,"RI=",E15.8,X5,"NPHI=",E15.8,X5),
      INPUT2("APPROXOS=",E15.8,X5,"NLAMBDA=",E15.8,X5,"N=",E15.8,X5,
       "EPS=",E15.8),
      TIMEL("TOTAL TIME IN LAMBDA=",F9.3," SECONDS"),

      TIMEPI"TOTAL PROCESSOR TIME=",F9.3," SECONDS"),
      TIMEIO"TOTAL I/O TIME=",F9.3," SECONDS"),
      RESULTI"P=",E19.8," WATTS/CM2");
   LABEL NEXTRAY;
   LABEL EXIT, NEXTRI;
   REAL PROCEDURE LAG(X, X0, DX, Y, N);
COMMENT ORDER 3 LAGRANGE INTERPOLATION. EQUAL INDEPENDENT STEP.          LAG   2
SINGLE DEPENDENT,INDEPENDENT VARIABLE.EXTRAPOLATE IF NOT X0≤X≤X0+N×DX.   LAG   3
X  = DESIRED INDEPENDENT VALUE                                           LAG   4
X0 = FIRST INDEPENDENT VALUE OF Y TABLE (FOR Y[0])                       LAG   5
DX = TABLE STEP FOR INDEPENDENT                                          LAG   6
Y  = NAME,DEPENDENT VARIABLE VALUE TABLE (MUST BE SINGLE SUBSCRIPT)      LAG   7
N  = MAX INDEX OF Y TABLE ( ≥ 4 ) ;                                      LAG   8
   VALUE X, X0, DX, N;                                                   LAG   8
   REAL X, X0, DX;                                                       LAG   9
   INTEGER N;                                                            LAG  10
   ARRAY Y[0);                                                           LAG  10
   BEGIN                                                                 LAG  12
      INTEGER I;                                                         LAG  12
      REAL S;                                                            LAG  12
      I← ENTIER(S←(X-X0)/DX);                                            LAG  12
      IF S=I THEN
         LAG← Y[I]
      ELSE
         LAG←(Y[I+1]-Y[I])×(S-I)+Y[I];
   END LAG;                                                              LAG  18
COMMENT DOLLAR OR DOUBLE DOLLAR CARD GOES HERE **********************;   00000000
   TIMEIT(GEIL);                                                         00000000
   READ(READER,/, R);
   READ(READER,/, NPHI, APPROXOS);
   READ(READER,/, N);
   READ(READER,/, EPS);
   READ(PASSKAPPA,*, BT, DT, ET);
COMMENT                              TEMPS AT WHICH KAPPALT IS GIVEN;
   READ(PASSKAPPA,*, NLAMBDA);
   READ(PASSKAPPA, NLAMBDA+1, ALAMBDA[*]);
   READ(READER,/, NR, FOR IR← 0 STEP 1 UNTIL NR DO T[IR]);
   WRITE(GEIL, RRI, NR, FOR IR← 0 STEP 1 UNTIL NR DO T[IR]);
   FOR ILAMBDA← 1 STEP 1 UNTIL NLAMBDA DO
      ALAMBDA[ILAMBDA]← ALAMBDA[ILAMBDA]×0-8;
   NT←(ET-BT)/DT;
   FOR IT← 0 STEP 1 UNTIL NT DO
      BEGIN
         READ(PASSKAPPA,*, FOR ILAMBDA← 1 STEP 1 UNTIL NLAMBDA DO KAPPA
          [ILAMBDA, IT]);
```

```
      READ(PASSKAPPA,*, X, X);
    END OF IT LOOP;
  READ(PASSG, 301, G[*]);
  IF FALSE THEN
    BEGIN
      (NLAMBDA* TIME(2);
      FOR IT* 0 STEP 1 UNTIL 300 DO
        BEGIN
          X* IT/10;
          G[IT]* ROMBERG(.000000001, 1.5707963268, 6, THETA, EXP(-
           X/(TEMP* SIN(THETA)))*TEMP)
        END OF IT LOOP;
      INLAMBDA* TIME(2)-INLAMBDA;
      WRITE(GEIL, OCLOCK, INLAMBDA/60);
      WRITE(PASSG, 30(, G[*]);
      WRITE(GEIL, OUTG, FOR IT* 0 STEP 1 UNTIL 300 DO(IT, G[IT]));
    END;
  DPHI* 3.(8(5926536/NPHI;
  IF FALSE THEN
    BEGIN
      WRITE(GEIL, TITLEKAPPA);
      FOR ILAMBDA* 1 STEP 1 UNTIL NLAMBDA DO
        WRITE(GEIL, PRINTKAPPA, ALAMBDA[ILAMBDA], FOR (T* 0 STEP 1
         UNTIL NT DO KAPPA[ILAMBDA, IT));
      WRITE(GEIL, LAMBDAALONE, FOR LAMBDA* 1 STEP 1 UNTIL NLAMBDA DO
       ALAMBDA[ILAMBDA]);
      WRITE(GEIL, TT, BT, DT, ET);
    END;
  WRITE(GEIL(OBL));
  FOR ILAMBDA* 2 STEP 1 UNTIL NLAMBDA DO
    DLAMBDA[ILAMBDA]* ALAMBDA[ILAMBDA]-ALAMBDA[ILAMBDA-1];
  DLAMBDA[1]* DLAMBDA[2];
  READ(READER,/, FOR I* 0 STEP 1 U[illegible] 21 DO AR[I])(NEXTRI);
NEXTRI:
  CLOSE(READER, RELEASE);
  NRI* I-1;
  FOR I* 0 STEP 1 UNTIL NRI DO
    BEGIN
      RI* ARI[I];
      COUNTS* 0;
      INLAMBDA* INS* INTHETA* INPHI* 0;
      WRITE(SAVEWR[I, 1,*], INOUT1, R, RI, NPHI);
      WRITE(SAVEWR[I, 2,*], INOUT2, APPROXDS, NLAMBDA, N, EPS);
      SUMF* 0;
      IF RI=1 THEN

        LPHI* 1.5707963268*DPHI/2
      ELSE
        LPHI* DPHI/2;
      HPHI* 3.1415926536-DPHI*.8;
      INPHI* INPHI-TIME(2);
      FOR PHI* LPHI STEP DPHI UNTIL HPHI DO
        BEGIN
          TAN2PHI*(TANPHI*(SINPHI* SIN(PHI))/COSPHI* COS(PHI))*2;
          SUM* 0;
          COSALPH*(RI/R*TAN2PHI-SQRT(1+TAN2PHI*(I-(RI/R)*2)))/(I+
           TAN2PHI);
          SINALPH* SQRT(1-COSALPH*2);
          IF ABS(SINALPH/(COSALPH-RI/R)-TANPHI)>.000000( THEN
            BEGIN
              COSALPH*(RI/R*TAN2PH(+SQRT((+TAN2PHI*(I-(RI/R)*2))
              )/((+TAN2PHI));
              SINALPH* SQRT((-COSALPH*2);
            END;
          INTHETA* INTHETA-TIME(2);
          LENGTH* SINALPH*R/SINPHI;
          FOR ILAMBDA* 1 STEP 1 UNTIL NLAMBDA DO
            EXPARG(ILAMBDA]* 0;
          IF NDS* ENTIER(LENGTH/APPROXDS)+1<N THEN
            DS* LENGTH/NDS
          ELSE
            DS* LENGTH/N;
          LS* DS/2;
          HS* LENGTH-LS*.8;
          VM* 0;
          INS* INS-TIME(2);
          FOR S* LS STEP DS UNTIL HS DO
            BEGIN
              COUNTS* COUNTS+1;
              RSMXY* SQRT((RI*S*COSPHI)*2+(S*SINPHI)*2);
              TM* LAG(RSMXY, 0, R/NR, T, NR);
              IBM* (.44022/TM;
              ZM* 0;
              INLAMBDA* INLAMBDA-TIME(2);
              FOR ILAMBDA* 1 STEP 1 UNTIL NLAMBDA DO
                BEGIN
                  LAMBDA* ALAMBDA[ILAMBDA];
                  KLM* LAG(TM, BT, DT, KAPPA[(LAMBDA,*], NT);
                  IBB* (.1925@-12/(LAMBDA*5*(EXP(TBM/LAMBDA)-1
                   ));
                  EXPARG[ILAMBDA]* TEMP* KLM*DS+EXPARG[ILAMBDA
```

```
                              ]}
                             IF TEMP$3D THEN
                                BEGIN
                                   YMT← KLM×[BB×LAG(TEMP, 0, .1, G, 300)]
                                   Z'4← ZM+YMT×DLAMBDA[ILAMBDA]}
                                END TEMP3D}
                          END OF LAMBDA LOOP}
                       INLAMBDA← INLAMBDA+TIME(2)}
                       VM← VM+ZM}
                    END OF S LOOP}
NEXTRAY}
                 INS← INS+TIME(2)}
                 SUM← SUM+VM×DS}
                 INTHETA← INTHETA+TIME(2)}
                 SUMF← SUMF+SUM×COSPHI}
              END OF PHI LOOP}
           INPHI← INPHI+TIME(2)}
           SUMF←-SUMF×4×DPHI}
           WRITE(SAVEWR[I, 0,*], RESULT, SUMF)}
           WRITE(SAVEWR[I, 3,*], TIMEL, INLAMBDA/60)}
           WRITE(SAVEWR[I, 4,*), TIMEP, TIME(2)/60)}
           WRITE(SAVEWR[I, 5,*], TIMEID, TIME(3)/60)}
        END OF RI LOOP}
     FOR I← 0 STEP 1 UNTIL NRI DO
        BEGIN
           WRITE(GEIL,'PAGE'))}
           FOR J← 0 STEP 1 UNTIL 5 DO
              WRITE(GEIL, 15, SAVEWR[I, J,*]))}
        END OF I LOOP}
EXIT}
END,
```

09:20:15 TUESDAY, NOVEMBER 9, 1965 PROCESSOR TIME = 5.83 SECONDS I/O TIME = 22.57 SECONDS